

Stony Brook University



OFFICIAL COPY

The official electronic file of this thesis or dissertation is maintained by the University Libraries on behalf of The Graduate School at Stony Brook University.

© All Rights Reserved by Author.

**The Function of *pqbp1*, a Causative Gene for Renpenning Syndrome, During
Early Neural Development in *Xenopus***

A Dissertation Presented

by

Jamina Oomen-Hajagos

to

The Graduate School

in Partial Fulfillment of the

Requirements

for the Degree of

Doctor of Philosophy

in

Genetics

Stony Brook University

May 2015

Copyright by
Jamina Oomen-Hajagos
2015

Stony Brook University
The Graduate School

Jamina Oomen-Hajagos

We, the dissertation committee for the above candidate for the
Doctor of Philosophy degree, hereby recommend
acceptance of this dissertation.

Gerald H. Thomsen, Ph.D. – Dissertation Advisor
Professor, Department of Biochemistry and Cell Biology

Howard I. Sirotkin, Ph.D. - Chairperson of Defense
Associate Professor, Department of Neurobiology and Behavior

Ken-Ichi Takemaru, Ph.D.
Associate Professor, Department of Pharmacological Sciences

Mustafa Khokha, M.D.
Associate Professor, Pediatrics (Critical Care) and Genetics
Yale University

This dissertation is accepted by the Graduate School

Charles Taber
Dean of the Graduate School

Abstract of the Dissertation

**The Function of *pqbp1*, a Causative Gene for Renpenning Syndrome, During
Early Neural Development in *Xenopus***

by

Jamina Oomen-Hajagos

Doctor of Philosophy

in

Genetics

Stony Brook University

2015

The *pqbp1* (polyglutamine tract-binding protein 1) gene has been associated with a number of developmental and neurodegenerative disorders, such as Huntington's disease, spinocerebellar ataxia type 1, and a variety of X-linked intellectual disabilities grouped together under the umbrella term Renpenning Syndrome. Renpenning Syndrome is an X-linked recessive disorder involving intellectual disability, as well as physical features such as microcephaly, microphthalmia, lean build, short stature, and small testes.

Work in the Thomsen Lab previously determined that a disruption in cellular levels of PQBP1 can impact crucial developmental processes such as gastrulation and neural tube closure. A reduction in PQBP1 levels was found to perturb the splicing regulation or transcription of two components of the FGF pathway (FGFR2 and FGF4), a critical developmental pathway. Specifically, changes were seen in the levels of the two FGFR2 transcripts. As these splice forms have different ligand binding affinities, this would be expected to alter the nature of FGF signaling, which performs an essential role in a variety of developmental processes. Several other critical signal transduction pathways - BMP, Activin, and Nodal - were not affected.

This project is particularly focused on investigating the impact of modulating PQBP1 levels on neural function, since increasing our knowledge in this area has direct relevance to human disease phenotypes. I am using a well-established model organism for studying early development, the frog *Xenopus*. Knockdown of PQBP1 levels by splice morpholino demonstrated a severe eye phenotype as well as a reduction in the length of the anterior-posterior body axis. These phenotypes could be rescued by *pqbp1* mRNA.

Knock down of PQBP1 in this neuralized animal caps affected a variety of early and later neural markers. *In situ* hybridization experiments on whole embryos revealed similar impacts on neural markers, in addition to changes in the specific regions of marker expression.

This work lends new insight into the aspects of early neural development that are impacted by PQBP1, and provides guidelines for further research into the developmental mechanisms underlying Renpenning syndrome and other *pqbp1*-related disorders.

Dedication Page

This work is dedicated to my all-time favorite genetics experiments: my children, Eli and Cheyenne Hajagos. You have been an unwavering source of inspiration to me. Thanks to both of you; you make me proud to be your Mom.

“Have big dreams. You will grow into them.”

-Unknown

Table of Contents

Chapter 1: Background and Significance

1.1 <i>Pqbp1</i> and its role.....	1
1.1.1 General background.....	1
1.1.2 Protein structure and evolutionary conservation.....	3
1.1.3 <i>Pqbp1</i> connections to disease.....	4
1.1.4 <i>Pqbp1</i> function in <i>Xenopus</i>	7
1.2 Overview of Renpenning syndrome.....	11
1.2.1 Presentation/clinical features.....	11
1.2.2 <i>Pqbp1</i> mutations and Renpenning.....	13
1.3 Introduction to <i>Xenopus</i> and its early development.....	15
1.3.1 <i>Xenopus</i> as a model system.....	15
1.3.2 <i>Xenopus</i> early development.....	17
1.3.3 Neural development in <i>Xenopus</i>	19
1.3.4 A note on the use of morpholinos in <i>Xenopus</i> studies.....	23
1.4 Figures and Tables.....	28

Chapter 2: *pqbp1* expression is largely localized to neural-fated regions in tailbud stage embryos

2.1 Introduction.....	44
2.2 Results.....	45
2.2.1 <i>pqbp1</i> expression in tailbud stage whole embryos.....	45
2.2.2 <i>pqbp1</i> expression in tailbud head sections.....	45
2.3 Discussion.....	45
2.4 Future Directions.....	47
2.5 Materials and Methods.....	48
2.5.1 mRNA probe synthesis and whole mount <i>in situ</i> hybridization.....	48
2.5.2 Embryo paraffin embedding and sectioning.....	49
2.6 Figures and Tables.....	50

Chapter 3: PQBP1 is essential for normal embryo development

3.1 Introduction.....	53
3.2 Results.....	54
3.2.1 PQBP1 knockdown and overexpression cause gastrulation and neurulation defects.....	54
3.2.2 PQBP1 knockdown impacts proper elongation of the <i>Xenopus</i> body axis.....	55
3.2.3 Targeted PQBP1 knockdown results in eye and anterior head defects.....	55
3.3 Discussion.....	56
3.4 Future Directions.....	59
3.5 Materials and Methods.....	60
3.5.1 PQBP1 morpholino design.....	60
3.5.2 Microinjections and embryo culture.....	61
3.5.3 Magenta-gal staining.....	62
3.5.4 In vitro transcription.....	62
3.5.3 Western blotting.....	63
3.6 Figures and Tables.....	65

Chapter 4: PQBP1 impacts neural development independent of mesodermal influences and may promote neural determination and differentiation

4.1 Introduction.....	79
4.2 Results.....	80
4.2.1 <i>Pqbp1</i> is expressed in neuralized animal caps.....	80
4.2.2 PQBP1 knockdown selectively impacts neural marker expression in an isolated neural context.....	81
4.2.3 PQBP1 knockdown in neural tissue may impact FGF signaling in a manner antagonistic to its function in mesoderm.....	82
4.3 Discussion.....	82
4.4 Future Directions.....	85
4.5 Materials and Methods.....	86

4.5.1 In vitro transcription and analysis of Chordin function.....	86
4.5.2 Microinjection and animal cap cutting.....	86
4.5.3 RNA extraction and cDNA synthesis.....	87
4.5.4 RT-qPCR.....	87
4.6 Figures and Tables.....	90
Chapter 5: PQBP1 selectively influences the neural developmental circuit	
5.1 Introduction.....	100
5.2 Results.....	100
5.2.1 Targeted PQBP1 knockdown in early neurula stages impacts a subset of neural markers.....	100
5.2.2 Marker expression is altered in tailbud stage embryos.....	101
5.3 Discussion.....	101
5.4 Future Directions.....	105
5.5 Materials and Methods.....	105
5.5.1 Microinjection and embryo culture.....	105
5.5.2 Whole mount <i>in situ</i> hybridization.....	105
5.6 Figures and Tables.....	108
Chapter 6: PQBP1 likely acts during early neural specification.....	111
Bibliography.....	112
Appendix A: <i>Pqbp1</i> Homeolog Alignment to Genomic Scaffold Showing Intron/Exon Boundaries and Morpholino Target Sites.....	127
Appendix B: TGF-β Interactants Morpholino Screen Preliminary Data.....	131

List of Figures and Tables

Figures:

<u>Figure 1:</u> Evolutionary conservation of PQBP1 protein sequence among Metazoan taxa.....	40
<u>Figure 2:</u> Sample Renpenning syndrome pedigrees and phenotypes.....	41
<u>Figure 3:</u> Photographs and drawings of 8, 6, and 32 cell stage embryos.....	42
<u>Figure 4:</u> A proposed gene regulatory network involved in the stabilization..... of neural fate	43
<u>Figure 5:</u> <i>Pqbp1</i> expression in whole embryos.....	51
<u>Figure 6:</u> Sections of <i>pqbp1</i> whole mount <i>in situ</i> embryos at..... NF Stages 33-34	52
<u>Figure 7:</u> In vitro transcribed <i>pqbp1</i> mRNA is expressed in <i>Xenopus</i> <i>laevis</i> embryos	66
<u>Figure 8:</u> Gels showing the presence of a smaller, alternate <i>pqbp1</i> splice product	66
<u>Figure 9:</u> Phenotypes of embryos injected bilaterally at the 2 cell stage..... with control or PQBP1 morpholino	70
<u>Figure 10:</u> PQBP1 splice morpholino produces milder phenotypes..... than PQBP1 translation-blocking morpholinos.	71
<u>Figure 11:</u> Bean plot showing the length distribution of PQBP1 splice..... morpholino-injected embryos as compared to control morpholino-injected embryos	72
<u>Figure 12:</u> PQBP1 splice morpholino produces eye defects.....	73
<u>Figure 13:</u> <i>Pqbp1</i> mRNA partial rescue of wild-type phenotype.....	76
<u>Figure 14:</u> Percent wild-type phenotypes observed in rescue experiments.....	77
<u>Figure 15:</u> Morpholino designs.....	78
<u>Figure 16:</u> Diagram showing the experimental procedure for RT-qPCR on neuralized animal caps	91

<u>Figure 17:</u> Test of <i>chordin</i> mRNA function.....	92
<u>Figure 18:</u> Sample whole embryos at NF Stage 20 and corresponding caps.....	93
<u>Figure 19:</u> <i>Pqbp1</i> is expressed in neuralized animal cap explants.....	94
<u>Figure 20:</u> <i>Brachyury</i> levels of expression in neuralized caps are minimal.....	95
<u>Figure 21:</u> Expression levels at NF Stages 18-21 and time courses of.....	96-97
neural marker expression (and the cement gland marker <i>XAG1</i>) in neuralized and non-neuralized animal caps	
<u>Figure 22:</u> PQBP1 morpholino and <i>pqbp1</i> mRNA appear to induce.....	98
similar changes in marker expression	
<u>Figure 23:</u> PQBP1 morpholino injection changes the relative levels of the.....	99
<i>FGFR2</i> spliceoforms in neuralized animal caps	
<u>Figure 24:</u> Representative <i>in situ</i> expression patterns in neurulae with	110
PQBP1 knocked down in one dorsal blastomeres at the 4-8 cell stage	
<u>Figure 25:</u> Representative <i>in situ</i> expression patterns in NF Stage 27.....	111
embryos with PQBP1 knocked down in one dorsal blastomeres at the 4-8 cell stage	
<u>Figure 26:</u> Proposed placement of PQBP1 in a simplified neural regulatory network.....	115
<u>Figure B-1:</u> TGF- β pathway interactants knocked down during the.....	128
preliminary morpholino screen.	

Tables:

<u>Table 1:</u> Early neural determination and differentiation genes.....	30
<u>Table 2:</u> Embryo survival by treatment.....	67
<u>Table 3:</u> Embryo phenotypes at NF Stage 15.....	68
<u>Table 4:</u> Embryo phenotypes at NF Stage 23.....	69
<u>Table 5:</u> Embryo length statistical comparisons.....	72
<u>Table 6:</u> Rescue experiment summary.....	74
<u>Table 7:</u> Phenotype breakdown of 4 cell stage rescue experiments (n=3).....	75
<u>Table 8:</u> Expression changes by marker (NF Stage 18-21 embryos).....	109

Acknowledgements

I am grateful to the many people who contributed in various ways to allow me to complete this work. I am thankful to my advisor, Dr. Gerald (Jerry) Thomsen, for being a supportive and flexible mentor. I feel that I have learned a great deal, not just about developmental biology, working with *Xenopus*, and my particular research topic, but also about how to think critically, troubleshoot, and collaborate with other research groups. Thank you also to my committee members for their time and valuable feedback.

Thank you to the members of the Thomsen lab, particularly Yasuno Iwasaki, Gina Sorrentino, Matt Dunn, and Francesca Gist Nakagawa, who have been a pleasure to work with and enriched my lab experience. I also want to particularly thank Qichen Wang, who provided valuable assistance on my project - I wish we could have worked together longer!

Thanks to Jerry and Dr. Amy Sater, Dr. Karen Liu, and Dr. Mustafa Khoka for allowing me to experience the magic that is the Cold Spring Harbor Cell & Developmental Biology of *Xenopus* Course, first as a student, and then for three years as an assistant. This introduction to the wonderful people who make up the frog community has been tremendously enriching and personally rewarding to me.

I owe a debt of gratitude to my friends, who have provided me with (mostly helpful) advice and good times together during my time in graduate school. I would like to especially thank my fellow Genetics students, particularly Stephanie Izzi, who has been an awesome support throughout and is just an all-around “good egg”, and Kimberly Bell, who has always been willing to help when asked, and has provided a listening ear when I needed one.

A big “thank you” goes out to Kate Bell, who is a true saint for dealing with all of us “gradual students”, and Dr. Martha Furie, Director of the Genetics Program, for her valuable guidance and advice. I also appreciate the financial support provided by the Genetics Program, the Biochemistry and Cell Biology Department, as well as the Ecology and Evolution Department.

I am grateful to my students at Suffolk County Community College for providing me with a wide variety of perspectives, and for continuing to surprise me every semester.

Last but not least, thank you to my family, particularly Janos, Cheyenne, and Eli Hajagos, whose support and patience have been an enormous source of strength to me for the past five years. Thank you to my parents, Lea Seeuws and Cornelius Oomen, for instilling a love of learning in me from a young age and exposing me to all sorts of exciting adventures, and my in-laws, Kathleen and Janos Hajagos, for always helping out and providing good company and delicious meals.

Chapter 1: Background and Significance

1.1 *pqbp1* and its role

1.1.1 *General background*

In humans, the *pqbp1* (polyglutamine tract-binding protein 1) gene (previously known as *NPW38*) is located on the X chromosome and codes for a 38 kDa nuclear protein involved in regulating transcription and pre-mRNA splicing (Komuro et al. 1999b; Komuro et al. 1999a; Tapia et al. 2010; Iwasaki & Thomsen 2014). PQBP1 is linked to aspects of the disease processes of various developmental and neurodegenerative disorders, including Huntington's disease, spinocerebellar ataxia type 1, and a variety of X-linked intellectual disabilities now grouped together under the umbrella term Renpenning Syndrome (Flynn et al. 2011; Stevenson et al. 1998; Germanaud et al. 2011; Stevenson et al. 2005; Kurosaki et al. 2012; Nasu et al. 2012).

PQBP1 was initially identified through its association with the polyglutamine (polyQ) sequence of BRN2 (POU3F2) (Waragai et al. 1999; Waragai et al. 2000). BRN2 belongs to a family of transcription factors that can bind to the octameric DNA sequence ATGCAAAT and appear to play an important role in both the development and eventual functioning of the nervous system, as well as the proper differentiation of other cell lineages (Waragai et al. 2000; Wapinski et al. 2013; Schreiber et al. 1993; Latchman 1999; Josephson et al. 1998; Komiyama et al. 2003; He et al. 1989; Shi et al. 2010). PQBP1 also colocalizes - and has been found to interact with - mutant forms of Ataxin-1 as well as Huntingtin (Busch et al. 2003; Okazawa et al. 2002). A variety of X-linked intellectual disabilities, including Sutherland-Haan syndrome, Renpenning syndrome,

Hamel cerebropalatocardiac syndrome, and Golabi-Ito-Hall syndrome, are associated with *pqbp1* mutations. Recently, these disorders, as a group, have generally been referred to as Renpenning syndrome (Lubs et al. 2006; Tapia et al. 2010; Martínez-Garay et al. 2007; Germanaud et al. 2011; Kunde et al. 2011; Golabi et al. 1984). The observation that a number of distinct physical anomalies occur with these syndromes (such as microcephaly, cardiac abnormalities, and short stature) strongly suggests the disruption of early development in these individuals (Golabi et al. 1984). Interestingly, in the nematode *C. elegans*, the *pqbp1* homolog appears to be involved in lipid metabolism (Takahashi et al. 2009).

Varying levels of *pqbp1* expression appear to be required during embryonic development, as well as for proper neural functioning in adulthood. In mice, it is expressed largely in embryos and newborn mice, with peak expression occurring around birth and down-regulated expression in adulthood (Qi et al. 2005). In *Xenopus laevis*, *pqbp1* is initially expressed maternally, and expression continues through tailbud stages (Iwasaki & Thomsen 2014). In adult *Drosophila*, the level of PQBP1 seems to be maintained within a narrow range for optimal function (Tamura et al. 2013).

Expression of *pqbp1* in the human brain was initially confirmed by northern blot (Imafuku et al. 1998). In the developing mouse embryo, *pqbp1* expression is largely confined to the CNS (Qi et al. 2005). However, in adult mice *pqbp1* is expressed ubiquitously throughout, but it remains more concentrated in the neurons of the central nervous system (CNS), particularly in the hippocampus, olfactory bulb, and cerebellar cortex (Waragai, Lammers et al. 1999). In *Xenopus laevis*, *pqbp1* is expressed maternally in the animal poles of 64-cell-stage embryos, and in neural plates and head

primordia of neurula-stage embryos. In later tailbud stages, *pqbp1* expression is found in the head, eye, spinal cord, and neural crest derivatives (Iwasaki & Thomsen 2014).

1.1.2 Protein structure and evolutionary conservation

The PQBP1 protein was named for the polar rich domain (PRD) it contains, which can bind polyglutamine stretches. This domain, when mutated, can be involved in producing disease phenotypes when mutated (Martínez-Garay et al. 2007). Studies showed that it binds to the Huntingtin, Ataxin-1, and POU3F2 (BRN2) proteins, which function in gene transcriptional regulation (Shi et al. 2010; Kunde et al. 2011; Thurber et al. 2011; Tong et al. 2011; Hogel et al. 2012). Expanded polyglutamine stretches are associated with diseases such as Huntington's disease and a number of ataxias, with a proposed causative mechanism being excessive protein aggregation (Shimohata et al. 2002; Shimohata et al. 2000; Robertson & Bottomley 2010; Schaefer et al. 2012). However, the details regarding whether, and if so, how PQBP1 protein may be involved in this process are currently largely unknown.

Another key feature of the PQBP1 protein is its WW domain, which is one of the smallest protein motifs known to interact with proline-rich peptides and has been shown to be involved in transcriptional regulation (Sudol et al. 2012). It contains the two conserved tryptophans and one proline that are considered typical of WW domains. However, it is worth mentioning that three hydrophobic amino acids are found near the second conserved Trp, whereas the comparable region is usually hydrophilic in most WW domains. It is thought that this may help define the ligand binding specificity of PQBP1 (Komuro et al. 1999b). The WW domain in PQBP1 was determined to function

as a transcriptional activator through a GAL4-DNA-binding assay in CHO cells. Mutating the three conserved WW residues abolished this transcriptional activation activity (Komuro et al. 1999b). It is noteworthy that there are a number of alternatively spliced *pqbp1* transcripts in humans, but all of these contain the WW domain (Iwamoto, Huang et al. 2000). Mutations in this region are found in a number of X-linked ID syndromes, such as Golabi-Ito-Hall syndrome, in which a missense mutation in the WW domain is present (Lubs, Abidi et al. 2006).

A survey of Metazoa indicates that the amino acid sequence of critical domains within PQBP1 is conserved across species (Figure 1). Although PQBP1 is conserved from human to sea anemone (*Nematostella vectensis*), the length and makeup of the polar rich domain (and, in fact, its presence) varies greatly among species (Nasu et al. 2012). In addition, the *Drosophila* homologue lacks the C-terminal domain and is rather divergent from the homologues found in other model systems.

1.1.3 *Pqbp1* connections to disease

As mentioned previously, mutations in *pqbp1* are associated with a variety of disorders, including Renpenning syndrome, which encompasses a number of diseases previously thought to be distinct. In addition, several polyglutamine diseases, such as Huntington's and a number of spinocerebellar ataxias, involve improper protein interactions with PQBP1 (Michalik & Van Broeckhoven 2003). The anatomical features observed with Renpenning syndrome, such as microcephaly, microphthalmia, and lean build, imply that PQBP1 may play a critical role in development (Flynn et al. 2011;

Stevenson et al. 1998; Martínez-Garay et al. 2007). However, the mechanisms by which PQBP1 influences early developmental events are still largely unknown.

Several studies have begun to address the question of whether an increase or a decrease (or both) in functional PQBP1 protein levels is causative of the observed disease phenotypes. A knockout mouse model system for studying the developmental importance of PQBP1 has not yet been generated, presumably due to an essential role for the protein in cells, and thus lethality of a complete knockdown (Okuda et al. 2003). A partial knockdown mouse exhibiting about half of the normal expression of PQBP1 does exist; however, it does not display developmental defects, but rather has an anxiety phenotype (Ito et al. 2009). A depletion of PQBP1 in mouse projection neurons reduced dendritic outgrowth and altered the alternative splicing of a number of mRNA transcripts associated with neuronal projection development (Wang et al. 2013). Supplementation with wild-type human PQBP1, but not mutant PQBP1 containing known disease-associated mutations, was able to rescue these defects. In addition, in utero gene therapy at E10 of conditional *pqbp1* knockout mice with microcephaly was successful at rescuing microcephaly and improving behavioral abnormalities (Ito et al. 2014).

A study in *Drosophila* in which PQBP1 is repressed through the insertion of *piggyBac* showed a decrease in the expression of the NMDA receptor subunit 1 (NR1) in projection neurons. A learning disturbance, which could be rescued through NR1 overexpression, was also observed (Tamura et al. 2010).

While these studies have established the deleterious effects of a reduction in *pqbp1* expression, negative impacts are also observed upon overexpression.

Transgenic mice that overexpress *pqbp1* show a late-onset neurological degeneration phenotype reminiscent of some of the disorders observed in humans with mutations in the *pqbp1* gene, such as spinocerebellar ataxia type-1 (Okuda et al. 2003). In addition, a study using *Drosophila* demonstrated that both insufficient and excess PQBP1 expression had a negative impact on lifespan (Tamura et al. 2013). Interestingly, a recent study found a full duplication of *pqbp1* in certain patients with Renpenning syndrome (Flynn et al. 2011). In addition, both knockdown and overexpression of *pqbp1* in *Xenopus* produces abnormal phenotypes (Iwasaki & Thomsen 2014). Therefore, a modulation of PQBP1 levels within a fairly narrow range appears to be essential for an optimal phenotype.

It is clear that the presence of PQBP1, at some level, is required for proper development as well as functioning in the adult organism. There has also been some investigation into the molecular mechanisms by which PQBP1 exerts its effects. Current evidence suggests that PQBP1 may have important functions in transcription and splicing. PQBP1 has been shown to interact with RNA polymerase II, and enhanced binding of PQBP1 to the C-terminal domain of the RNA polymerase II large subunit caused by mutant Ataxin-1 led to reduced levels of phosphorylated Pol II and transcription (Okazawa et al. 2002). Also, a mutated *pqbp1* in which the complex with WBP11, with which it interacts through its WW domain, was compromised led to a pre-mRNA splicing defect (Komuro et al. 1999a; Tapia et al. 2010). Furthermore, PQBP1 may play a significant role in cytoplasmic RNA metabolism and the transport of RNA granules in dendrites. In addition to being found in nuclear speckles, it is present in a cytoplasmic pool, where it interacts (and co-localizes in punctate structures) with RNA-

binding proteins that have been shown to function in RNA processing, translation, and neuronal RNA transport (Kunde et al. 2011). These interacting proteins include WBP11 (SIPP1), K-homology (KH)-type splicing regulatory protein (KSRP), and polypyrimidine tract-associated splicing factor (PSF), all proteins associated with neuronal RNA transport granules. In addition, PQBP1 is recruited into stress granules, which are complexes of mRNAs and associated proteins formed during conditions in which translation needs to be downregulated (Kunde et al. 2011).

PQBP1 forms nuclear inclusions with at least one of its binding partners (WBP11). These inclusions are highly dynamic and are mostly found in neurons, due to the higher concentration of *pqbp1* found in those cells. A number of mutations in PQBP1 were found to disrupt this interaction (Nicolaescu et al. 2008).

1.1.4 PQBP1 function in *Xenopus*

The Thomsen lab has been investigating the role of PQBP1 in early development, using the *Xenopus* model system. The experiments have mostly utilized *Xenopus laevis* but also, to a lesser extent, *Xenopus tropicalis*. In *X. laevis*, which is pseudotetraploid, there are two *pqbp1* homeologs: *pqbp1a* and *pqbp1b*. cDNA was obtained for *pqbp1a* using RT-PCR with primers designed based on the homology of *X. laevis* expressed sequence tags (ESTs) to the known human *pqbp1* sequence. PQBP1a and b are 97% identical to each other at the amino acid level. Therefore, it is likely that they perform the same function in the embryo; although their relative contributions may vary based on levels of expression. As compared to human PQBP1,

the *X. laevis* PQBP1a homeolog has 79% and 85% amino acid identity on the N-terminal and C-terminal halves, respectively.

In situ hybridization results revealed that *pqbp1* expression becomes more localized during the course of early embryonic development. Expression was seen in the animal pole of 64-cell stage embryos, in the neural plate and presumptive head region of neurula stage embryos, and the head, eye, spine and neural crest derivatives of tailbud stage embryos (Iwasaki & Thomsen 2014).

Loss of PQBP1 function was investigated in the *Xenopus* system using three different morpholino oligonucleotides (MOs) that were designed to block mRNA translation. Morphant embryos showed a variety of defects, including the disruption of gastrulation and neurulation movements, a shortened anterior-posterior (AP) axis, small heads, missing tail structures, perturbed movement of dorsal mesoderm tissue, and shedding of the epidermis following neurulation. Injection of a morpholino targeting both homeologs led to more severe phenotypes than homeolog-specific morpholinos. However, when combining the two morpholinos targeting *pqbp1a* and *pqbp1b*, a severe phenotype was obtained. Therefore, this suggests that the observed effects were in fact due to lowered levels of PQBP1. In addition, these results imply that the two homeologs play largely redundant (but required) roles in the early *X. laevis* embryo (Iwasaki & Thomsen 2014).

In addition to whole embryo injections, more targeted knockdown of PQBP1 was also performed. Dorsal injection of morpholino prevented the formation of the head, and disrupted neural folding and gastrulation movements, in some cases leaving the morphant embryos with an open blastopore. This suggests a function for PQBP1 in

early neural development of the *X. laevis* embryo. The observed defects were partially rescued by the injection of *pqbp1* mRNA (point mutated to confer resistance to the morpholino) (Iwasaki & Thomsen 2014).

The impact of PQBP1 knockdown was further investigated by looking at marker gene expression using *in situ* hybridization. The expression of *chordin*, a dorsal mesoderm marker, was not significantly affected despite the observed perturbation of dorsal mesoderm tissue movement in the morpholino-injected embryos. The pan-mesodermal marker *brachyury* and the neural marker *NCAM* showed a large reduction at injected sites, as did the early marker *sox2* and the neural crest marker *slug* (Iwasaki & Thomsen 2014). Interestingly, it has recently been shown that, in mouse neural stem progenitor cells (NSPCs), *sox2* transcriptionally regulates *pqbp1* (Li et al. 2013).

PQBP1 knockdown was not found to impact BMP, Nodal, or Wnt signaling pathways, but did affect FGF signaling. Fibroblast growth factors (FGFs) are a family of secreted molecules that activate FGF tyrosine kinase receptors. These receptors in turn activate a number of signal transduction pathways, including Ras/MAP kinase and phospholipase-C gamma. Several developmental processes are regulated at least in part by FGF signaling. These include morphogenesis, cell proliferation or migration, differentiation, and patterning (Thisse & Thisse 2005).

qRT-PCR analysis on RNA obtained from morphant embryos showed that expression of *fgf4* and its direct target *cdx4* was lowered by PQBP1 knockdown. This observed reduction of these markers was seen upon injection with any of three PQBP1 morpholinos, and it was rescued upon co-injection of *pqbp1* mRNA resistant to the morpholinos. PQBP1 knockdown in *Xenopus tropicalis* also showed a similar reduction

in *fgf4* and *cdx4* expression, further suggesting that these changes are specifically due to PQBP1 knockdown (Iwasaki & Thomsen 2014).

Given that prior studies showed that PQBP1 influences splicing (Sudol et al. 2012), it was thought that the knockdown of PQBP1 protein levels could affect splicing patterns, specifically those impacting FGF signaling. Since *fgf4* and *fgf8* were found to have splicing variants of different activity (Fletcher et al. 2006; Fletcher & Harland 2008), the impact of PQBP1 knockdown on *fgf4* and *fgf8* splicing was examined first. No difference was seen, although the level of *fgf4* transcript decreased by about 50%, indicating a possible direct or indirect transcriptional effect.

Next, the splicing variants of FGF receptors were studied. FGFRs 1-3 each have two common alternative splice forms (known as b and c variants) that affect their ligand binding affinities (Holzmann et al. 2012). FGFR2 has an exon a-including form (FGFR2IIIb, also known as Keratinocyte Growth Factor Receptor, KGFR), and an exon 8b-including form (FGFR2IIIc, also known as the bek form). These two major isoforms are produced by alternative splicing of the C-terminal portion of the IgIII domain (Mai et al. 2010). The b and c forms are differentially distributed among tissues, with FGFR2IIIb being primarily found in ectoderm-derived tissues as well as endothelial organ linings, while FGFR2IIIc is mostly localized to mesenchyme, including craniofacial structures (Orr-Urtreger et al. 1993). The b form binds to FGFs 1, 3, 7, 10 and 22, while the c form binds to FGFs 1, 2, 4, 6, 8, 9, 17, and 18 (Ornitz et al. 1996). Since the various FGF ligands perform specific functions during early development, any changes in the localization and/or quantity of these splice forms could be expected to impact development. Semi-quantitative RT-PCR was conducted using primers specific to each

Xenopus FGFR2 splice form. This analysis determined that the knockdown of PQBP1 elevated the level of *FGFR2IIIb*, while decreasing the level of *FGFR2IIIc*. Since only the *IIIc* form can respond to FGF4 ligand, it is reasonable to hypothesize that this switching of FGFR2 receptor splice forms can significantly impact the FGF4 response. In addition, partial rescue of *fgf4* expression was achieved in PQBP1 knockdown embryos by the introduction of *FGFR2IIIc* (Iwasaki & Thomsen 2014).

1.2 Overview of Renpenning syndrome

1.2.1 Presentation/clinical features

Even though a number of earlier clinical studies described cases of X-linked mental retardation (XLMR), after 1962 “Renpenning syndrome” became the general term used for both syndromic and nonsyndromic forms of XLMR (Lenski et al. 2004). Hans Renpenning, a medical student, and his coauthors described a family containing 20 mentally disabled males in their 1962 case study (Renpenning et al. 1962). They determined that the defect had appeared in three successive generations, and was likely transmitted in a sex-linked recessive manner. In addition, they stated that, since there were no clear defining physical or biochemical features, the disorder was non-specific, and so performing biochemical tests on the mothers of the affected sons was not advisable (Renpenning et al. 1962).

Later papers further examined families with X-linked intellectual disabilities and refined the description of Renpenning syndrome to include specific clinical features, including microcephaly, microphthalmia, short stature, and small testes in affected

males, with female carriers unaffected (Lenski et al. 2004). Initially, what are now considered variants of Renpenning were defined as separate disorders, including Golabi-Ito-Hall, Hamel cerebropalatocardiac, Porteous, and Sutherland-Haan syndromes. Eventually these syndromes, which share many clinical and genetic features, were united under the term Renpenning syndrome (Stevenson et al. 2005; Stevenson et al. 1998; Archidiacono et al. 1987; des Portes 2013; Lubs et al. 2006; Golabi et al. 1984).

Initially, phenotypic descriptions of Renpenning syndrome patients were obtained from a limited number of case reports, and the descriptions were heterogeneous. In addition, information regarding brain imaging results and behavioral or cognitive observations were rarely included (Germanaud et al. 2011; Stevenson et al. 2005). Recently, a more clearly defined clinical as well as radiological phenotype was described following detailed assessments of 13 French patients with *pqbp1* mutations, from 7 unrelated families (Germanaud et al. 2011). In addition to the already defined symptoms of microcephaly, leanness and short stature, the authors described several new clinical features: progressive muscular atrophy of the upper back, metacarpophalangeal ankylosis of the thumb as well as velar dysfunction. Gyri in the cortex were found to be normal based on MRI imaging of six of the patients. This study helped define the clinical phenotype of Renpenning syndrome, which will aid in future diagnoses of the disorder (Germanaud et al. 2011).

1.2.2 *Pqbp1* mutations and Renpenning

The coding region of *pqbp1* in humans consists of six exons and five introns, and at least five alternatively spliced transcripts have been found (Iwamoto et al. 2000) (see also Figure 15 and Appendix A). These transcripts were uniformly found to retain the WW domain, although much variation was observed in their C-terminal domains. Several transcripts lacked the region required for interaction with polyglutamine tracts, as well as a nuclear localization signal (NLS) (Iwamoto et al. 2000).

A number of different *pqbp1* mutations have been identified in patients with Renpenning syndrome (Figure 2). Duplications, insertions, deletions, and missense mutations have all been linked with the disorder (Tapia et al. 2010; Lubs et al. 2006; Rejeb et al. 2011; Kunde et al. 2011; Musante et al. 2010; Cossée et al. 2006; Martínez-Garay et al. 2007). Symptoms resembling Renpenning syndrome were even observed in the case of a whole-gene duplication (Flynn et al. 2011). It is interesting that, as in the case of animal studies, both a reduced and increased level of PQBP1 in humans may lead to abnormal function.

Nine out of the 13 *pqbp1* mutations known to be involved in Renpenning syndrome (as of 2010) disrupt the AG hexamer in exon 4 (within the PRD domain), leading to frameshifts and premature termination codons (Musante et al. 2010; Martínez-Garay et al. 2007; Kleefstra et al. 2004). At the cellular level, a range of defects is observed related to these mutations. One major category of dysfunction relates to the role of PQBP1 in pre-mRNA splicing. The spliceosomal protein U5-15kD interacts with a YxxPxxVL motif in PQBP1; mutations in this motif prevent this interaction from occurring, presumably disrupting splicing (Mizuguchi et al. 2014). In addition, a mutation

within the WW domain of *pqbp1* reduces the binding ability of the WW domain with proline rich ligands, including the WBP11 splicing factor (Tapia et al. 2010). The protein interaction network of PQBP1 is in fact enriched for splicing regulators and components of the spliceosome complex (Wang et al. 2013). The presence of disease-linked *pqbp1* mutants reduces the association with the splicing factor 3B (SF3B) protein, causing significant changes in alternative splicing patterns. In particular, in neurons, factors involved in neurite outgrowth, such as NCAM, are affected (Wang et al. 2013).

Nonsense-mediated decay (NMD) and nonsense-associated altered splicing (NAS) pathways appear to be involved in the pathology of *pqbp1*-associated disease. Depending on the specific *pqbp1* mutation, levels of *pqbp1* transcripts carrying the mutation tend to be reduced in patients by NMD. However, the amount of reduction ranges widely, with the largest decrease being associated with the most severe clinical phenotype. In addition, the NAS response serves to increase the level of alternatively spliced *pqbp1* transcripts with a premature termination codon. The proteins produced from these transcripts may function in a dominant-negative manner, or demonstrate a gain of function phenotype. Therefore, the clinical manifestations in Renpenning syndrome could conceivably result from a combination of reduced levels of wild-type protein and the presence of truncated protein (Musante et al. 2010).

1.3 Introduction to *Xenopus* and its early development

1.3.1 *Xenopus* as a model system

Since it was first described at the beginning of the nineteenth century, *Xenopus laevis* (and since relatively recently, a related species, *Xenopus tropicalis*) has become one of a handful of “model” organisms used to study development. *X. laevis* originate from Southern and Central Africa, and, due to a number of features, have attained a prominent role in the field of developmental biology. *Xenopus*, which are wholly aquatic, are relatively hardy and easy to maintain in a laboratory setting. As vertebrates, they share many similarities with other vertebrates in terms of cellular signaling pathways and gene function (Dawid & Sargent 1988). In addition, female *Xenopus* can be induced to lay large numbers of eggs year round, and these eggs are relatively large and easy to use for manipulations such as microinjection and microsurgery (Gurdon & Hopwood 2000a). Embryos develop relatively rapidly, and this rate can be controlled to an extent by changes in incubation temperature.

In the 1930s, *Xenopus* became used for pregnancy testing (the “Hogben test”, named after Lancelot Hogben), after it was discovered that the injection of pregnant women’s urine would reliably promote ovulation. By the end of World War II, *Xenopus* colonies could be found in laboratories as well as medical clinics throughout the world. Captive breeding was still considered to be relatively difficult, until it was found that the injection of hormone preparations into both female and male frogs induced coupling and fertilized egg production (Gurdon & Hopwood 2000b; Shapiro & Zwarenstein 1935). This allowed many more researchers to effectively utilize *Xenopus* in their research.

Pioneering researchers such as John Gurdon and Pieter Nieuwkoop demonstrated and expanded the possibilities of *Xenopus* as a model system (Laskey et al. 1977; Gurdon 1971; Nieuwkoop 1977; Nieuwkoop 1973).

Soon, *Xenopus* became the animal of choice for studying induction – interactions between cells or groups of cells that affect their differentiation – and other aspects of embryogenesis. The frog was found to be especially suited for those studies that took place where molecular and developmental biology met. Some areas of study in which *Xenopus* research has played a critical part include the role of localized cytoplasmic elements and inductive interactions in the establishment of embryonic polarity and initial differentiation of tissue, the examination of genes to identify RNA components of the ribosome and how their expression is regulated, and the use of *Xenopus* oocytes in research focused on transcription and translation (Dawid & Sargent 1988). The *Xenopus* system has been part of many “firsts” - the first isolation of a eukaryotic gene, as well as the first studies on gene amplification. It was also used to provide the earliest example of accurate transcription of a cloned eukaryotic gene, as well as the isolation, cloning, and characterization of a eukaryotic transcription factor (Dawid & Sargent 1988).

It should be noted that another major advantage of the *Xenopus* model system is the fact that fate maps for early cleavage stages (particularly useful are the 16 and 32 cell fate maps) are available, and individual blastomeres can be readily identified (Figure 3). This allows for relatively straightforward targeting of specific regions in the developing embryo, making *Xenopus* particularly useful for targeted

knockdown/overexpression experiments (Moody & Kline 1990; Moody 1987b; Moody 1987a).

1.3.2 *Xenopus* early development

In the minutes following fertilization, the *Xenopus laevis* embryo exhibits a contraction of the highly pigmented animal cap, and a densely pigmented region on the ventral side becomes visible. At 22 degrees Celsius, the first three cleavages occur in a two-hour interval. The dorsoventral pigmentation becomes asymmetrical during this time, and this difference is maintained through a number of subsequent divisions (Sive et al. 2000). The cleavages that take place during the first four to five hours postfertilization produce a blastula (stage 7-8 according to Nieuwkoop and Faber's generally accepted staging system) (Nieuwkoop et al. 1995; Nieuwkoop & Faber 1956).

Gastrulation begins around nine hours post fertilization (stage 10) when the blastopore first becomes apparent. At this time, the animal cap is in the embryonic region fated to become epidermis, with the marginal zone having neural and mesodermal fates, and the vegetal yolk mass destined to form endodermal derivatives (Sive et al. 2000). Gastrulation is a highly complex process that takes place over several hours (ending at NF stage 12) (Keller et al. 1992). The result of this process is the movement of mesoderm and endoderm into the embryo, displacing the blastocoel within and forming the archenteron. The appearance of a condensed region of pigmentation on the dorsal side of the embryo marks the first sign of gastrulation. At this time, bottle cells with an endodermal origin elongate, and involution of dorsal marginal zone tissue begins to occur. This involution then extends to lateral tissues and then to

the ventral side of the embryo. Movement of cells from ventral and lateral regions toward the dorsal midline of the embryo leads to elongation of tissues along the anteroposterior (AP) axis. Although it is difficult to define morphological boundaries between germ layers at the start of gastrulation, these can be identified by looking at gene expression domains of markers such as *gooseoid* and *noggin*, which localize to dorsal mesoderm that will later become notochord (Sive et al. 2000) .

Following gastrulation, the developing neural plate becomes increasingly prominent on the dorsal side of the embryo. The neural plate is made up of a flat and thick region of ectoderm destined to form the central nervous system (CNS), with the edges (the region between the neural plate and future epidermis) producing the neural crest (Baker & Bronner-Fraser 1997). Convergence extension movements caused by cell rearrangements in the ectoderm form the neural plate. NF stages 14 through 20 encompass neurulation, which involves folding of the neural plate to form the neural tube (Schoenwolf & Smith 2000).

Organogenesis in *Xenopus* takes place after neural tube closure, and, while it can be challenging to identify particular tissue anlagen (embryonic regions capable of forming specific structures), gene expression studies provide a useful tool to elucidate these regions (Sive et al. 2000).

Xenopus tropicalis development occurs in a manner highly similar to that described above, albeit more rapidly, and often at a higher temperature.

1.3.3 Neural development in *Xenopus*

In vertebrate embryos, neurulation takes place in two phases – primary and secondary neurulation. Amphibians such as *Xenopus* only exhibit primary neurulation, which is the formation of the neural plate and the following morphogenetic movements that produce the neural tube. Although humans have both primary and secondary neurulation, primary neurulation is more clinically significant because, if this process does not occur correctly, neural tube defects such as spina bifida and anencephaly can occur (Schoenwolf & Smith 2000).

There are four stages to the process of primary neurulation: 1) formation of the neural plate, 2) neural plate shaping, 3) bending of the neural plate and neural fold fusion, and 4) closure of the neural groove. The neural plate itself contains pseudostratified columnar epithelium that is formed into a thickened ectoderm. Two kinds of inductive cellular interactions take place to form the neural plate. One of these is vertical interactions between the endoderm and mesoderm underlying the neural plate ectoderm, and the other involves horizontal interactions between the organizer and the neural plate surrounding it (Schoenwolf & Smith 2000).

Ectoderm has the ability to differentiate into either epidermal or neural tissue. On a molecular level, neural induction requires the formation of a BMP gradient involving the secretion of bone morphogenetic protein (BMP) antagonists such as Chordin, Noggin, Follistatin, Cerberus, and XNr3 by the Spemann-Mangold organizer. The organizer is a cluster of cells that can induce the formation of neural tissue (Rogers et al. 2009). It forms in response to signals from a region known as the Nieuwkoop Center, located in the nearby presumptive endoderm. Although the organizer itself forms dorsal

mesoderm, this region signals the bordering regions to adopt a neural fate (Rogers et al. 2009). The factors secreted by the organizer bind to BMPs (such as BMP4 and BMP2) and prevent BMP receptor activation. Knockdown of three of these BMP antagonists (Chordin, Noggin, and Follistatin, or Cerberus, Chordin, and Noggin) leads to a catastrophic failure to generate CNS structures (Khokha et al. 2005; Kuroda et al. 2004).

While BMPs are secreted ventrally (mainly BMP2 and BMP4), dorsal secretion of BMPs such as Admp and BMP7 also occurs, and this can help compensate for a loss of signals from the ventral side of the embryo, while dorsal signaling is prevented by Chordin binding. If both dorsal and ventral BMPs are depleted, ubiquitous neural induction results. Organizer gene transcription occurs when the levels of BMPs are low; conversely, ventral gene transcription takes place in the presence of high BMP levels (De Robertis & Kuroda 2004; De Robertis 2006).

A Wnt/beta-catenin signaling gradient also plays an important role in early neural induction. The Wnt gradient is perpendicular to the BMP gradient, and the combination of both helps define the dorsoventral (DV) and anteroposterior (AP) body axes. Accumulation of the Wnt effector beta-catenin is required for establishment of the Nieuwkoop Center. Canonical Wnt/beta-catenin signals induce neural fate through blocking of *BMP4* transcription in the dorsal ectoderm, as well as by increasing the expression of BMP antagonists. However, later on in embryonic development, Wnt signals switch from a pro-neural to an anti-neural role, encouraging the formation of epidermis rather than neural tissue. The organizer produces the secreted Wnt antagonists Frzb1, Cerberus (which also inhibits BMP4), and Dkk1, which move to the

anterior pole of the embryo during gastrulation. The resulting Wnt/beta-catenin gradient determines the AP polarity of the developing neural plate. It is important to note, however, that the role of Wnt signaling in neural induction may be indirect, rather than direct, and it has been shown that overexpression of a dominant negative form of beta-catenin can inhibit the neural markers *sox2* and *sox3* (Heeg-Truesdell & LaBonne 2006)

Fibroblast growth factor (FGF) and insulin-like growth factor (IGF) signaling are active in neural induction as well. FGF appears to play a role in reinforcing BMP antagonism (Rogers et al. 2009). Ectopic neural tissue is formed from non-neural ectoderm when BMP signaling is inhibited in the presence of FGF. FGF also seems to be specifically required for AP patterning of the neural plate (Gould & Grainger 1997). IGF signaling promotes anterior neural induction by inhibiting both BMP and Wnt signals (Pera et al. 2014).

Neural induction signals are integrated by differential phosphorylation of the Smad1/5/8 transcription factor. Noggin and Chordin function to block the phosphorylation of Smad1 at the C-terminal end. This enables ectoderm to establish a neural fate. High levels of BMP in the ventral region of the embryo, mediated by BMP receptor kinase activation, increase Smad1 signaling and direct the ectoderm to follow an epidermal fate. Mitogen-activated protein kinase (MAPK), upon activation of IGF or FGF receptors, phosphorylates Smad1 in its central linker region. This inhibits Smad1 transcriptional activity, promoting neural induction. GSK3-mediated linker phosphorylation subsequently promotes the ubiquitination and degradation of Smad1, which then terminates the BMP signal. Wnt signaling, on the other hand, inhibits GSK3 and stabilizes Smad1, allowing BMP signaling to continue (Pera et al. 2014). Retinoic

acid and Hedgehog signaling also participate to further promote and refine neural induction.

Following neural induction, many “neural fate stabilizing” (NFS) transcription factors are required in the presumptive neural ectoderm, as well as the developing neural tube and finally in neural stem cells (Rogers et al. 2009). Although many details of how the molecules involved work together to stabilize neural fate are not known, a proposed gene regulatory network of factors involved in neural fate stabilization is shown in Figure 4 (from Rogers et al. 2009).

Many of the required transcription factors are coexpressed in rather broad overlapping domains; for example, mRNAs of *geminin*, *sox3*, *sox11*, and *soxD* are located throughout the dorsal ectoderm at the beginning of gastrulation. Others (such as *foxD5*, *sox2*, *zic1*, *zic2*, and *zic3*) are localized in a broad band in the region of the blastopore lip. Yet others (*Xiro1*, *Xiro2*, *Xiro3*) are found near the blastopore lip, in two dorsolateral bands (Rogers et al. 2009). While the transcripts of some of these factors are of maternal origin, most can be detected around the beginning of gastrulation and through the formation of the neural tube. Although none of these transcription factors appear to have the ability to induce ectopic neural tissue independently, dorsal overexpression through mRNA injection can expand the region of the neural plate (Rogers et al. 2009). While much work still remains to be done before a detailed network of factors involved in *Xenopus* neural development can be defined, the major roles of a number of individual neural transcription factors that appear to be critical players in this process are summarized in Table 1.

1.3.4 A note on the use of morpholinos in *Xenopus* studies

As morpholino antisense oligonucleotides (MOs) are used in many of the experiments conducted in this study, it is important to address the issues surrounding their proper use. Morpholinos are synthetic oligonucleotides that are resistant to degradation. They contain about 25 subunits and incorporate morpholine ring instead of the ribose ring found in DNA and RNA (Eisen & Smith 2008). They can target either mRNA translation or splicing and are generally used to knock down specific target genes. Effectiveness, apparent specificity, and longevity of morpholinos during embryonic development in *Xenopus laevis* as well as *X. tropicalis* were initially documented in GFP-reporter lines (Nutt et al. 2001), where inhibition of GFP translation could be easily seen.

Inhibiting the function of specific genes is a powerful tool in studying the molecular basis of early embryonic development. A number of different techniques to accomplish this are available, including RNA interference (RNAi), the use of antisense RNA, and antisense oligonucleotides (which function by hybridizing to endogenous RNAs and mediating their degradation via RNaseH) (Eisen & Smith 2008). These tools, unfortunately, were generally not very successfully used in *Xenopus* to examine the function of zygotically expressed genes (Eisen & Smith 2008). Morpholinos offered another option for gene expression knockdown in a variety of organisms, initially mainly in frog and zebrafish (Nasevicius & Ekker 2000; Ekker 2000; Heasman et al. 2000). Following the introduction of this technology using these two models, other researchers quickly adapted their use to their individual study organisms, and morpholinos became widely used in *Xenopus tropicalis*, chick, tunicate, mouse oocytes, and sea urchins,

among others (Eisen & Smith 2008; Khokha et al. 2002). There has been some concern, especially in the last year, regarding the specificity of morpholinos (Kok et al. 2014), so this is an important consideration when designing experiments using this tool .

In addition, gene editing technologies involving sequence-specific designer nucleases, such as zinc finger nucleases (ZFNs), transcription activator-like effector nucleases (TALENs) and clustered, regularly interspaced, short palindromic repeats (CRISPR/Cas9) have become available (Maggio & Gonçalves 2015). CRISPR/Cas9 techniques in particular have great potential in creating mutant lines of interest, and both have been shown to function in *Xenopus laevis* and *tropicalis*, as well as a variety of other organisms including zebrafish (Nakayama et al. 2013; Nakajima et al. 2013; Guo et al. 2014; Lei et al. 2012; Wang et al. 2015). These tools can also be used to look at phenotypes in generation 0 (G0) embryos, as shown by a recent study using *X. laevis* (Wang et al. 2015). While the off-target rate for *X. tropicalis* was found to be low, the rate in *X. laevis* has not yet been studied. Although CRISPR/Cas9 appears to be an extremely useful method to use in basic research, it is not ready to be applied in a clinical setting due to mosaicism and a large number of off-target effects, as a recent study using inviable pre-implantation human embryos has shown (Liang et al. 2015). As a whole, all gene knockdown/editing technologies mentioned here could be expected to have some level of off-target effects.

Although many research groups are now primarily using CRISPR/Cas9 for gene knockout, most of the work in this study was conducted using morpholinos (although some preliminary work involving CRISPR/Cas9 has also been done). A number of studies have addressed factors that should be considered when designing an

experiment involving MOs (Eisen & Smith 2008; Bill et al. 2009; Stainier et al. 2015). Essentially, proper morpholino design as well as the use of proper experimental controls should be carefully considered. Going forward, given the technology currently available, it would be prudent to compare any morpholino phenotypes to the observed phenotypes in a null background (for example, through CRISPR/Cas9 knockout). However, this is not always feasible, especially in the short term. CRISPR/Cas9 can result in mosaic effects in G0 embryos, so in this case it would be necessary to first create a mutant line, if viable, to observe the knockout phenotype. In addition, in many cases multiple transgenic reports are required for phenotypic analyses, in which case crossing a mutation into the necessary reporter lines could take a significant amount of time. In these cases, as well as in the case of data already collected (as in this study), researchers should attempt to control for off-target morpholino effects by following several best practices (Stainier et al. 2015).

It is critical to ensure that any morpholino design will affect only the intended gene target; this can be done by conducting a thorough search of the genome to eliminate morpholino designs that bind to other sites (with up to 4 mismatches – 5 mismatches are not expected to bind). With the availability of a relatively complete genome for both *X. laevis* and *X. tropicalis*, a search would be expected to be sufficiently thorough for this purpose. Other important considerations in MO design, such as a GC content of around 50%, are discussed further in Eisen & Smith 2008.

Titration of morpholino amounts should be carefully performed in order to determine the lowest level at which reliable phenotypes are seen, but at which the control morpholino (used alongside the experimental MO in the same amounts) is not

toxic. The importance of using a control morpholino treatment (rather than only uninjected controls) in these experiments cannot be understated, since the physical trauma of embryo injection and the toxicity of introducing a foreign substance (even if not targeted to a specific gene) need to be accounted for. As uninjected embryos tend to develop at a slightly faster rate than injected ones, comparing development without control MO embryos is unreliable for this reason as well. Obtaining a large number of replicates is important since, particularly for smaller embryos, it can be a challenge to inject precise volumes of MO (Eisen & Smith 2008). Fortunately, *Xenopus* embryos are relatively large, and having a large sample size will help equalize any variation.

If possible, the amount of knockdown achieved using a specific morpholino should be documented. This can be somewhat challenging in the case of a translation-blocking MO where a reliable antibody is not available, but can be evaluated if an antibody is available, or in the case of a splice morpholino that would be expected to produce a different-sized splice product (which can then be evaluated on a gel). A full knockdown of a gene product is not necessarily required to produce a phenotype (and in fact may not be desired if knockdown is highly deleterious or lethal), but it is important to understand the level of knockdown in order to interpret the results correctly.

The use of multiple morpholinos (for example, a translation blocking and a splice blocking MO) for the same gene target helps provide confirmation that a phenotype is likely specific, if a similar phenotype is seen for both (with the caveat that a splice MO does not target maternal transcript and so could potentially have a milder phenotype).

mRNA rescue of a MO phenotype is always ideal. Rescue can be performed in different ways; for example, one can look at overall phenotype, markers by RT-qPCR,

expression by *in situ* hybridization, etc. It may be necessary to try several methods of rescue, since, especially in the case of gene products that are specific to small regions within an embryo, it would be difficult to compensate adequately for MO in these areas while avoiding overexpression in others. It can also be challenging to obtain rescue by mRNA injection if the RNA in question has pleiotropic effects (Heasman 2002; Eisen & Smith 2008).

Finally, experimental protocols should always be detailed and clear, so that information such as the frequency and variability of phenotypes is readily available. While the use of morpholinos is not without its concerns, these can be largely alleviated by proper MO design and the use of appropriate controls.

1.4 Figures and Tables

Table 1: Early Neural Determination and Differentiation Genes

Gene	Major Function(s)	Expression	Induction	Knockdown Phenotype	Overexpression Phenotype
<i>NCAM</i>	Cell adhesion; mediator of neurite outgrowth	Early in the neural plate; later in neural tube	<i>Noggin</i>	Defects in morphology of the subventricular zone, olfactory bulb, cerebellum, retina, and hippocampus (mouse)	Intact neural tube formation; morphological abnormalities in organization of epidermis and somites (frog)
<i>Sox2</i>	Promote neural ectoderm competence; neural progenitor maintenance	Expression begins at onset of neural induction, in neural ectoderm only; expressed in retina; expressed throughout CNS development	FGF and Wnt signaling; induced in animal cap explants by <i>Zic1</i>	Diminished neurogenesis in mouse retina, anophthalmia in humans	Loss of neurogenesis in cranial placodes (frog and fish), expansion of neural progenitors in frog and chick neural tube at the expense of epidermal development and neuronal differentiation (frog and chick)
<i>Sox3</i>	Promote neural ectoderm competence; neural progenitor maintenance; antagonizes <i>BMP4</i> signaling pathway	Pan-ectodermal until mid-gastrula, then dorsal ectoderm; strong expression in otic placodes; expressed in developing lens; expressed throughout CNS development	Inhibition of BMP signaling; restricted to neural plate by <i>Vent1</i> and <i>Vent2</i>	Craniofacial abnormalities and abnormal pituitary development (mouse)	Loss of neurogenesis in cranial placodes (frog and fish), expansion of neural progenitors in frog and chick neural tube at the expense of epidermal development and neuronal differentiation (frog and chick)

Continued on next page

Gene	Major Function(s)	Expression	Induction	Knockdown Phenotype	Overexpression Phenotype
<i>Zic1</i>	Promote neural ectoderm competence; increases sensitivity of ectoderm to neural induction by <i>Noggin</i>	Maternally expressed; at early gastrulation, expressed in presumptive neural ectoderm; later restricted to lateral margins of neural plate; dorsal expression in forebrain, midbrain, and hindbrain; likely expressed in immediate response to neural induction (30-60 min after <i>Chordin</i>)	Inhibition of BMP signaling	Cerebellar abnormalities (human)	Expansion of neural plate and neural crest; repression of epidermal fate; activates <i>Nrnp1</i> and <i>Sox2</i> in AC explants; expand expression of bHLH genes involved in neural determination/differentiation (promote transition to neural differentiation) (frog)
<i>Zic2</i>	Promote neural ectoderm competence	Expressed from egg to tailbud stages; at early gastrulation, expressed in presumptive neural ectoderm; later restricted to lateral margins of neural plate; expressed in eye vesicles; dorsal expression in forebrain, midbrain, and hindbrain; likely expressed in immediate response to neural induction (30-60 min after <i>Chordin</i>)	Inhibition of BMP signaling	Neurulation delay, holoprosencephaly, spina bifida (mouse); holoprosencephaly (human)	Expands neural plate and neural crest; represses epidermal fate; represses neural bHLH genes and counteracts the formation of ectopic neurons formed following <i>Ngnr1</i> mRNA injection (may maintain cells in a more immature progenitor state) (frog)

Continued on next page

Continued from previous page

Gene	Major Function(s)	Expression	Induction	Knockdown Phenotype	Overexpression Phenotype
<i>Zic3</i>	Promote neural ectoderm competence	Expression begins at late blastula stages; in early gastrulation, expressed in presumptive neural ectoderm; later restricted to lateral margins of neural plate; dorsal expression in forebrain, midbrain, and hindbrain; likely expressed in immediate response to neural induction (30-60 min after <i>Chordin</i>)	Inhibition of BMP signaling	Left-right abnormalities; less severe neural tube defects (human)	Expands neural plate and neural crest; represses epidermal fate; expand expression of bHLH genes involved in neural determination/differentiation (promote transition to neural differentiation) (frog)

Continued on next page

Continued from previous page

Gene	Major Function(s)	Expression	Induction	Knockdown Phenotype	Overexpression Phenotype
<i>Geminin</i>	Maintain immature neural state by inhibiting reinitiation of DNA replication (preventing cell cycle exit); antagonizes BMP4 signaling pathway; antagonizes the ability of neural bHLH transcription factors (such as <i>Neurogenin</i> and <i>NeuroD</i>) to promote neurogenesis; induces expression of <i>Ngnr-1</i> in ectodermal explants	Maternal expression in animal pole ectoderm; enriched dorsally during gastrulation, then restricted to neural ectoderm (with anterior bias); region of expression wider than those of <i>Sox2</i> or <i>Sox3</i> ; maintained in proliferative regions of developing nervous system	Inhibition of BMP signaling; <i>TCF3</i> (Wnt signaling effector) regulation; <i>Vent1</i> and <i>Vent2</i> restrict expression to dorsal side of the embryo; activation by <i>Sox3</i> and <i>FoxD5</i>	Suppression of neural differentiation; dorsal misexpression produces islands of epidermal gene expression in the neuroectodermal territory (frog)	Inhibition of epidermal development and neuronal differentiation; expansion of neural progenitor population (frog)

Continued on next page

Continued from previous page

Gene	Major Function(s)	Expression	Induction	Knockdown Phenotype	Overexpression Phenotype
<i>FoxD5</i>	Maintain undifferentiated neural ectoderm during early steps of neural plate formation; reduces nuclear localization of BMP signaling effectors, phosphorylated <i>SMAD1/5/8</i> and ventral epidermal expression of <i>BMP4</i> target genes; upregulates the expression of <i>Szl</i> , a secreted BMP antagonist	Maternal transcripts in animal pole; zygotic transcripts more restricted at gastrulation compared to <i>Sox3</i> and <i>Geminin</i> in presumptive neural ectoderm; expression ceases as neural folds elevate and fuse, with the exception of the mid/hindbrain junction and the tail bud	Maternally regulated <i>Stamois</i> pathway via <i>Cerberus</i> (no strong induction by <i>Noggin</i> , and none by <i>Chordin</i>)	Reduced expression of <i>Sox2</i> , <i>Sox11</i> , <i>SoxD</i> , <i>Zic1</i> , <i>Zic3</i> , and <i>Iro1-3</i> at beginning of gastrulation; and <i>Geminin</i> , <i>Sox3</i> , and <i>Zic2</i> by late gastrulation (frog)	Expansion or transient weak reduction of <i>Sox2</i> , <i>Sox3</i> (conflicting studies), expansion of <i>Otx2</i> , <i>Geminin</i> , <i>Zic2</i> expression; repression of <i>Zic1</i> , <i>Zic3</i> , <i>SoxD</i> , <i>Iro1-3</i> ; neural patterning (<i>En2</i> , <i>Krox20</i>) and neural differentiation and neural differentiation (<i>Ngnr-1</i> , <i>NeuroD</i> , <i>N-tubulin</i>) genes (frog)
<i>SoxD</i>	Promote expression of neural determination/differentiation bHLH genes (unique to amphibians)	Detected at late blastula stages in embryonic ectoderm; becomes restricted to dorsal ectoderm during gastrulation	Inhibition of BMP signaling; induced in AC explants by <i>Zic1</i> ; MEK5/ERK5 pathway may be involved	Suppression of neural tissues (not rescuable by <i>Sox2</i>) (frog)	Expansion of neural progenitors; induction of neural determination bHLH gene <i>Ngnr-1</i> ; inhibition of epidermal gene expression (frog)

Continued on next page

Continued from previous page

Gene	Major Function(s)	Expression	Induction	Knockdown Phenotype	Overexpression Phenotype
<i>Sox11</i>	Promote expression of neural determination/differentiation bHLH genes; antagonizes Wnt signaling	Expressed in developing nervous system; induces pan-neural (<i>NCAM</i>) and anterior neural (<i>Otx2</i> , <i>En2</i>) markers by interactions with NLK MAP kinase	Inhibition of BMP signaling by <i>Chordin</i> ; ectopic expression of <i>FoxD5</i>	Weak phenotype (mouse); likely functionally redundant with <i>Sox4</i> and <i>Sox12</i> ; increase in cell apoptosis in eye when knocked down with <i>Sox4</i> (frog)	Associated with mantle cell lymphoma (human); lethal cardiac defects and ectopic bone formation (mouse)
<i>Iro1</i>	Involved in specification of the Spemann organizer, neuroectoderm, mid-hindbrain boundary, and neural crest; activate proneural bHLH genes; likely function downstream of early neural genes but upstream of neural bHLH genes; antagonize <i>BMP4</i> signaling pathway	Restricted bands in neural ectoderm, before earliest expressed neural bHLH genes (<i>Ngnr-1</i> and <i>NeuroD</i>); later in dorsolateral neural tube and neural crest	Weakly by <i>Noggin</i> ; enhanced greatly by posteriorizing factors such as Wnt and FGF; also Hedgehog and retinoic acid signaling	Ectopic <i>BMP4</i> expression; inhibition in expression of preplacodal markers and specific placed markers (neural plate markers not affected)	Expansion of neural plate and onset of neural differentiation; reduction of neural crest; suppression of terminal neuronal differentiation

Continued on next page

Continued from previous page

Gene	Major Function(s)	Expression	Induction	Knockdown Phenotype	Overexpression Phenotype
<i>Iro2</i>	Involved in specification of the Spemann organizer, neuroectoderm, mid-hindbrain boundary, and neural crest; activate proneural bHLH genes; likely function downstream of early neural genes but upstream of neural bHLH genes	Restricted bands in neural ectoderm, before earliest expressed neural bHLH genes (<i>Ngnr-1</i> and <i>NeuroD</i>); later in dorsolateral neural tube and neural crest	Weakly by <i>Noggin</i> ; enhanced greatly by posteriorizing factors such as Wnt and FGF; also Hedgehog and retinoic acid signaling	Induction of <i>Otx2</i> expression; cerebellar structures converted to tectum (chick)	Expansion of neural plate and onset of neural differentiation; reduction of neural crest; suppression of terminal neuronal differentiation
<i>Iro3</i>	Involved in specification of the Spemann organizer, neuroectoderm, mid-hindbrain boundary, and neural crest; activate proneural bHLH genes; likely function downstream of early neural genes but upstream of neural bHLH genes	Restricted bands in neural ectoderm, before earliest expressed neural bHLH genes (<i>Ngnr-1</i> and <i>NeuroD</i>); later in dorsolateral neural tube and neural crest	Weakly by <i>Noggin</i> ; enhanced greatly by posteriorizing factors such as Wnt and FGF; also Hedgehog and retinoic acid signaling	Represses organizer formation (fish)	Expansion of neural plate and onset of neural differentiation; reduction of neural crest; suppression of terminal neuronal differentiation; induces <i>Otx2</i> when expressed in animal cap explants

Continued on next page

Gene	Major Function(s)	Expression	Induction	Knockdown Phenotype	Overexpression Phenotype
<i>Ngnr-1</i> (<i>Ngn2</i>)	Neuronal commitment; activates network of downstream differentiation factors and promotes exit from the cell cycle to allow terminal differentiation; activates Notch-mediated lateral inhibition to restrict the number of cells undergoing neuronal differentiation; induces <i>NeuroD</i> and <i>Ebf2</i>	One of the earliest genes expressed in regions of primary neurogenesis; expressed in discrete patches in dorsal ectoderm at gastrulation; localized to posterior neural plate in three bilateral stripes during neurulation, specifically in trigeminal-profundal placodes; in tail bud embryos localized throughout brain and spinal cord, and in the epibranchial placodes	Notch-Delta lateral inhibition determines density of cells expressing <i>Ngnr-1</i>	Loss of cranial and spinal sensory ganglia and ventral spinal cord neurons (mouse)	Induces ectopic expression of target genes, including <i>Ebf2</i> , <i>Ebf3</i> , and <i>NeuroD</i> ; ectopic neurogenesis
<i>NeuroD</i>	Neuronal differentiation; downstream mediator of <i>Neurogenin</i> activity	Initially expressed in all areas of the brain, spinal cord, peripheral ganglia, and sense organs that express <i>Ngn1</i> , <i>2</i> , or <i>3</i> ; then becomes localized to the cerebellum and hippocampus as the neurons mature	Induced by <i>Ngnr-1</i>	Loss of cerebellar and hippocampal granule cells, inner ear sensory neurons, and retinal photoreceptor cells; other regions do not exhibit gross deficits (mouse)	Premature and more extensive neuronal differentiation in CNS; loss of non-neurogenic cephalic neural crest and expansion of neurogenic cephalic neural crest; induces ectopic <i>N-tubulin</i> expression (frog)

Continued on next page

Continued from previous page

Gene	Major Function(s)	Expression	Induction	Knockdown Phenotype	Overexpression Phenotype
<i>Coc2 (Ebf2)</i>	Stabilizes process of neuronal differentiation; helps maintain or increase pro neural gene expression (can activate <i>Ngnr-1</i> and <i>NeuroD</i>)	Precursors of primary neurons after <i>Ngnr-1</i> but before <i>NeuroD</i>	Induced by <i>Ngnr-1</i>	Defective neuronal migration (mouse); prevention of neuronal differentiation (frog)	Ectopic expression of neuronal-specific markers such as <i>N-tubulin</i> (frog); ectopic differentiation of neurons in both neural plate and epidermis (frog)
<i>Ebf3</i>	Functions during later stage of neuronal differentiation; expressed in three stripes of primary neurons after <i>NeuroD</i> ; reinforces <i>Ngnr-1</i> expression and may also target <i>NeuroD</i>	Differentiating neurons in mantle layer of neural tube; expression and activity are resistant to lateral inhibition	Direct downstream target of <i>NeuroD</i>	Defects in axonal pathfinding of thalamocortical and olfactory receptor neurons (mouse); pathfinding defects of motor neurons (<i>C. elegans</i>)	Induces neurogenesis but does not impact <i>NeuroD</i> , <i>Ngnr-1</i> or <i>Ebf2</i> expression; ectopic expression of <i>N-tubulin</i> (frog)
<i>N-tubulin (Tubb2b)</i>	Primary neurogenesis; required for proper neuronal migration	Postmitotic, differentiated neurons	Downstream of <i>NeuroD</i>	Bilateral asymmetrical polymicrogyria (human); neuronal migration impairment (rat); lethality and abnormal cortical development (mouse)	Ectopic neurogenesis (frog)

Continued on next page

Continued from previous page

Gene	Major Function(s)	Expression	Induction	Knockdown Phenotype	Overexpression Phenotype
<i>Pax6</i>	Lens placode formation; oculogenesis	Presumptive anterior neural plate at late gastrula stage; later, in presumptive lens ectoderm	Response to neuralizing factors such as <i>Noggin</i> , <i>Chordin</i> , <i>Follistatin</i>	Aniridia (human); anophthalmia, CNS defects and lethality, iris hypoplasia and corneal, lens, and retinal defects (mouse); underdeveloped iris, cataracts, corneal defects, severe eye abnormalities and changes in brain development (frog)	Ectopic eye development (Drosophila and frog)
<i>Otx2</i>	Promotes cement gland formation; prevents cells from performing convergent extension movements; promotes bipolar cell fate in frog retina; required for anterior olfactory, lens, and trigeminal character	Dorsal bottle cells during gastrulation; fore/midbrain; later in presumptive cement gland territory	Combination of low levels of <i>FGF8</i> together with Wnt- and BMP-antagonists	Lens, olfactory, inner ear defects (mouse); absence of forebrain and midbrain regions (mouse); missing cement gland and other head structures (frog)	Anteriorized embryos with gastrulation defects; formation of ectopic cement glands (frog); overexpression found in medulloblastoma cell lines (human)
<i>XAG1</i>	Promotes cement gland formation/differentiation	Extreme anterior ectoderm (cement gland region and hatching gland region)	Activated by <i>Otx2</i> (indirectly) and others	Improper cement gland formation	Ectopic hatching gland and cement gland cell expression (frog)

Continued on next page

Continued from previous page

Gene	Major Function(s)	Expression	Induction	Knockdown Phenotype	Overexpression Phenotype
<i>En2</i>	Repels axons originating from the temporal retina; attracts nasal axons; topographic map formation in vertebrate visual system	Midbrain/hindbrain boundary	Wnt, <i>Pax2/5</i>	Reduction in size of cerebellum (mouse); deficits in social behavior (mouse); absence of midbrain and upper pons (human); blocked turning responses of nasal and temporal growth cones (frog)	Increased cell cycle exit and neuronal differentiation (mouse)
<i>Cbfa2i2</i> (<i>XETOR</i>)	Inhibitory factor for primary neurogenesis; helps regulate the size of pro neural domains at later stages (thus helping to define the correct number of primary neurons)	Neuronal territories; three bilaterally symmetrical stripes at each side of dorsal midline	Pronеural genes (such as <i>Ngnr-1</i> and <i>NeuroD</i>)	Expansion of <i>N-tubulin</i> expression domain without change in neuron density (frog)	Represses expression and activity of downstream pro neural genes, including <i>NeuroD</i> , but does not affect <i>Ngnr-1</i> expression; inhibits <i>Delta1</i> expression (frog)
Concluded					

Compiled from: Altmann et al. 1997; Anderson 1995; Andreatzoli et al. 1997; Gammill and Sive 1997; Arresta et al. 2005; Baker and Bronner-Fraser 1997; Bang et al. 1997; Bellefroid et al. 1998; Vernay et al. 2005; Bertrand et al. 2000; Brunet et al. 2005; Cavodeassi et al. 2001; Chang and Hemmati-Brivanlou 1998; Cheh et al. 2006; Delaune et al. 2005; Dubois et al. 1998; Dubrulle and Pourquié 2004; Eisaki et al. 2000; Ellis et al. 2004; Fletcher et al. 2006; Gammill and Sive 2001; Glavic et al. 2004; Green and Vetter 2011; Halder et al. 1995; Hansen et al. 2008; Holowacz and Sokol 1999; Hongo et al. 1999; Jaglin et al. 2009; Kenyon et al. 2001; Kintner 1988; Kintner and Melton 1987; Yellajoshiyula et al. 2012; Seo et al. 2007; Kroll et al. 1998; Lamb and Harland 1995; Lee et al. 1995; Mancini et al. 2013; Martha et al. 1995; McMahon and Merzdorf 2010; Nagai et al. 2000; Nakata et al. 1998; Nakayama et al. 2015; Nishida et al. 2003; Ono et al. 1994; Pozzoli et al. 2001; Rabinowitz et al. 1996; Rebsam and Mason 2008; Rogers et al. 2009; Rossman et al. 2014; Sarnat et al. 2002; Sato et al. 2005; Singh et al. 2002; Steventon et al. 2012; Stottmann et al. 2013; Sugiyama et al. 2009; Tzoulaki et al. 2005; Wardle et al. 2002; Xu and Li 2010; Yan et al. 2009; Zuber et al. 2003

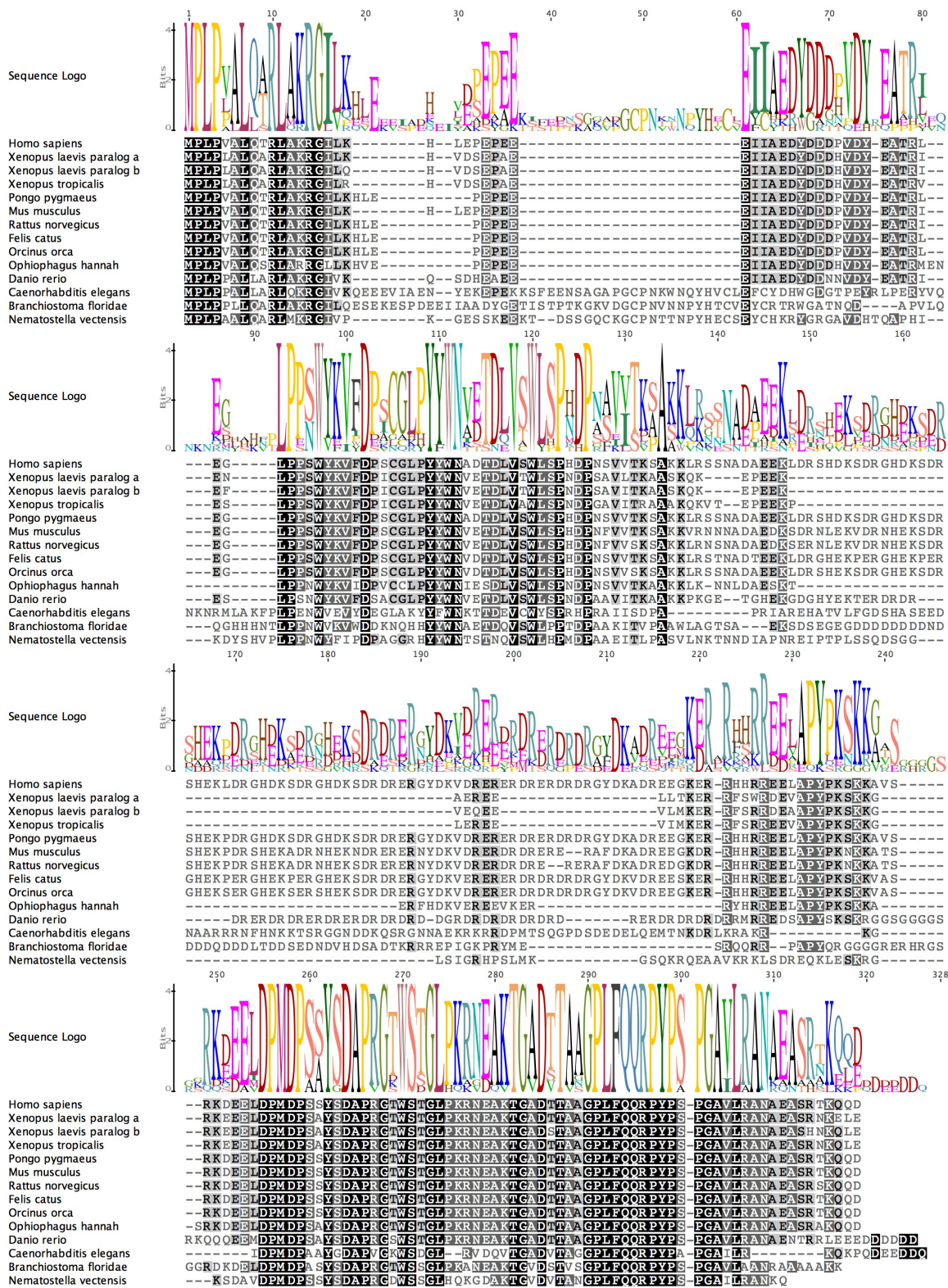


Figure 1: Evolutionary conservation of PQBP1 protein sequences among Metazoa. Alignment was performed using Geneious software (version 6.1.7) using the MUSCLE algorithm. Sequences were obtained from NCBI databases. Darker boxes indicate higher levels of conservation among species shown.

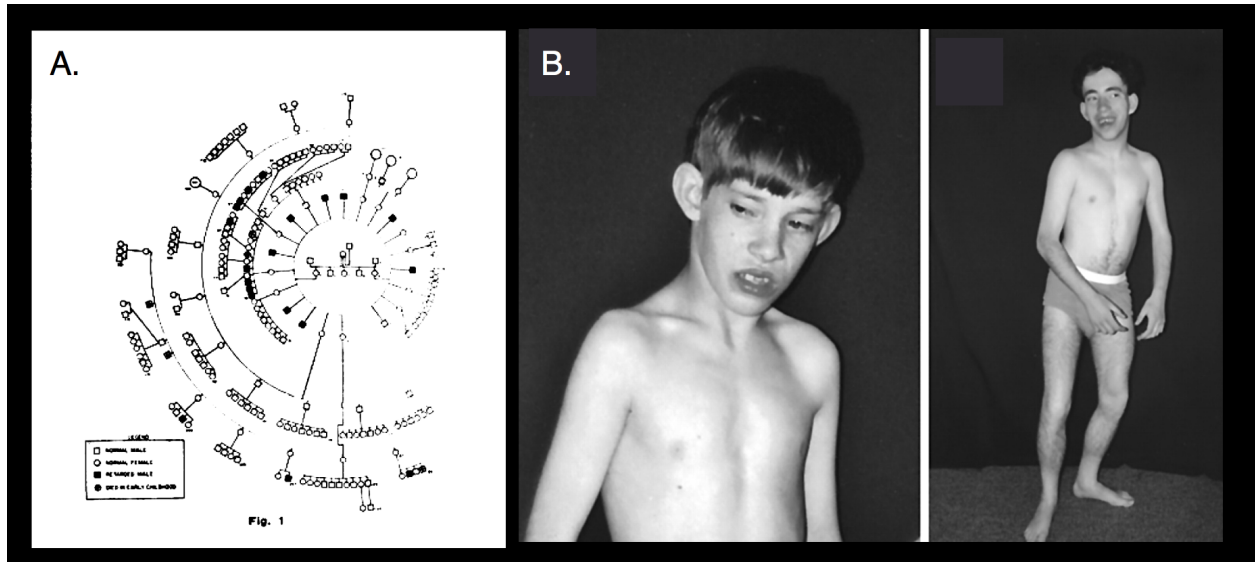
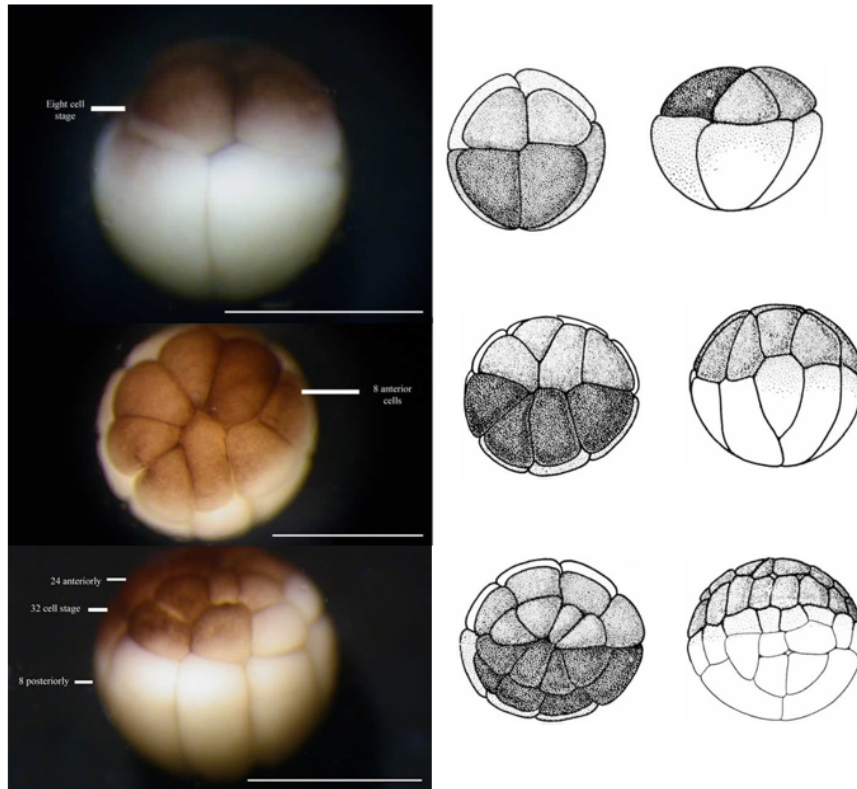


Figure 2: Renpenning family pedigree and characteristic phenotype. A. Family pedigree from the original paper describing Renpenning syndrome (Renpenning et al. 1962). B. Renpenning syndrome patient showing characteristic clinical features (Lubs et al. 2006).



Stage	blastomere b2		contributes to:		
32-cell	animal	dorsal	major:	moderate:	minor:
ventral		dorsal	dorsal brain, spinal chord, neural crest	retina, cranial ganglia, lens, otocyst, head epidermis	
			central somite	branchal arch, head somite	notochord
				pharynx, foregut, archenteron roof	ventral hindgut
	vegetal		mapping data based upon Moody (1987)		

Figure 3: Photographs and drawings of 8, 16, and 32 cell stage embryos, showing the clearly defined blastomeres. A sample fate map of one blastomere in a 32 cell stage embryo is shown on the bottom.

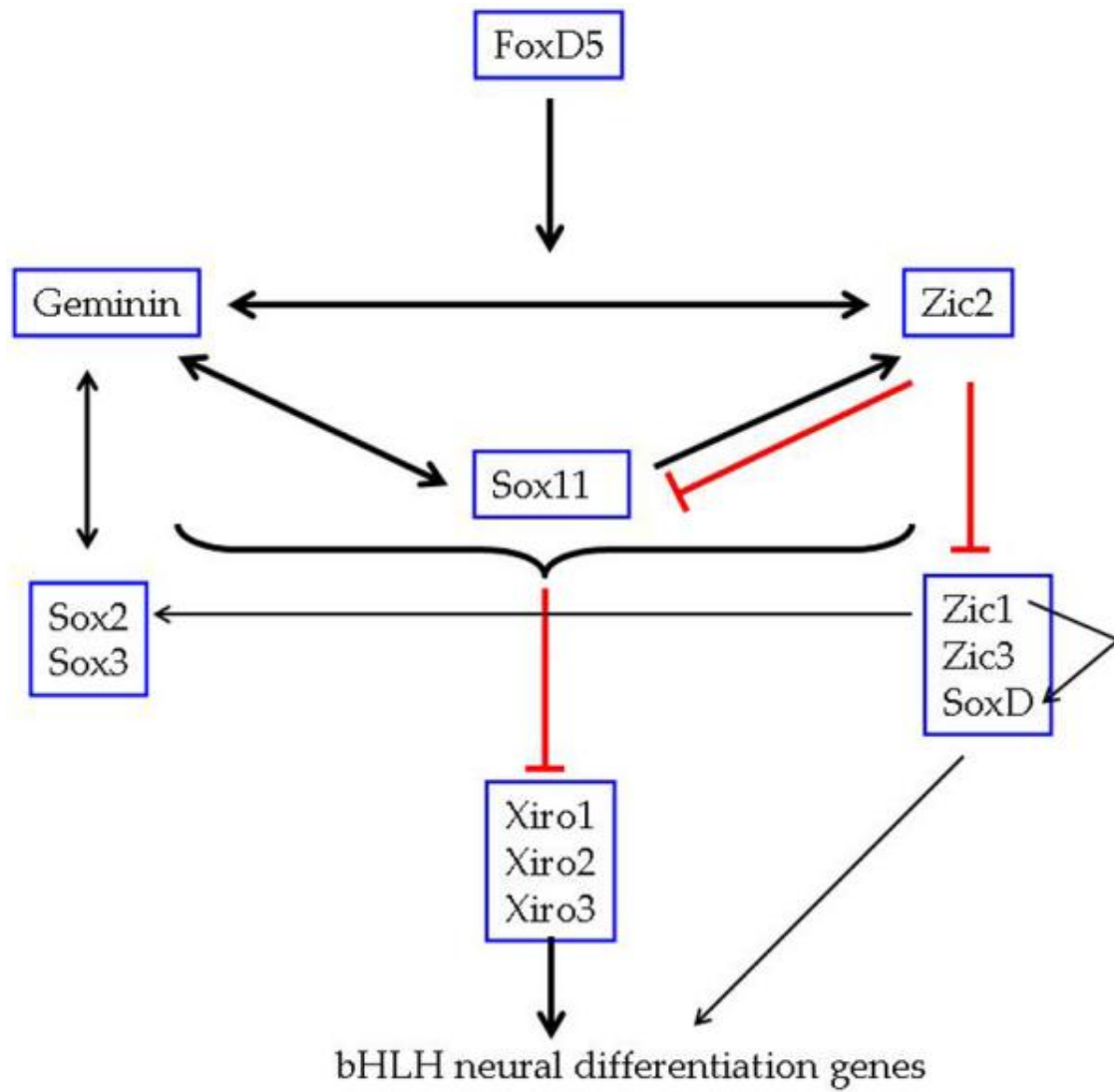


Figure 4: A proposed gene regulatory network involved in the stabilization of neural fate. (From Rogers et al. 2009)

Chapter 2: *pqbp1* expression is largely localized to neural-fated regions in tailbud stage embryos

2.1 Introduction

Our current body of knowledge clearly shows that *pqbp1* mutations are causative of disorders involving early developmental phenotypes (neural and otherwise), and that PQBP1 is also involved in neurodegenerative disorders. However, many questions remain regarding how the PQBP1 protein functions, both in normal and disease contexts. This work aims to elucidate the mechanism(s) by which PQBP1 is helping to regulate early nervous system development, and the first goal was to determine, in more detail, where *pqbp1* is expressed during early neural development in the *Xenopus* embryo.

Prior work in the Thomsen lab defined the expression patterns of *pqbp1* during relatively early developmental stages (up to early tailbud stages) (Iwasaki & Thomsen 2014). Tailbud stages in *Xenopus* range from Stages 22-44 (Nieuwkoop & Faber 1956; Whetzel et al. 2011). During these stages, neurulation is completed and tail formation begins. Feeding begins at Stage 44, the end of the tailbud stages.

Following up on what is already known, I performed *in situ* hybridization using *pqbp1* probe and examined whole embryos as well as head sections at later tailbud stages in an attempt to define more precise regions of expression. The localization of *pqbp1* expression could provide clues as to where PQBP1 might be acting during the development of neural structures.

2.2 Results

2.2.1 *Pqbp1* expression in tailbud stage whole embryos

Figure 5 shows *pqbp1* expression in early-to-mid tailbud stages. *Pqbp1* expression is seen throughout the head and brain region, but appears to be especially strong in the branchial arches, ear vesicle, optic vesicle, and olfactory placode (Figure 5B). Expression is also observed in the spinal cord, although the intensity of the staining appears to diminish at later tailbud stages.

2.2.2 *Pqbp1* expression in tailbud embryo head sections

Figure 6 shows sections of whole mount *in situ* embryos stained for *pqbp1* expression. Transverse sections at the level of the midbrain show high levels of expression in the brain (mesencephalon), with lower levels in the developing lens. Some expression is also observed in epidermis in both the midbrain and mid-body sections.

2.3 Discussion

The results of these experiments are consistent with what was already known about *pqbp1* expression (Iwasaki & Thomsen 2014); in addition, the regions of expression in tailbud stages are further defined. In whole embryos, the ear vesicle, optic vesicle, olfactory placode, and branchial arches exhibit concentrated staining. More

diffuse staining is seen throughout the head region. During the course of embryonic development, the amount of expression in the spinal cord appears to diminish; in NF Stage 34 tailbud embryos (as in Figure 5D) it is barely visible. Interestingly, based on the sections made from NF Stage 33-34 embryos, expression in the head region appears to be largely localized to the brain itself (mesencephalon in these sections) as well as the developing lens and epidermal ectoderm. These regions of *pqbp1* expression allow for a wide range of effects on neurogenesis, neuronal migration, and other aspects of early brain development.

Pqbp1 is expressed in a number of cranial placodes, such as the olfactory, otic, and lens placodes, or their derivatives. Placodes are specialized regions of embryonic ectoderm that can give rise to a variety of non-epidermal cell types such as neurons, glia, and secretory cells (Schlosser 2006). All placodes appear to originate from a common primordium located around the neural plate, and they share properties such as proliferative ability, the capacity for morphogenetic movements, and neuronal differentiation (Schlosser 2006).

The olfactory placode in *Xenopus laevis* is known to send nerve projections to three different parts of the developing brain – the telencephalon, diencephalon, and myelencephalon. Removal of the placode after NF Stage 41 led to a loss of olfactory organs in addition to hypoplasia of both the olfactory bulb and the telencephalon (Graziadei & Monti-Graziadei 1992; Stout & Graziadei 1980). Therefore, the olfactory placode contributes to the final structure of anomalous brain regions, and, therefore, a disruption in proper neuronal development in this region could be expected to influence overall brain function.

The otic vesicle, derived from the otic placode, is an invagination of neural ectoderm, which develops into inner ear structures. It can give rise to a variety of cell types, including support cells, hair cells, sensory epithelial cells, as well as neurons (including the auditory and vestibular neurons) (Appler & Goodrich 2011). Again, as in the case of the olfactory placode, a perturbation in otic vesicle formation and differentiation could lead to defects in brain or sensory function.

The lens placode, unlike the majority of cranial placodes, is non-neurogenic, possibly due to a downregulation of *Ngnr-1* in the prospective lens ectoderm (Schlosser & Ahrens 2004) . It produces the lens vesicle by invagination, and the lens vesicle subsequently produces crystallin-accumulating cells that comprise the mature lens. Since *Ngnr-1* downregulation is needed for proper lens development, any impact on *Ngnr-1* levels during early development would be expected to perturb proper eye formation.

It is possible that additional placodes, such as the epibranchial or lateral line placodes, which are located near the branchial arches, also show higher levels of *pqbp1* expression; however, additional sectioning would be required to confirm this, since there is at least diffuse staining in this entire region.

2.4 Future Directions

In order to extend our knowledge of the precise regions of *pqbp1* expression, it would be useful to repeat the whole mount *in situs* on a time course of tailbud stage embryos. By collecting embryos from a larger number of stages between NF Stages 22

and 44, it would be possible to determine any temporal shifts in overall expression that may be developmentally relevant. It is possible that whole mount *in situ* on late tailbud stage embryos will exhibit high levels of background staining (this was observed in preliminary tests using the same *pqbp1* probe. This might necessitate the optimization of either the *in situ* protocol or the probe used. Alternatively, much of the same information could be obtained from section *in situ*.

As we know that *pqbp1* is expressed in the developing *Xenopus* brain, conducting *in situ* on isolated brains would be warranted. This would provide more precise information regarding brain regions that may be particularly susceptible to *pqbp1* activity. Doing a time course as with the whole mount *in situ* would provide complementary information regarding what is happening to the overall embryo and specifically brain tissue during the same development time periods. If transverse section *in situ* covering most of the embryo could be obtained, this would also expand our understanding of expression regions, not just in neural tissue, but also in additional anatomical regions which may be hard to define in the whole mount *in situ* embryos. Section *in situ* of the isolated brain may also be informative.

2.5 Materials and Methods

2.5.1 mRNA probe synthesis and whole mount in situ hybridization

In situ hybridization was performed on MEMFA-fixed embryos using digoxigenin-labeled probes as previously described (Harland 1991). BM purple (Roche) was used as the chromogenic substrate. Embryos were incubated with BM purple at 4 degrees to

minimize background. Template plasmids used for probe generation were pCS-*pqbp1* and pXT1-*brachyury*, as described in prior work (Iwasaki & Thomsen 2014).

2.5.2 Embryo paraffin embedding and sectioning

Embryos were embedded in Paraplast, using a modified published protocol (Protocol 14.1.in Sive et al. 2000). The following modifications were made: Embryos in fixation buffer (4% PFA in 1X phosphate buffered saline (PBS) were rinsed with 1x PBS rather than a sucrose solution, and xylene was used rather than a xylene substitute. Sectioning was performed as described in the published protocol. Sections were cut to 8 μm thickness. No additional staining was performed following sectioning.

2.6 Figures and Tables

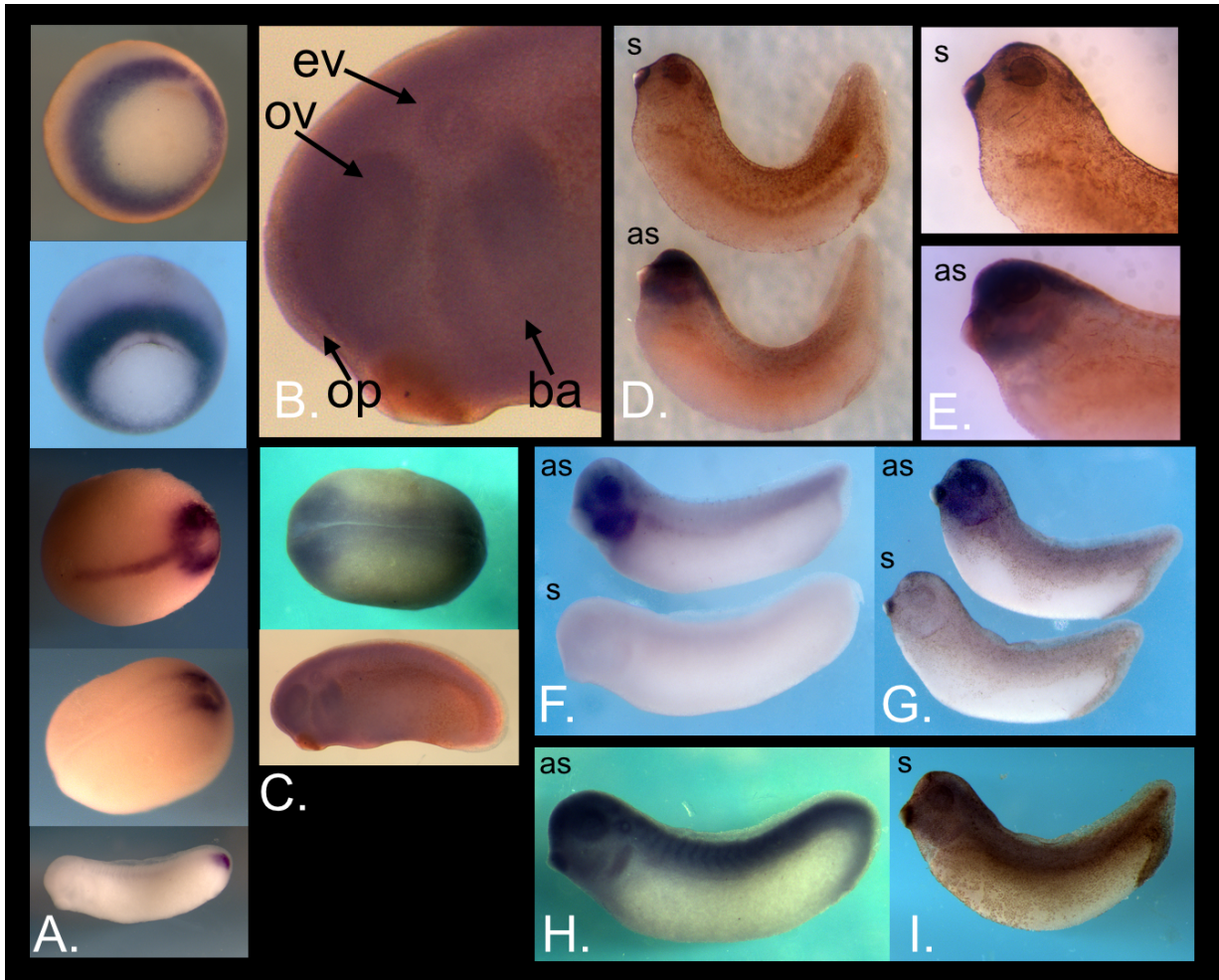


Figure 5: *Pqbp1* expression in whole embryos. A. *Brachyury* expression controls. B. Closeup of head showing staining of the ear vesicle (ev), optic vesicle (ov), olfactory placode (op) and branchial arches (ba) (same embryo as in C (bottom)). C. *pqbp1* expression in NF Stage 22 (top) and Stage 24 (bottom) tailbud embryos. D-E, F-G, and H-I. Replicates of *pqbp1* staining in NF Stage 29-34 embryos, showing staining in head regions and spinal cord. Spinal cord staining appears to diminish in later tadpole stages (see D compared to H). Note that the closeups in E. are of the same embryos shown in D. s = sense, as = antisense

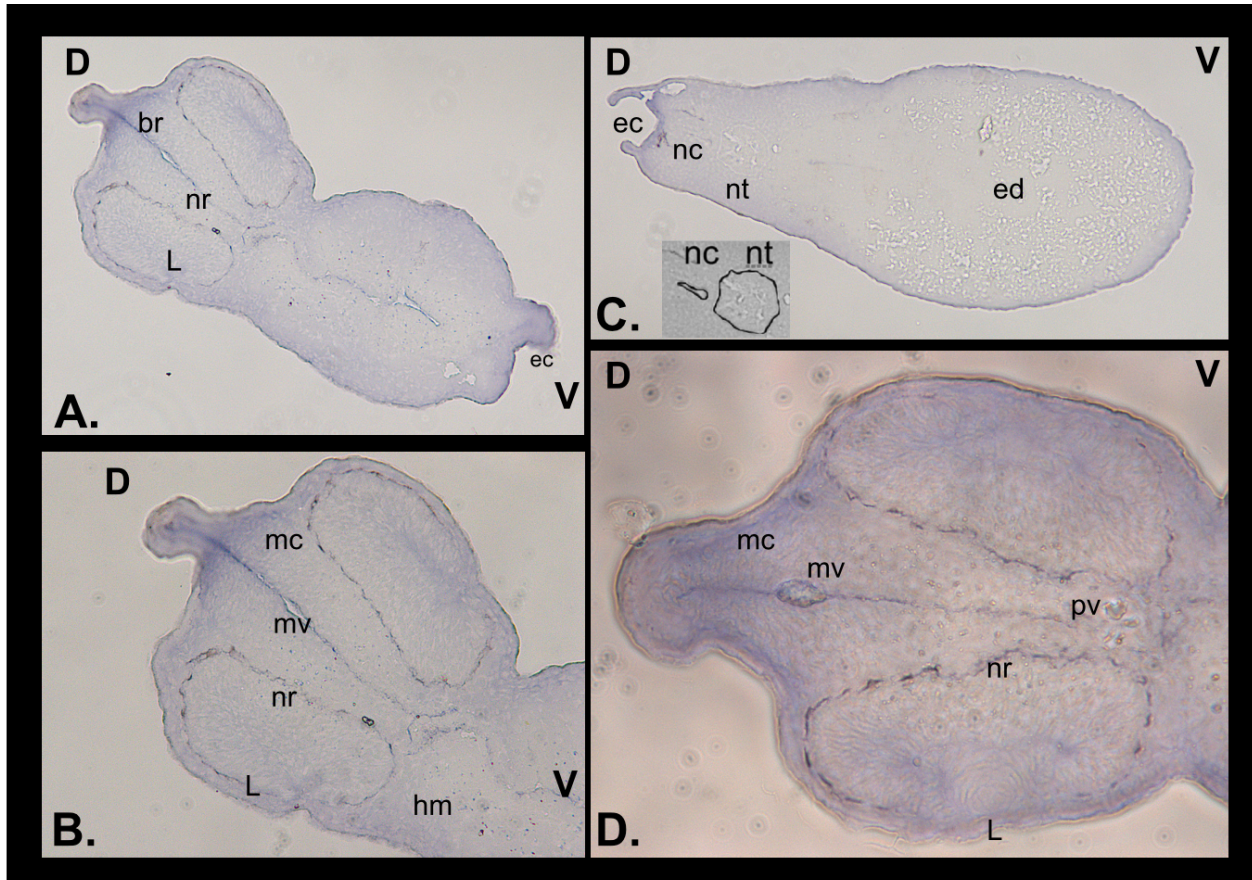


Figure 6: Sections of *pqbp1* whole mount *in situ* embryos at NF Stages 33-34. A. Transverse section at the level of the midbrain. B. Closeup of the developing eye region in A. C. Transverse section at the mid-body level of the same embryo shown in A and B (inset shows closeup of the notochord and neural tube region, with key features outlined). D. Transverse section at the midbrain level of another embryo, with additional features detailed. D = dorsal, V = ventral, br = brain, nr = neural retina, L = lens, ec = ectoderm (epidermal), nt = neural tube, nc = neutochord, ed = endoderm cells, mc = mesencephalon, mv = mesencephalic ventricle, pv = prosencephalic ventricle.

Chapter 3: PQBP1 is essential for normal embryo development

3.1 Introduction

Prior work in the Thomsen lab (Iwasaki & Thomsen 2014) demonstrated that knockdown using PQBP1 translation blocking (ATG) morpholino can cause gastrulation and neurulation defects in both *Xenopus laevis* and *Xenopus tropicalis* embryos (Figure 2). These defects were partially rescuable by coinjection of *pqbp1* mRNA. In order to further investigate the function of PQBP1 in the developing embryo, I first conducted knockdown and overexpression experiments to determine if they worked in my hands. In addition, a different set of optimized morpholinos (MOa and MOb, as described in Materials & Methods) were used here than the one used in most of the previously published phenotypic analysis, so it was necessary to confirm that comparable phenotypes were obtained (Iwasaki & Thomsen 2014). In addition, phenotypes were recorded in detail and rescue using morpholino-resistant *pqbp1* mRNA was attempted in several different ways.

Since translation blocking (ATG) morpholinos inhibit translation of both maternal and zygotic transcripts, they would be expected to have a greater effect than splice morpholinos on the knock down target. Since embryos injected into all blastomeres with PQBP1 ATG morpholinos died prior to finishing neurulation or lacked all head structures, it was not possible to observe specific neural defects using this morpholino. In order to focus on neural tailbud stage phenotypes, I switched to using a splice morpholino for the majority of these experiments. Translation of the in vitro transcribed *pqbp1* mRNA was confirmed using western blot (Figure 7), and I determined that the

expected alternatively spliced product was present in knock down embryos (Figure 8). Since the effects of the splice MO were indeed milder than that of the ATG MOs, I was able to make relevant observations of later tailbud stage embryos.

In addition to targeting the entire embryo, neural-fated blastomeres were individually targeted at the 4-8 cell stage in order to reduce the effects on other tissues. These embryos were observed into mid-tailbud stages for phenotypic changes, and phenotypic rescue was completed.

3.2 Results

3.2.1 PQBP1 knockdown and overexpression cause gastrulation and neurulation defects

Injection of ATG morpholino into whole embryos produced both gastrulation and neurulation defects (Table 2). Although knockdown embryos generally survived into neurulation, those injected with *pqbp1* mRNA often showed a high rate of nonspecific death by gastrulation (NF Stage 10.5). The survival rate appeared to depend largely on the embryo batch injected (batches in which overall survival among treatments was low were excluded from analysis). In some batches, embryos injected with the same amount of *pqbp1* mRNA (0.5 ng) did not show an obvious phenotype (mRNA from the same in vitro transcription reaction was used throughout). In the case where high death rates in the mRNA-injected embryos were observed, the survival rate was rescuable by co-injection of PQBP1 ATG morpholino in a statically significant manner (Table 2).

In cases where the mRNA did not have a lethal effect at early developmental stages, the “rescue” conditions (Tables 3 and 4) appeared to have an additive deleterious effect at both NF Stage 15 and NF Stage 23. The phenotype observed in these embryos by NF Stage 23 was generally a cessation of development around the start of neurulation, followed by cell dissociation. Figure 9 shows representative phenotypes of embryos in one of these experiments. While the *pqbp1* mRNA injected embryo looks phenotypically normal, both of the “rescue” conditions demonstrate a more severe phenotype than the PQBP1 ATG MOs alone.

*3.2.2 PQBP1 knockdown impacts proper elongation of the *Xenopus* body axis*

Embryos injected into both dorsal blastomeres with PQBP1 splice MO at the 4 cell stage survived past neurulation but appeared less elongated than corresponding control MO-injected embryos (Figure 10). This difference in body axis length was quantified relative to the average of the controls (Figure 11). The length difference between the two groups was statistically significant (Table 5). In addition, the range of body lengths was greater in the knockdown embryos.

3.2.3 Targeted PQBP1 knockdown results in eye and anterior head defects

Embryos injected with 25 ng total PQBP1 splice morpholino into two dorsal blastomeres at the 8 cell stage or one dorsal blastomere at the 4 cell stage showed a range of eye and anterior head defects (Figure 12 shows representative phenotypes). Approximately 35% of knockdown embryos were wild type in appearance, but the remainder (with the exception of a few “deformed” embryos that showed nonspecific

phenotypes) had either reduced or missing eyes. The eye phenotype was partially rescuable; embryos injected with *pqbp1* mRNA along with the splice MO largely recovered wild-type eye phenotypes (5 experiments are summarized in Table 6). Embryos in which *pqbp1* was overexpressed also showed phenotypes, with a number of embryos having reduced eye structures or a nonspecific deformed appearance (usually involving a twisted body).

Table 7 shows the phenotypic range observed in three of the experiments conducted. Data from these experiments were used to generate Figure 13, which shows a partial recovery of the wild-type phenotype in the rescue conditions. This stacked bar graph clearly shows that both overexpression and knockdown of PQBP1 can cause similar phenotypes, although in different proportions. In Figure 14, the data from five rescue experiments were grouped into wild type and abnormal phenotypes by control, splice MO, and rescue condition. This shows that the wild-type phenotype was rescuable by mRNA co-injection at a highly statistically significant level.

The level of *pqbp1* mRNA required for optimal rescue varied among experiments, possibly due to the fact that different embryo batches appeared to respond either more strongly or weakly to the mRNA.

3.3 Discussion

The first set of experiments, involving use of the ATG morpholino to observe phenotypes and attempt a rescue, show that the two morpholinos used here recapitulate the phenotypes observed in prior studies by the Thomsen lab (Iwasaki &

Thomsen 2014). In addition, rescue of the survival rate was possible by co-injection of *pqbp1* mRNA, although in some batches of embryos the mRNA did not lead to a distinguishable phenotype.

This variation was not due to the use of different sets of mRNA, since all experiments used mRNA generated in the same in vitro reaction. It also could not be due to mRNA degradation over time, as the same aliquots that did not produce a phenotype when injected sometimes led to high rates of death when injected into later embryo batches. Changes in needle size, calibration, or injection site are unlikely culprits since the same level of “noise” was not seen in the other treatments. Therefore, I would hypothesize that the variation could be largely due to the inherent differences in embryo health among batches. Although perhaps less likely, it cannot be ruled out that variation is caused partially by genetic differences among frogs; not, as can be the case with a morpholino, because of variation in the target sequence, but rather because of other factors that may impact the ability of the mRNA to be translated or of the protein to interact with its targets or binding partners (Waldman et al. 2011). In addition, environmental factors such as stress and temperature have been shown to affect translation efficiency; since embryos can be kept at a variety of temperatures during development (generally from 16-22 degrees Celsius) this could have had an impact as well (Huch & Nissan 2014; Rodnina et al. 2011). Any changes due to genetic differences could be minimized by utilizing J-strain frogs, an inbred strain in which genetic variation is greatly reduced.

Data from the splice morpholino injection experiments show that, when only zygotic *pqbp1* transcript levels are knocked down in both dorsal blastomeres of a 4cell

stage embryo, embryos can survive past neurulation and develop at least partial head structures. The body axis in knockdown embryos was significantly shorter than in control embryos. Since similar morphogenetic movements are involved in convergent extension (CE) of both mesoderm as well as overlying neural ectoderm in the posterior neural plate, the observed elongation defect could be due to a change in either or both of these factors (Wallingford & Harland 2001). However, inhibition of mesoderm CE tends to produce a shortened, but straight, body axis, while inhibition of neural ectoderm CE usually leads to a bent body axis. Therefore, it is likely that the change seen in these *pqbp1* knockdown embryos is due to mesodermal effects.

Embryos injected into single blastomeres at the 4 cell stage or two dorsal blastomeres at the 8 cell stage showed clear phenotypic differences between the injected side and the control side of each individual embryo. Injection of PQBP1 splice morpholino at a higher concentration in this more restricted region showed fewer elongation defects but consistent eye phenotypes (Figure 14). Approximately 64% of embryos exhibited either reduced or missing eye structures. In addition, many of these embryos also had reduced anterior head structures. This suggests that PQBP1 has a function in the proper development of the eye field. In addition, since the level of properly spliced *pqbp1* was reduced only moderately in knockdown embryos, even a relatively modest change in levels of PQBP1 could be expected to have a significant impact on proper neural development in these regions. Although there is a significant mesodermal component to the cells that help structure the eye, the complete lack of visible eye structures implies that neural tissue is involved, either independently of or in conjunction with mesoderm. Interestingly, *pax6*, a homeobox gene that functions as a

master regulator of eye development, was shown to consistently be expressed in an expanded region in knockdown embryos. This observation will be further addressed in Chapter 5.

Interestingly, almost 20% of embryos injected with *pqbp1* mRNA (700 pg) also had clear eye defects. Given what we know about the levels of PQBP1 required in cells, it is reasonable that both overexpression and knockdown would produce similar phenotypes (Okuda et al. 2003; Tamura et al. 2013; Ito et al. 2009). Therefore, it is very possible that the level of PQBP1 inside cells is very tightly regulated. Perhaps this is why it was difficult to determine a consistent amount of mRNA and morpholino that would produce a robust rescue. Figure 13 shows that a partial rescue of the wild-type phenotype relative to the morpholino only treatment is obtained – these data represent equal amounts of mRNA injected into each rescue embryo (3 experiments total). When the data from 5 experiments, utilizing the most effective rescue condition for each experiment, are combined into wild-type and abnormal groups, a more robust, highly statistically significant rescue is obtained (Figure 14). These data demonstrate that a rescue can be obtained, but the exact amount of mRNA required for an optimal response varied from one embryo batch to another.

3.4 Future Directions

Although an incorrectly spliced form of *pqbp1* is seen on the gels in Figure 10, there are several additional higher bands present. This could be due to an issue with the primer, so it would be beneficial to order additional primers and/or perform additional

PCR optimization to obtain a clearer quantitation of the reduction in correctly spliced *pqbp1*.

It would be highly informative to utilize CRISPR/Cas9 to produce knockdown F0 embryos for further experimentation. It may be impossible to establish a knockout mutant line, since *pqbp1* knockout was found to be lethal in mice (Okuda et al. 2003) and knock down experiments in *Xenopus* via ATG morpholino (this and prior work from the Thomsen lab) show that many embryos do not complete neurulation or have major head defects if they do. However, it would be possible to observe F0 embryos, which could later be genotyped to determine the efficacy of knockdown. In addition, newer CRISPR technology is making gene replacement using this system more feasible; modifying the *pqbp1* sequence to mimic the mutations seen in Renpenning syndrome would provide a powerful tool to examine the clinical implications of these mutations. Finally, inducible CRISPR techniques would provide more temporal control over the knockdown, since currently it is difficult to inject *Xenopus* embryos beyond the 32 cell stage.

3.5 Materials and Methods

3.5.1 PQBP1 morpholino design

PQBP1 morpholinos were designed with the assistance of Gene Tools. The ATG morpholinos were previously tested and described (Iwasaki & Thomsen 2014).

Homeolog-specific morpholinos were used to knock down translation: *pqbp1a* MO (MOa) (5'-AGCTCTTGTTCTAACTCCCCGCCGT-3') and *pqbp1b* MO (MOb)

(5'-ACCGACACGCTCCTGCTCCTACTCT-3'). The splice morpholino (Figure 15) sequence is: 5'CAGCAAACAACATACCTTTCTGCTT-3'

The control morpholinos used were the Gene Tools standard scrambled MO (5'-CCCTTACCTCAGTTACAATTTATA-3') or their randomized control MO.

3.5.2 Microinjections and embryo culture

Xenopus laevis egg laying was induced by the injection of 400-600 units of HCG (Chorulon or Sigma HCG). Egg laying commenced 12-24 hours post induction, depending on the environmental temperature and the individual females. Embryos were produced by in vitro fertilization as previously described (Sive et al. 2000). Fertilized embryos were de-jellied using a 3% cysteine solution in 0.1X Marc's Modified Ringers (MMR) solution (pH 7.8-8.2).

Microinjection needles were pulled and calibrated to the desired volume. Embryos were injected with morpholino, mRNA, or both at the 2-8 cell stage (stages for each experiment are specified in figure legends). In all experiments except for the initial characterization of the PQBP1 splice morpholino phenotype (Figure 10), *lacZ* mRNA encoding β -galactosidase was co-injected as a lineage tracer. Following microinjections, embryos were incubated at 16-23 degrees until NF Stage 7-9 in 4% Ficoll + 0.5X MMR + 10 μ g/mL gentamycin, after which they were transferred to 0.1X MMR + 10 μ g/mL gentamycin.

3.5.3 Magenta-gal staining

Magenta-gal staining was performed on β -galactosidase injected embryos following 30 minutes of fixation at room temperature in 4% paraformaldehyde in 1X PBS. Embryos were washed 3 times for 5 minutes with 1X PBS, and then once for 5 minutes with 1 mM MgCl_2 in 1X PBS. Samples were then stained in the dark at 37 degrees until visible staining was apparent. The composition of the staining solution (for 10 mL total volume) was as follows:

476 μl 20X PBS

952 μl 50 mM potassium ferricyanide

952 μl 50 mM potassium ferrocyanide

9.5 μl 1M MgCl_2

476 μl 2% Magenta-gal in dimethylformamide

7,133 μl DEPC H_2O

Following staining, embryos were re-fixed in MEMFA (0.1 M MOPS pH 7.4, 2 mM EGTA, 1 mM MgSO_4 , 3.7% formaldehyde) for 2.5 hours at room temperature. Samples were stored in 100% methanol at -20 degrees.

3.5.4 *In vitro* transcription

Nuclear β -galactosidase was transcribed from XhoI-linearized pSP64T- β -galactosidase plasmid using the AmpliCap SP6 High Yield Message Maker kit (CellScript). A poly(A) tail was added using a poly(A) tailing kit (Ambion).

Pqbp1 morpholino-resistant mRNA was transcribed from a plasmid previously described in the literature (pCS2+-*pqbp1mut38*) (Iwasaki & Thomsen 2014). The *pqbp1* sequence encoded by this plasmid contains nine nucleotide mismatches at the *pqbp1* ATG morpholino recognition site; however, wild type amino acid coding was maintained. The plasmid was linearized with SacII and in vitro transcription was completed as described above.

RNA integrity was confirmed using a bleach gel as previously described (Aranda et al. 2012), and the RNA concentration was measured using a Nanodrop spectrophotometer.

3.5.5 Western blotting

The presence of PQBP1 protein was assessed using a western blot. Whole embryos were lysed by pipetting up and down in lysing solution containing 10 mM Tris-HCl (pH 7.5), 100 mM NaCl, 5 mM EDTA, and 0.5% Nonidet P-40, together with a proteinase inhibitor (Roche). Lysates were spun at 4 degrees. The visible fat layer at the top was removed, lysates were spun once more, and these lysates were then mixed 1:1 with loading buffer and heated. The solubilized proteins were then separated using 12.5% sodium dodecyl sulfate-polyacrylamide gel electrophoresis (SDS-PAGE). Proteins were transferred to nitrocellulose membrane (Bio-Rad) at 24 volts for 1 hour. Ponceau staining was used to confirm successful protein transfer. After washing with PBS, the membrane was blocked with 1% casein in PBS for 1 hour at room temperature.

The membrane was incubated overnight at 4 degrees with C-terminal PQBP1 primary antibody (1:200) (Thomsen lab custom antibody). The membrane was again washed with PBS three times and incubated with Alexa dye-conjugated rabbit anti-goat secondary antibody at 1:10,000 (Molecular Probes). The protein ladder used was the ColorPlus Prestained Protein Ladder, Broad Range (10-230 kDa) (New England Biolabs).

3.6 Figures and Tables

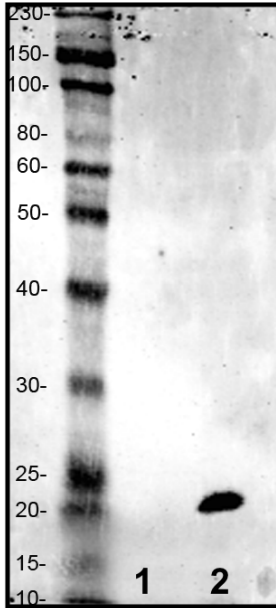


Figure 7: Western blotting of total cell lysates prepared from *Xenopus laevis* embryos injected with in vitro transcribed *pqbp1* mRNA. Lane 1 is uninjected embryos, lane 2 is *pqbp1* mRNA injected embryos. The equivalent of 1 embryo was loaded in each lane. Endogenous *pqbp1* mRNA was not detectable.

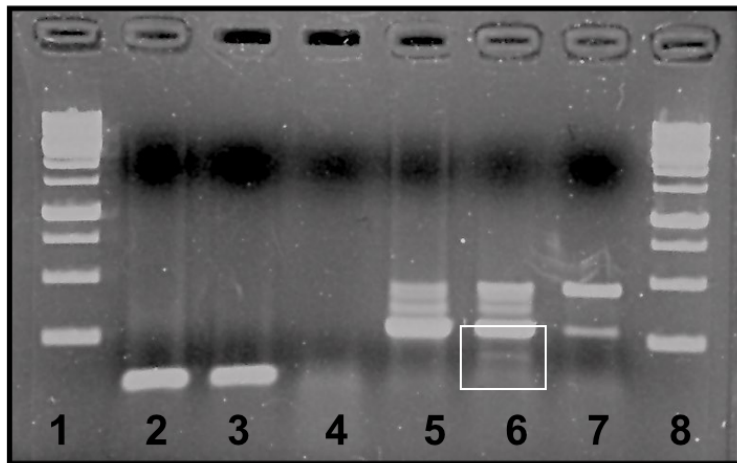


Figure 8: Gels showing the presence of a smaller, alternate splice product (white box) in PQBP1 splice morpholino injected embryos.

1. Ladder (Morganville Scientific 1 kb)
2. GAPDH Uninjected (+ control)
3. GAPDH PQ Splice Mo (+ control)
4. GAPDH RT- (- control)
5. PQBP1 Uninjected
6. PQBP1 PQ Splice MO
7. PQBP1 RT-
8. (Top only) Ladder (Morganville Scientific 1 kb)

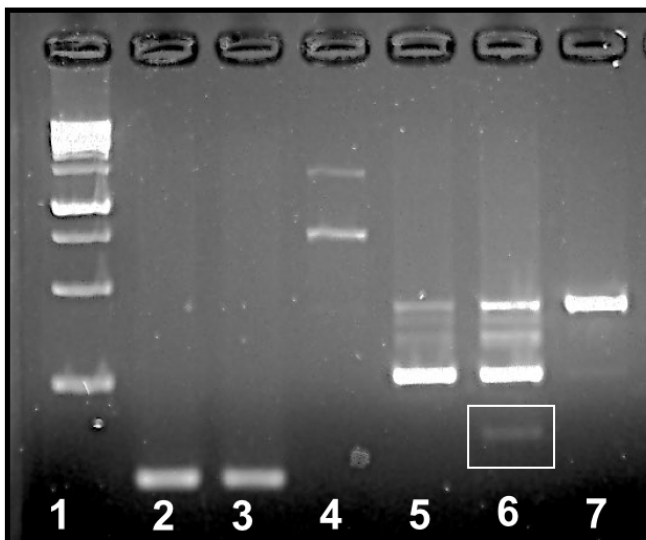


Table 2: Embryo Survival By Treatment

Treatment	Number Healthy at NF Stage 10.5	Number Sick/Dying at NF Stage 10.5	Percentage Dying
Uninjected	35	0	0
Control MO (40 ng)	21	1	5
PQBP1 MO (40 ng)	26	1	4
PQBP1 mRNA (0.5 ng)	16	14	47**
Rescue (40 ng MO + 0.5 ng mRNA)	32	6	16**

** The difference between these two groups is statistically significant at $p = 0.0076$ (Fisher's exact test). The difference between the rescue group and the control MO group is not significant. Embryos were injected with 10 nl total volume into one blastomere at the 2-cell stage.

Table 3: Embryo Phenotypes at NF Stage 15

Treatment	Living/Total	Wild Type Appearance	Blastopore Open	Cell Dissociation	Neural Folds Open	Neurulating but Delayed
Uninjected	43/43	43	0	0	0	0
Co MO (30 ng)	23/23	23	0	0	0	0
PQBP1 MO (30 ng)	20/20	0	5	0	8	7
<i>pqbp1</i> mRNA (1 ng)	14/14	13	0	0	0	1
PQBP1 MO (30 ng) + <i>pqbp1</i> mRNA (500 pg) "RESCUE LOW"	22/22	0	20	0	2	0
PQBP1 MO (30 ng) + <i>pqbp1</i> mRNA (1 ng) "RESCUE HIGH"	16/16	0	9	0	2	5

Embryos were injected with 10 nl volume in each blastomere at the 2-cell stage (amounts listed are totals for the entire embryo).

Table 4: Embryo Phenotypes at NF Stage 23

Treatment	Living/Total	Wild Type Appearance	Neural Folds Open	Delayed	Sphere Shape with Cell Dissociation	Other Abnormal
Uninjected	43/43	41	0	0	0	2
Co MO (30 ng)	23/23	23	0	0	0	0
PQBP1 MO (30 ng)	19/20	0	12	7	1	0
<i>pqbp1</i> mRNA (1 ng)	14/14	14	0	0	0	0
PQBP1 MO (30 ng) + <i>pqbp1</i> mRNA (500 pg) "RESCUE LOW"	21/22	0	0	1	21	0
PQBP1 MO (30 ng) + <i>pqbp1</i> mRNA (1 ng) "RESCUE HIGH"	0/16	0	0	0	16	0

Embryos were injected with 10 nl volume in each blastomere at the 2-cell stage (amounts listed are totals for the entire embryo).

NF Stage

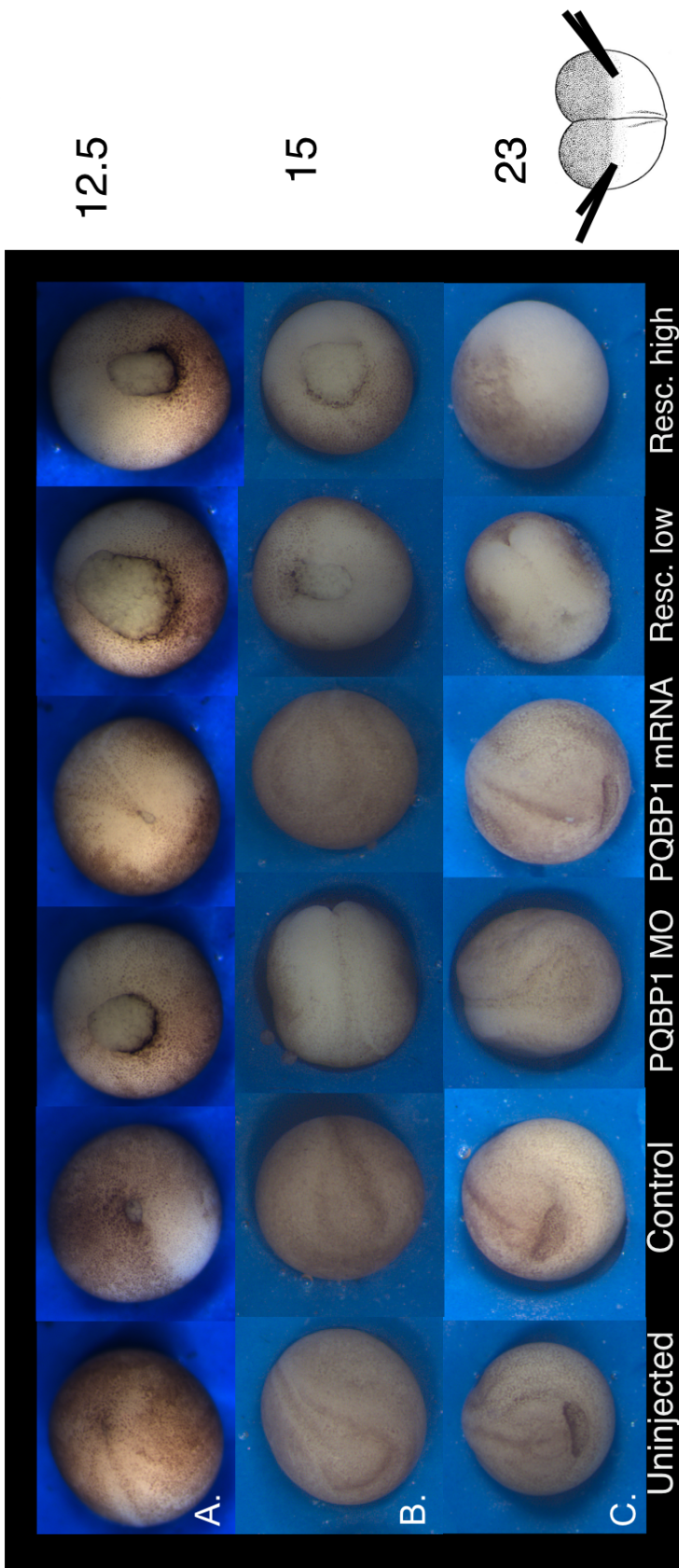


Figure 9: Phenotypes of embryos injected bilaterally at the 2 cell stage. A. NF Stage 12.5. B. NF Stage 15. C. NF Stage 23. Rows from left to right: uninjected, control MO (randomized control, 30 ng), PQBP1 MO (15 ng MOa + 15 ng MOb), *pqbp1* mRNA (30 ng Co MO + 1 ng mRNA); rescue low (30 ng PQBP1 MO + 500 pg *pqbp1* mRNA), rescue high (30 ng PQBP1 MO + 1 ng *pqbp1* mRNA).

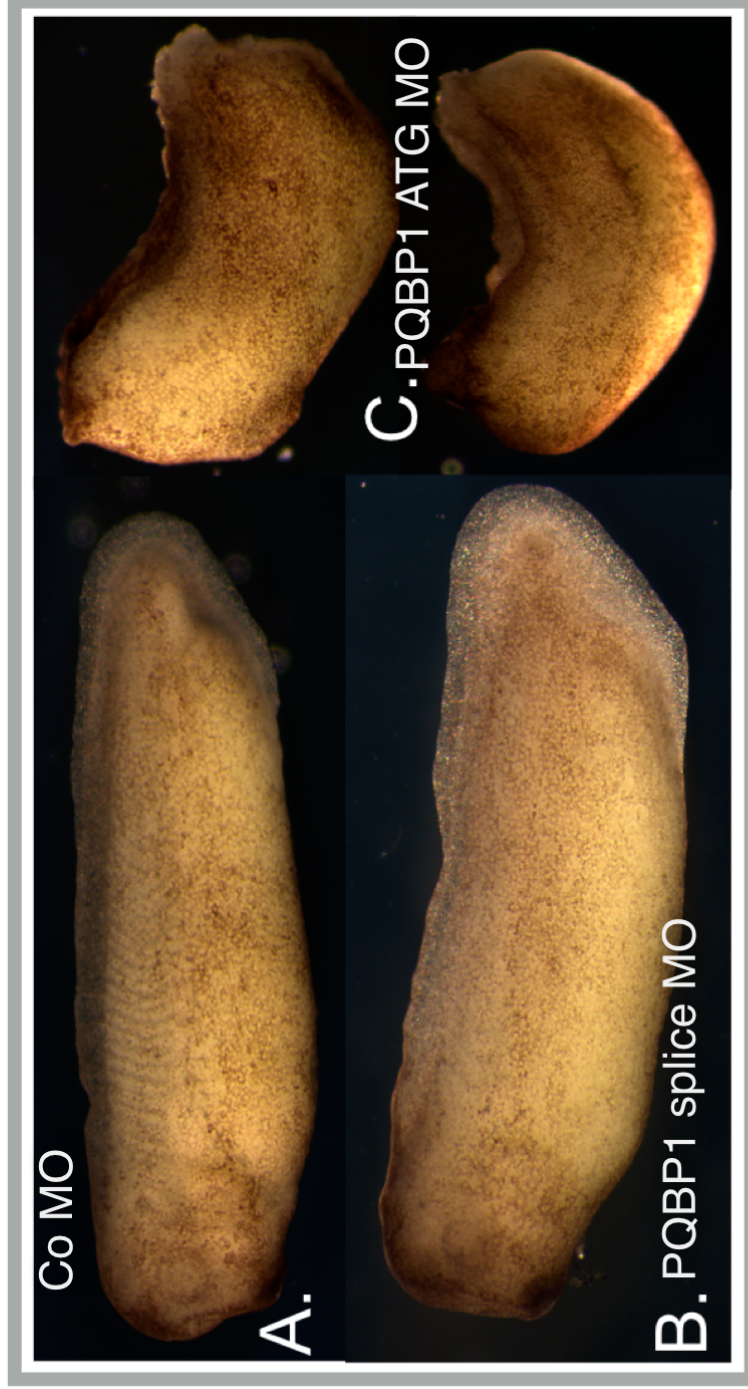


Figure 10: P.QQBP1 splice morpholino produces milder phenotypes than P.QQBP1 translation-blocking morpholinos (MOa and MOb). Representative phenotypes at NF Stage 30. Treatments: A. Control MO (randomized control, 25 ng). B. P.QQBP1 splice MO (25 ng). C. (Top and Bottom) P.QQBP1 translation blocking MOs (12.5 ng each MOa and MOb). (All bilateral dorsal injections in 5 nl volume at the 4-cell stage; amounts are the totals for the entire embryo.) (Refer to Appendix A for details on morpholino targets.)

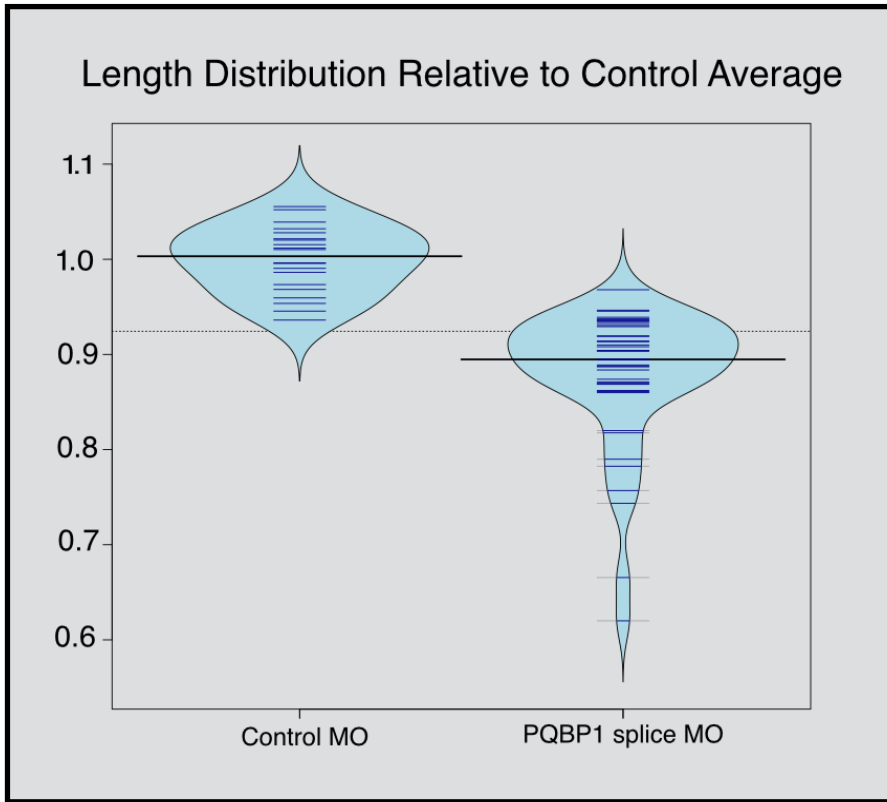


Figure 11: Bean plot showing the length distribution of PQBP1 splice morpholino-injected embryos (bilateral injections of 25 ng total splice morpholino at the 2-cell stage) as compared to control morpholino-injected embryos. (All at NF Stage 32.) Table 5 (below) shows the statistical breakdown of these data.

Table 5: Embryo Length Statistical Comparison

	Control MO	Splice MO
Upper Whisker	1.06	0.97
3rd Quartile	1.02	0.93
Median	1	0.89
1st Quartile	0.97	0.87
Lower Whisker	0.94	0.78
Number of Data Points	20	44

Student's T-test $p < 0.001$
 Embryo length was measured relative to the median of the Control MO injected embryos.

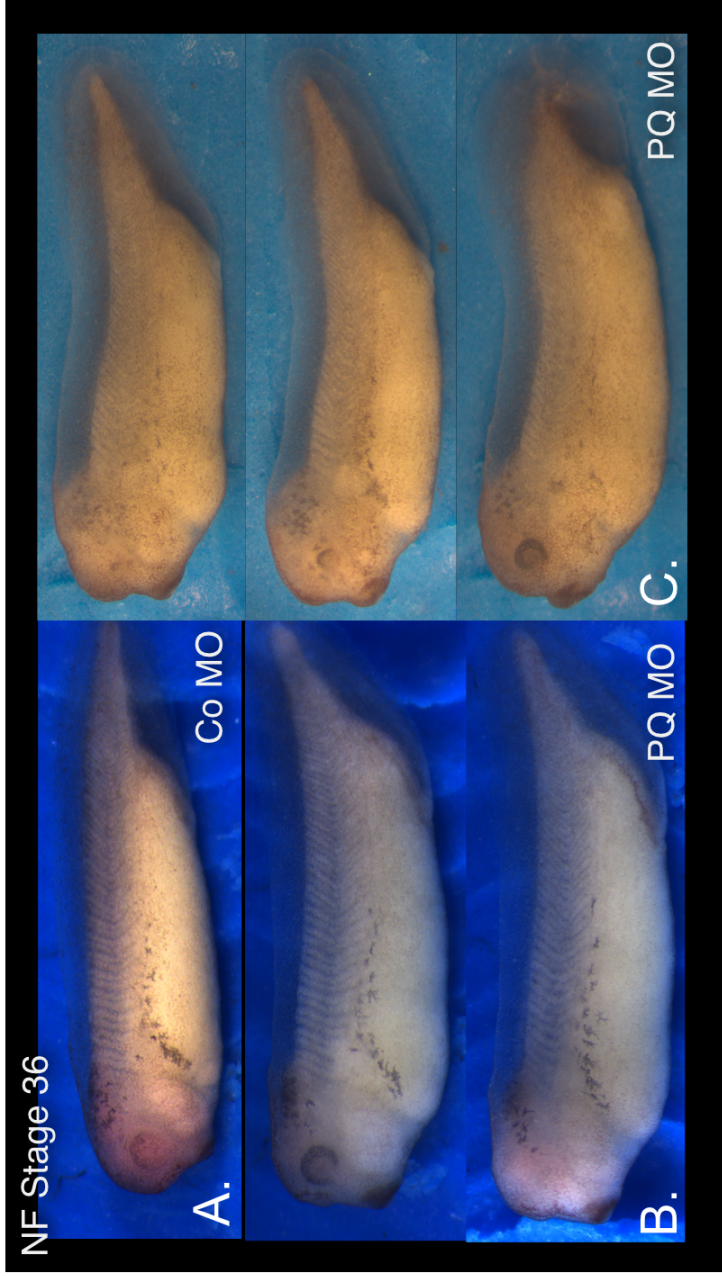


Figure 12: PQBP1 splice morpholino produces eye defects. All embryos are at NF Stage 36 and were injected into 2 dorsal blastomeres at the 8-cell stage. A. Embryo injected with 25 ng randomized control MO (fluoro-ruby shows injection targeting). B. Embryo injected with 25 ng PQBP1 splice MO. Top shows the uninjected side. C. Range of eye phenotypes produced by injection of 25 ng PQBP1 splice MO (the other side of each embryo was normal).

Table 6: Rescue Experiment Summary

Stage and Location Injected	Percent Normal with MO	Percent Normal with MO + RNA (rescue)	Best Rescue Condition	Significance*
8 cell, one dorsal blastomere	29 (5/17)	83 (10/12)	250 pg mRNA	p = 0.0049
8 cell, one dorsal blastomere	33 (5/15)	46 (6/13)	150 pg mRNA	p = 0.50
4 cell, both dorsal blastomeres	40 (14/35)	83 (24/29)	500 pg mRNA	p = 0.00058
4 cell, both dorsal blastomeres	30 (10/33)	56 (9/17)	300 pg mRNA	p = 0.12
4 cell, both dorsal blastomeres	30 (10/33)	39 (13/33)	300 pg mRNA	p = 0.44

*N-1 Chi-Square test

8 cell, one dorsal blastomere pooled significance: p = 0.015

4 cell, both dorsal blastomeres pooled significance: p = 0.0010

Table 7: Phenotype Breakdown of 4 Cell Stage Rescue Experiments (n=3)

Treatment	Percent (Number) Wild Type Appearance	Percent (Number) Small Eye	Percent (Number) Missing Eye	Percent (Number) Deformed	Total Embryos
Uninjected	96 (138)	3 (5)	0 (0)	1 (1)	144
Control MO (25 ng)	96 (79)	4 (3)	0 (0)	0 (0)	82
PQBP1 splice MO (25 ng)	34 (34)	48 (48)	17 (17)	2(2)	101
<i>pqbp1</i> mRNA (300 pg)	80 (75)	9 (9)	0 (0)	11 (10)	94
<i>pqbp1</i> mRNA (700 pg)	68 (53)	19 (15)	1 (1)	12 (9)	78
PQBP1 splice MO (25 ng) + <i>pqbp1</i> mRNA (300 ng)					
"RESCUE LOW"	38 (35)	39 (36)	16 (15)	8 (7)	93
PQBP1 splice MO (25 ng) + <i>pqbp1</i> mRNA (500 ng)					
"RESCUE MEDIUM"	44 (35)	34 (27)	14 (11)	9 (7)	80
PQBP1 splice MO (25 ng) + <i>pqbp1</i> mRNA (700 ng)					
"RESCUE HIGH"	14 (11)	66 (50)	13 (10)	7 (5)	76

All embryos were injected with 5 nl total volume into one dorsal blastomere at the 4 cell stage.

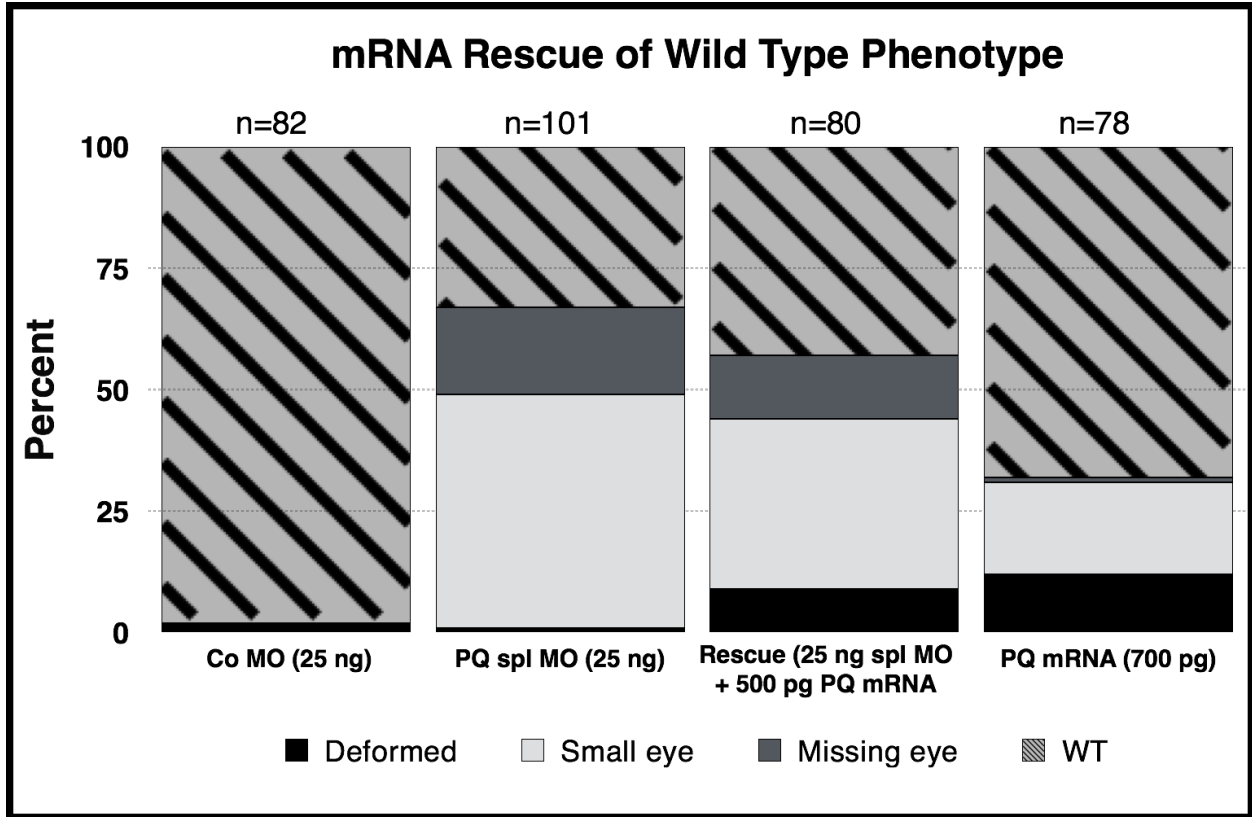
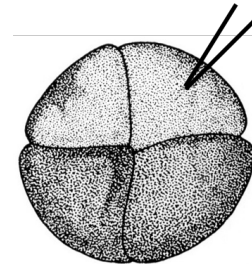


Figure 13: *Pqbp1* mRNA partial rescue of wild-type phenotype, showing only data for the “medium rescue” condition (Table 7). Combined data from 3 sets of 4 cell stage injections into 1 dorsal blastomere. Details are shown in Table 7.



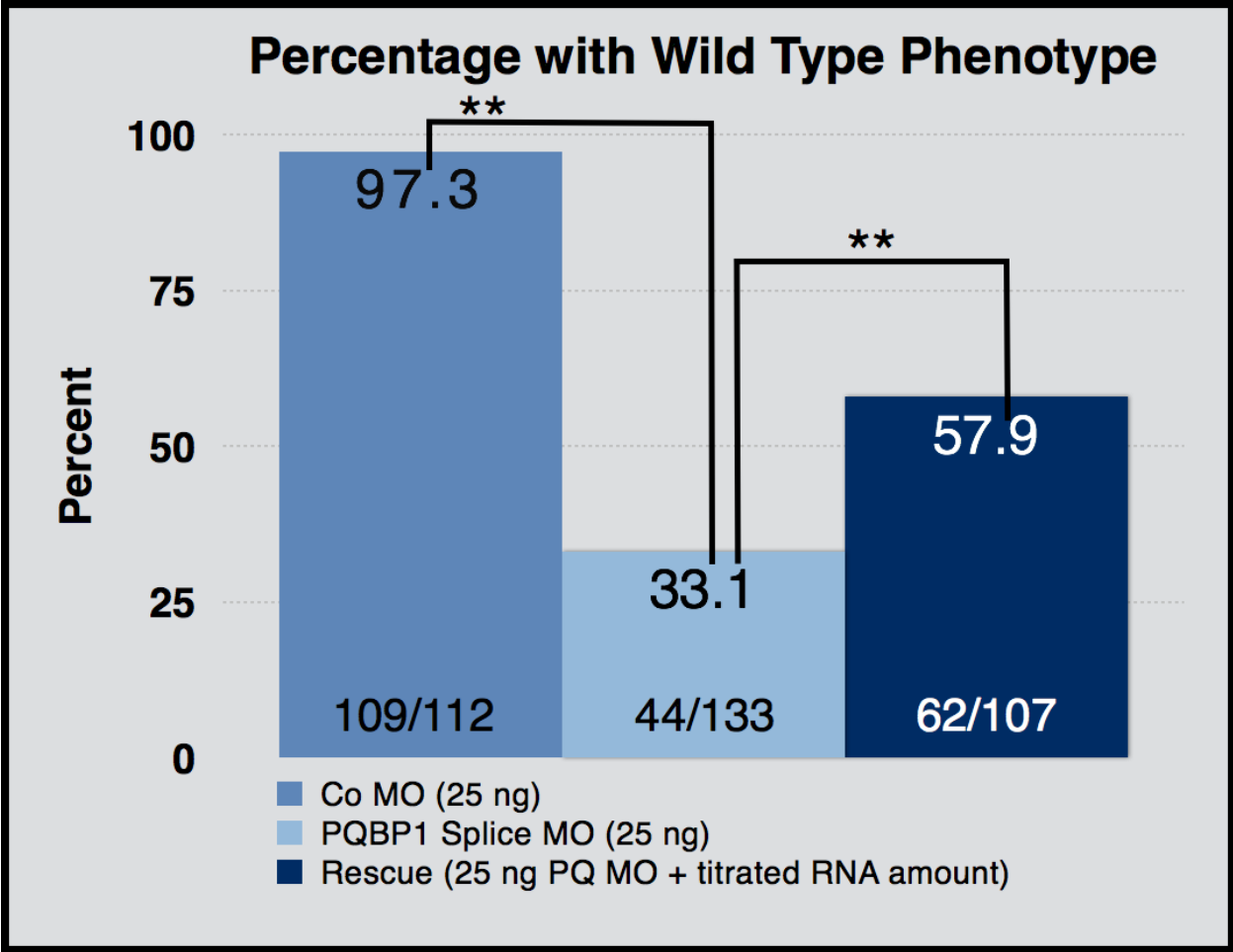


Figure 14: Percent and number/total wild-type phenotypes observed (data compiled from 5 experiments shown in Table 6). ** $p < 0.01$ calculated from one-way ANOVA and Tukey's HSD test.

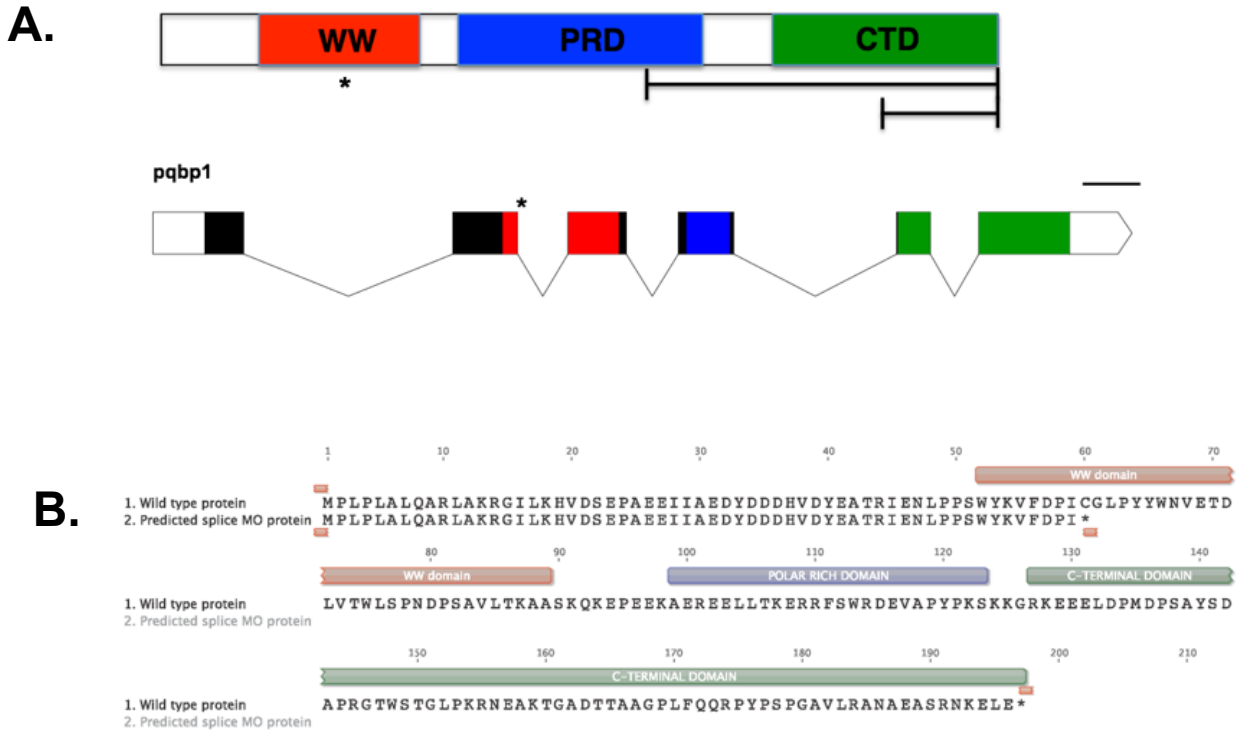


Figure 15: Pqbp1 protein domains, intron/exon structure, and expected splice MO truncation product. A. (Top) Diagram of Pqbp1 showing its major domains (WW: WW domain, PRD: polar rich domain, CTD: C-terminal domain) and common sites of mutations or truncations linked to Renpenning syndrome (lines and asterisk). (Bottom) Intron/exon structure of *pqp1* showing the target location of the Pqbp1 splice morpholino. B. Pqbp1 protein sequence showing the predicted truncated protein expected by blocking the exon 2/intron 2 junction using the Pqbp1 splice morpholino.

Chapter 4: PQBP1 impacts neural development independent of mesodermal influences and may promote neural determination and differentiation

4.1 Introduction

Although knockdown and overexpression of PQBP1 in the context of the whole embryo was certainly useful in determining the overall function of the protein, in order to further investigate and focus on neural development, it was necessary to consider the effects of PQBP1 in the absence of mesodermal tissues. In the intact embryo, it is difficult to distinguish whether effects on neural development are occurring through neural-fated or mesodermal tissues. Fortunately, obtaining neuralized tissue in *Xenopus* is relatively straightforward. *Xenopus* animal cap explants are an extremely useful tool, as they allow for the isolation of pluripotent cells from NF Stage 8-9 embryos, which can be induced to form neural tissue independent of the rest of the embryo through the injection of *chordin* mRNA (Figure 16).

After establishing that the in vitro transcribed *chordin* worked properly, several sets of neuralized caps were cultured alongside whole embryo controls and then utilized for RT-qPCR as shown in Figure 16. The cDNA produced from these caps was first used to whether *pqbp1* is in fact expressed in neuralized caps, and to eliminate the possibility of significant mesodermal contamination in the tissue. The levels of a variety of neural markers, as well as XAG1, a cement gland marker were then determined for each treatment. Table 1 outlines the major functions of the markers in a wild-type

embryo. I also examined whether it was possible to rescue marker levels by co-injection of *pqbp1* mRNA.

In addition to the neural markers and *XAG1*, I also considered the relative frequencies of the splice isoforms of *FGFR2*, since those had previously been noted to change in the whole embryo upon PQBP1 knockdown (Iwasaki & Thomsen 2014).

4.2 Results

4.2.1 *Pqbp1* is expressed in neuralized animal caps

Chordin mRNA was injected either ventrally or dorsally into one blastomere of 4 cell stage embryos, to ensure the *chordin* mRNA was effective. Figure 17 shows the results of this experiment. *Chordin* injection successfully dorsalized the embryos, which is evident by the second axis observed in the ventrally injected embryos, and the radial embryo with radial retinal pigment and cement gland (10a on the DAI index) produced by dorsal injection (see Figure 17C) (Kao & Elinson 1988). Based on these results, 500 pg of *chordin* was used for the animal cap injections.

Figure 18 shows a sample set of animal cap injections alongside the whole embryo controls that underwent the corresponding treatments. Many of the PQBP1 morpholino injected neuralized caps exhibited elongation by NF Stage 18-21, which did not occur in the control neuralized caps.

The level of *pqbp1* expression in neuralized caps relative to uninjected caps at various times during neurulation was determined through RT-qPCR (Figure 19). Expression was observed at NF Stage 14, 18, and 21, with expression relative to

uninjected caps increasing over time. The graph also shows expression in the whole embryo at Stage 14 to ensure that cap expression was not significantly lower than that in the entire embryo (at least at NF Stage 14).

In order to account for possible mesodermal contamination of the caps (due to incorrectly cut explants), the level of *brachyury* (*T*), a mesodermal marker, was measured (Figure 20). The levels of this marker relative to NF Stage 14 whole embryos were shown to be very low at NF Stage 14, 18, and 21.

4.2.2 PQBP1 knockdown selectively impacts neural marker expression in an isolated neural context

Figure 21 shows the levels of various markers in non-neuralized control caps, neuralized caps, and neuralized caps injected with PQBP1 morpholino, as well as the time courses of expression for these markers (data for expression levels was compiled from a minimum of 3 replicates). At NF Stage 18-21, at which replicate sets of caps were collected, a number of neural markers (as well as *XAG1*), both early and late, showed either decreased or increased expression relative to control neuralized caps. Among early markers, most (*sox2*, *NCAM*, *sox3*) decreased, but *geminin* levels increased. Later markers *otx2* and *XAG1* were also reduced, while *N-tubulin* levels went up. Time course data from independent experiments corroborate the changes in expression seen at NF Stages 18-21.

I attempted to rescue marker expression using co-injection of *pqbp1* mRNA along with the PQBP1 splice morpholino. In the case of *XAG1*, *sox2*, as well as *otx2* (Figure 22), it appeared that the *pqbp1* mRNA led to similar changes as the morpholino.

In addition, although *XAG1* levels appear to be rescued through the co-injection of MO and mRNA, in the case of the other two markers there is a cumulative effect, shown by an amplified response following co-injection.

4.2.3 PQBP1 knockdown in neural tissue may impact FGF signaling in a manner antagonistic to its function in the whole embryo

Prior work (Iwasaki & Thomsen 2014) indicated that, in whole embryos, the levels of *FGFR2* spliceoforms were altered following PQBP1 knockdown. Specifically, levels of *FGFR2IIIb* increased, while levels of *FGFR2IIIc* decreased, relative to overall *FGFR2* expression. In the neuralized caps, however, the opposite pattern was seen, with *FGFR2IIIc* increasing and *FGFR2IIIb* decreasing (Figure 23).

4.3 Discussion

By observing marker changes in the neuralized context of the *chordin*-injected *Xenopus* animal cap, mesodermal influences of PQBP1 activity can be discounted. This provides a clearer picture of the potential neural-specific impacts. At NF Stages 18-21, differences in both early and late neural markers are seen, although the magnitude as well as direction of these changes vary. It appears that PQBP1 knockdown reduces early neural determination and differentiation markers such as *NCAM*, *sox2*, and *sox3*, while increasing *geminin*, which maintains neural precursors in an undifferentiated state. Therefore, PQBP1, at least in isolated neural tissue, may promote neural determination and differentiation. The reduction in *pax6*, a master regulator of eye development,

suggests a role for PQBP1 in eye development. The reduction in *pax6* is consistent with the smaller or missing eye structures seen in PQBP1 splice morpholino-injected whole embryos.

The decrease in *otx2* and *xag1* levels, both markers that indicate cement gland development, implies an indirect or direct impact for PQBP1 on this process as well. The *Xenopus* cement gland is a relatively simple mucus-secreting structure in the extreme anterior of the developing embryo, in a region where ectoderm and endoderm are directly juxtaposed (Wardle & Sive 2003). Despite the observed marker reduction, the cement gland appears to form correctly in a whole embryo context. Since *otx2* does not just induce formation of the cement gland but neural structures as well, it is likely that the neural induction properties, rather than those related to the cement gland, are largely inhibited in the context of PQBP1-expressing neural-fated regions. In addition, *otx2* is a known inducer of *xag1*, which would explain the concurrent reduction in that marker (Michiue et al. 2007). Also, in addition to ectodermal influences, cement gland development requires input from mid-gastrula dorsoanterior yolky endoderm as well as dorsal mesoderm. Signals coming from these regions may compensate for reduced *xag1* expression (Bradley et al. 1996). These data indicate the PQBP1 is unlikely to play a primary role in cement gland development. However, the downregulation of *otx2* could help explain the lack of anterior head structures often observed in knockdown embryos, since *otx2* is known to be involved in the development of this region (Ip et al. 2014).

The increase in *N-tubulin* expression seen following PQBP1 knockdown suggests that PQBP1 may play a role in downregulating neuronal differentiation during later neural development. However, the observation that *in situ* hybridization results

consistently suggest that *N-tubulin* expression is reduced at earlier neurula stages implies that this may be a delayed effect due to a temporal delay in neuronal differentiation caused by PQBP1 knockdown. Therefore, it is more likely that PQBP1, in a wild type context, helps promote neuronal differentiation during earlier stages. This is consistent with early neural determination and differentiation markers that show a reduction following PQBP1 knockdown, as well as the observed increase in *geminin*. In addition, a reduction in *N-tubulin* during early neurogenesis, combined with the observed reduction in anterior head structures upon PQBP1 knockdown, would mimic human clinical phenotypes seen in the case of hypomorphic *N-tubulin* expression (Jaglin et al. 2009).

The change in *FGFR2* splicing observed in neuralized caps is the opposite of that seen in whole embryos. Given the previously identified role of PQBP1 in splicing, *FGFR2* may very well be a direct target (Tapia et al. 2010; Wang et al. 2013; Iwasaki & Thomsen 2014). Since the different isoforms bind to distinct groups of FGF ligands, changes in isoform expression could have significant developmental implications (Orr-Urtreger et al. 1993; Mai et al. 2010; Holzmann et al. 2012). FGFs 1, 2, and 8 appear in particular appear to have critical roles during neural development (Rash et al. 2013; Fukuchi-Shimogori & Grove 2001; Garel et al. 2003; Reuss & Von Bohlen Und Halbach 2003). If FGF signaling is blocked, neural induction as measured by markers such as *sox3* is disrupted. *FGFR2IIIb* is primarily found in ectodermal regions and endothelial organ lining, while *FGFR2IIIc* is mostly mesenchymal. FGFs 2 and 8 only bind to *FGFR2IIIc*; since this is the less common isoform in control neuralized caps, perhaps a limited amount of this isoform needs to be present in order for neural development to

proceed correctly. Increases in the level of FGFR2IIIc could, therefore, disrupt the required balance of FGF ligand activity.

4.4 Future Directions

While the data presented here imply a role for PQBP1 in neural determination and differentiation, they do not specify whether any of these markers are direct PQBP1 splicing targets or interacting partners. Therefore, identification of additional splicing targets, especially in an isolated neural context, would provide useful data regarding the role of PQBP1 in neural development and allow for a clearer determination of the mechanism by which it may be acting. The animal cap experiments used to obtain cDNA for marker RT-qPCR each involved RNA extraction from 30-50 animal caps per treatment, and sufficient RNA remains to conduct an RNA-seq experiment comparing control caps, neuralized control caps, and neuralized PQBP1 knockdown caps. This would greatly increase the ability to identify possible targets, which could then be followed up on by knockdown/overexpression experiments, (isoform-specific) RT-qPCR, epigenetic analysis, and so on.

In addition, following up on the data regarding differential impacts of PQBP1 knockdown on FGFR2 isoform expression in mesoderm versus neural tissue would help define, more specifically, the significance of the function of PQBP1 in FGF signaling in both tissues. This would increase not only our understanding of PQBP1 itself, but also of general FGF signaling during neural development in the early embryo.

4.5 Materials & Methods

4.5.1 *In vitro* transcription and analysis of Chordin function

Chordin mRNA was transcribed from a plasmid procured from the European *Xenopus* Resource Center (EXRC) (Clone number CC-6, pCS2+ vector). Not1-linearized plasmid was used with the AmpliCap SP6 High Yield Message Maker Kit (CellScript). A poly(A) tail was added using a poly(A) tailing kit (Ambion). RNA integrity was assayed using a bleach gel (Aranda et al. 2012), and the concentration was measured using a Nanodrop spectrophotometer.

Chordin function was determined by injecting varying amounts of mRNA into one dorsal or ventral blastomere of 4 cell stage embryos. Amounts injected were 0.25 ng, 0.5 ng, and 1 ng. The presence of a secondary axis in ventrally injected embryos or a radialized phenotype in dorsally injected embryos indicated functional Chordin. All embryos injected with 1 ng died at an early stage. Since embryos appeared to tolerate 0.5 ng without difficulty, this amount was used for the animal cap experiments.

4.5.2 *Microinjection and animal cap cutting*

Microinjections were performed as in 3.4.2; however, no lineage tracer was added. Animal caps were removed at NF Stages 8-9, cleaned several times by transfer to a clean 6-well plate, and cultured in 0.5X MMR + 10 µg/mL gentamycin until whole embryo controls (cultured in 0.1X MMR) reached NF Stage 18-21 (due to variation among embryos, staging could not be more precisely defined).

4.5.3 RNA extraction and cDNA synthesis

Total RNA was extracted from 30-50 caps or 3-5 whole embryos (per treatment) using the Direct-zol RNA MiniPrep with TRI-Reagent kit (Zymo Research) including the optional DNase treatment. RNA was dissolved in nuclease-free water (Qiagen). cDNA was synthesized using Superscript II (Invitrogen) or ProtoScript II reverse transcriptase (New England Biolabs) at 42 degrees, following the recommended protocols from the manufacturers. 1 µg of RNA was used as a template. The cDNA was diluted in 100 µl of nuclease-free water prior to RT-qPCR analysis.

4.5.4 RT-qPCR

Real time quantitative PCR (RT-qPCR) was conducted using the StepOnePlus system (Applied Biosystems) using *Power* SYBR Green Master Mix. 1 µl of cDNA template was used in a 20 ul reaction volume. The optimal amount of template to use was initially determined by running an experiment using multiple dilutions. Technical duplicates were run for each sample. The majority of primers had annealing temperatures around 60 degrees and product sizes ranging from 100-200 bp. PCR conditions were: initial denaturation for 10 minutes at 95 degrees, annealing/elongation for 60 seconds at 60 degrees (modified to 55 degrees for some primers), and denaturation for 15 seconds at 95 degrees (40 cycles).

Results were analyzed using LinRegPCR software, which determines the baseline fluorescence and then performs a baseline subtraction (Ramakers et al. 2003). The starting concentration per sample (C_q), expressed in arbitrary fluorescence unit is

calculated. This information was then used to normalize expression levels relative to the housekeeping genes ODC or GAPDH (initial experiments determined that both were suitable).

The primers used are listed below:

ODC U: GCCATTGTGAAGACTCTCTCC
D: TTCGGGTGATTCCTTGCCAC (Iwasaki & Thomsen 2014)

GAPDH U: TAGTTGGCGTGAACCATGAG
D: GCCAAAGTTGTCGTTGATGA (Bentaya et al. 2012)

Brachyury U: TTCTGAAGGTGAGCATGTCTG
D: GTTTGACTTTGCTAAAAGAGACAGG (Thomsen lab)

NCAM U: CACAGTTCCACCAAATGC
D: GGAATCAAGCGGTACAGA (Yasuno Iwasaki)

Sox2 U: GATCAGTATGTACCTACCTGG
D: AGTGGAGAGCCACAGTTTGTC (Evguenia Alexandrova)

Sox3 U: AGACACTTACGCGCACATGA
D: TACCTGTGCTGGATCTGCTG (Bentaya et al. 2012)

Geminin U: TGAAGTGGCTGTTGATCCAG
D: TCTTCGTTCCCTCTGCAACCT

XAG1 U: CTGACTGTCCGATCAGAC
D: GAGTTGCTTCTCTGGCAT (Alexandrova & Thomsen 2006)

Pax6 U: CGATGGGCAACAATCTAC
D: GACTGACACTCCAGGGGA (Tuzer Kalkan)

Otx2 U: CGGGATGGATTTGTTGCA

D: TTGAACCAGACCTGGACT (Evguenia Alexandrova)

N-tubulin U: TGCTGATCTACGCAAAGTGG
D: CTGTCAGGGCTCGGTATTGT

Fgfr2 ex8a U: TCCAGTGCTGAAGTGCTGAAACTG
D: TCGTCCGCTTCGGTCACATT (Iwasaki & Thomsen 2014)

Fgfr2 ex8b U: ACATTCTGCCTGGTTGACGGT
D: CCAGCATCCTCAAAGAAACATTCCTG (Iwasaki & Thomsen 2014)

Fgfr2 ex9 D: TCTTCTTGGCTCCTTGCCGC (Iwasaki & Thomsen 2014)

Pqbp1 Primers used were 38-3A and 38-3S (Iwasaki & Thomsen 2014)

4.6 Figures and Tables

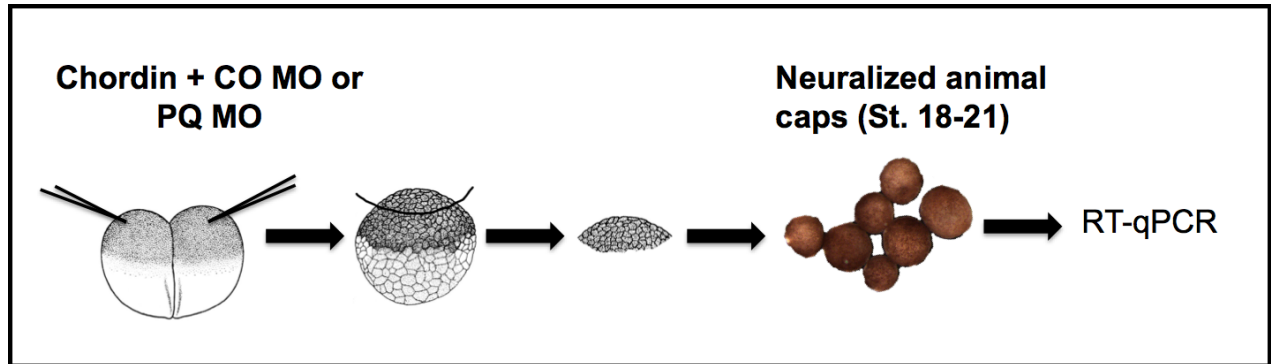
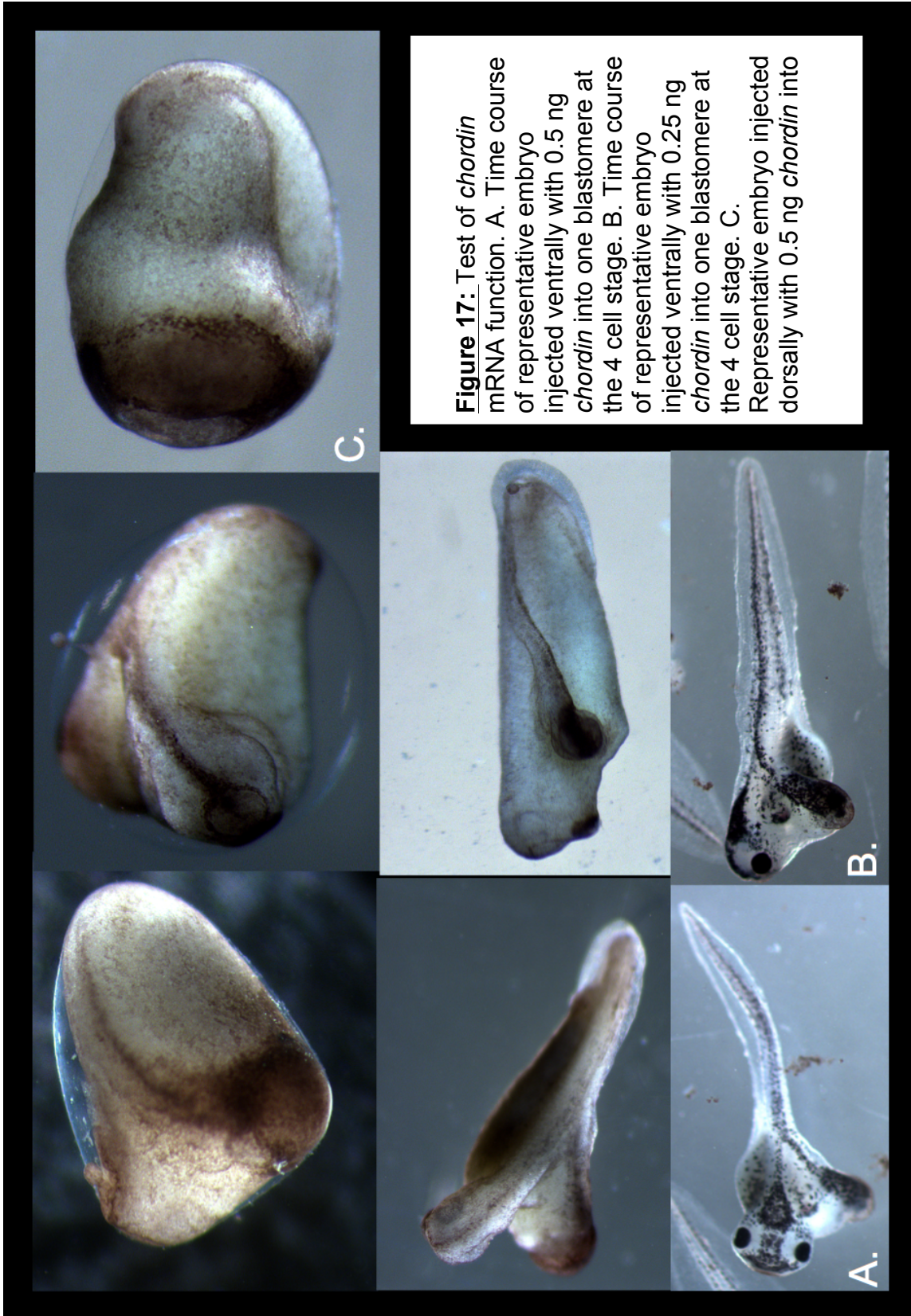


Figure 16: Diagram showing the experimental procedure for RT-qPCR on neuralized animal caps. The animal poles of each blastomere of 2 cell stage embryos are injected with *chordin* along with control or PQBP1 morpholino. The animal cap is removed at NF Stages 8-9, and cultured separately alongside several intact embryos (for staging). Caps are collected around NF Stages 18-21; RNA is extracted from these caps, cDNA is produced, which can then be used for RT-qPCR.



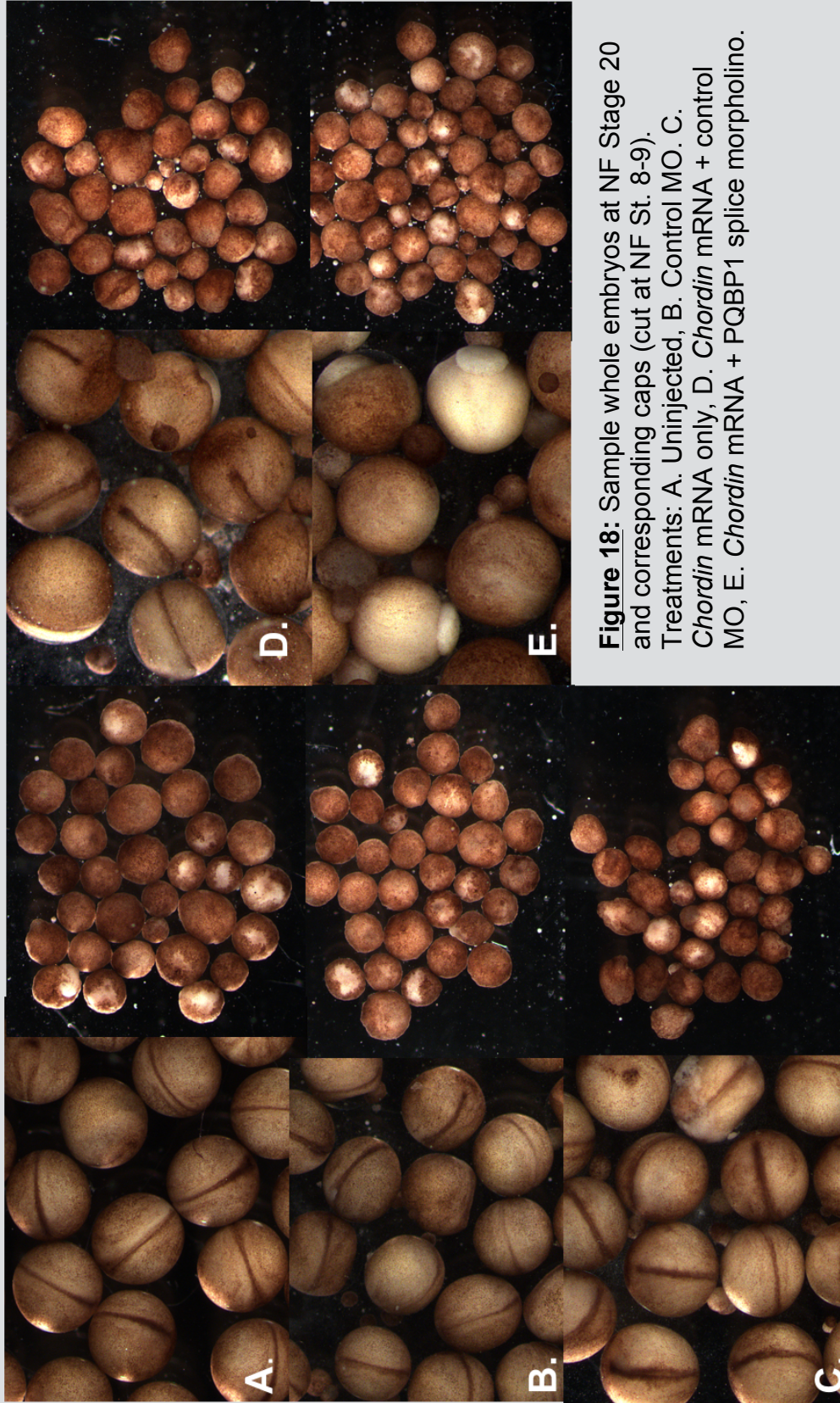


Figure 18: Sample whole embryos at NF Stage 20 and corresponding caps (cut at NF St. 8-9). Treatments: A. Uninjected, B. Control MO. C. *Chordin* mRNA only, D. *Chordin* mRNA + control MO, E. *Chordin* mRNA + PQBP1 splice morpholino.

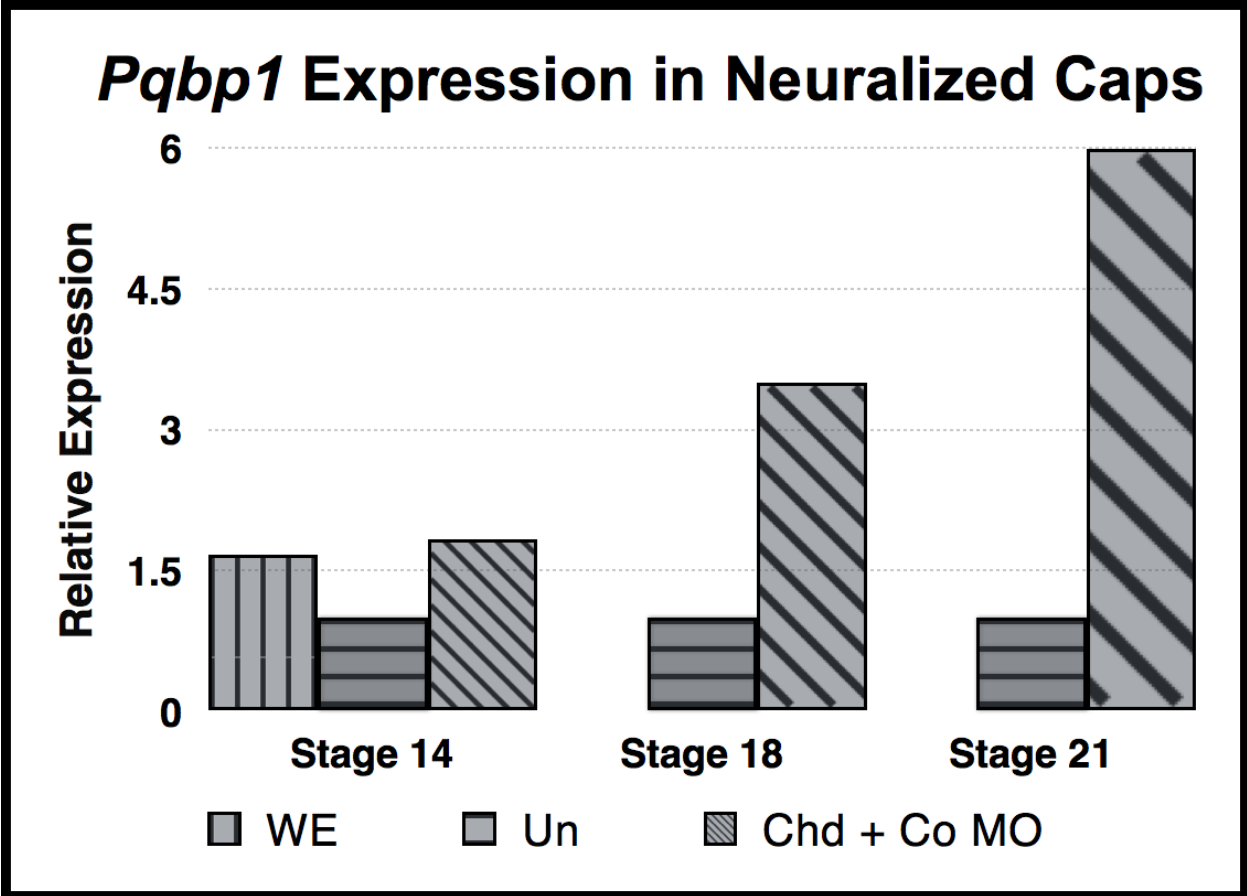


Figure 19: *Pqbp1* is expressed in neuralized animal cap explants. Expression is relative to uninjected caps at each stage.

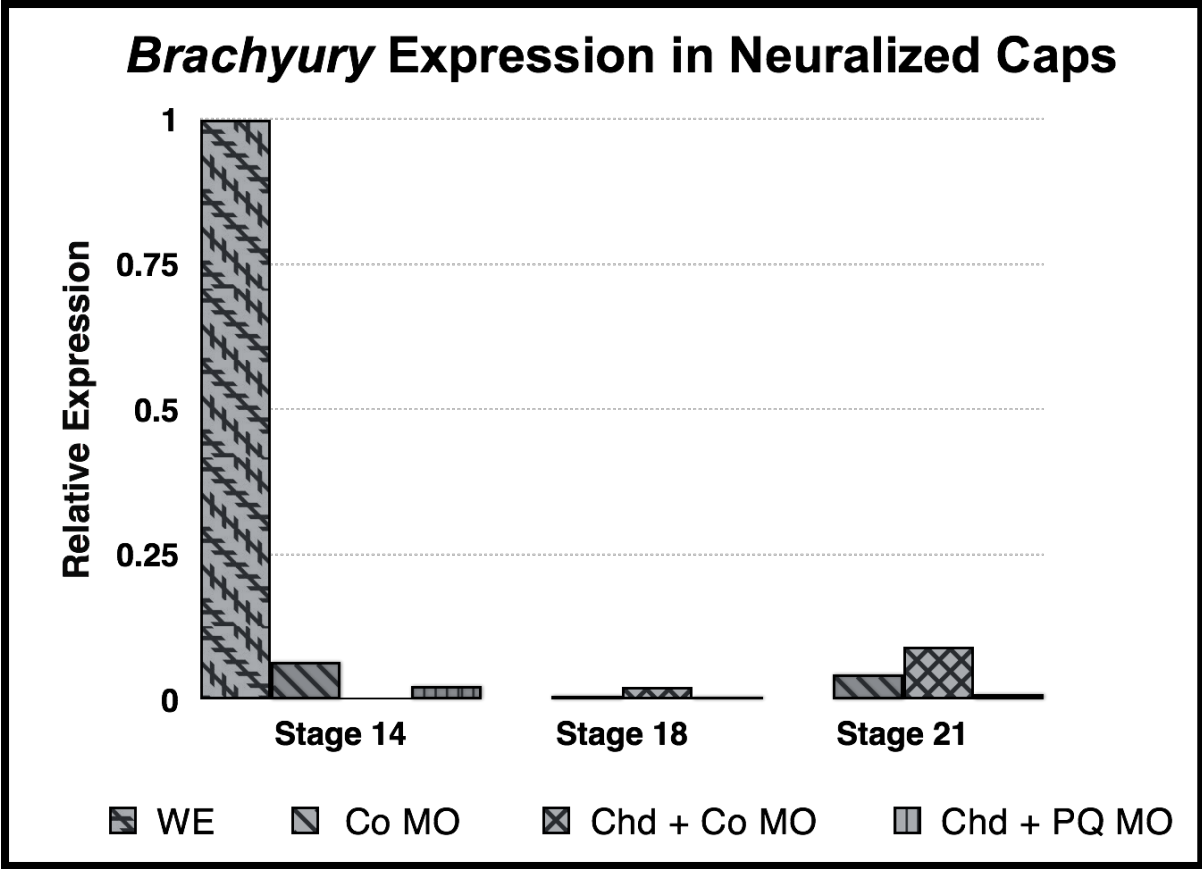
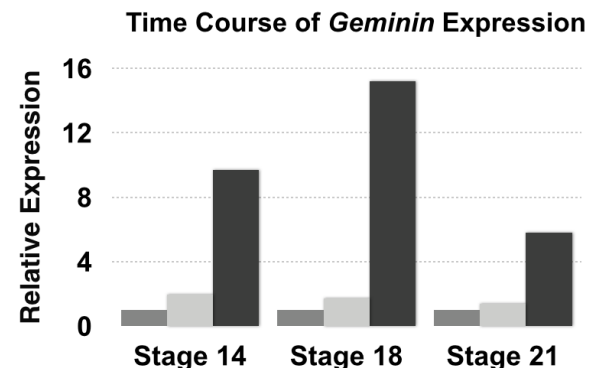
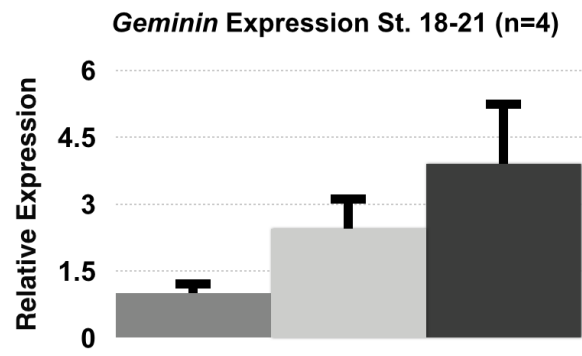
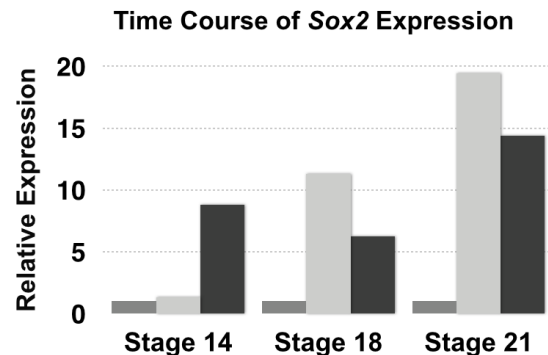
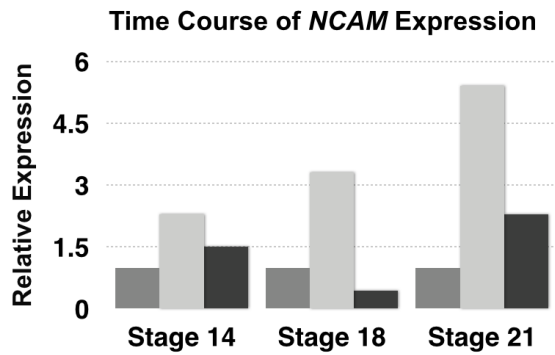
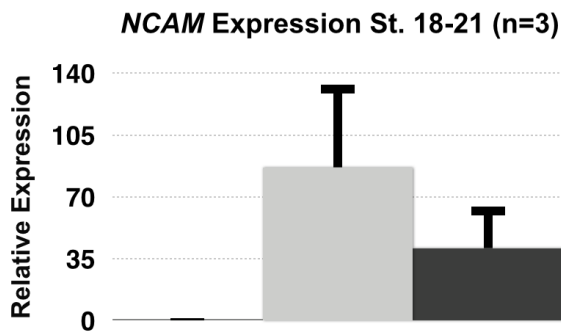


Figure 20: *Brachyury (T)* levels of expression in neuralized caps are minimal. Expression is relative to NF Stage 14 whole embryos (WE).



■ Co MO ■ Chd + Co MO ■ Chd + PQ MO

(Continued)

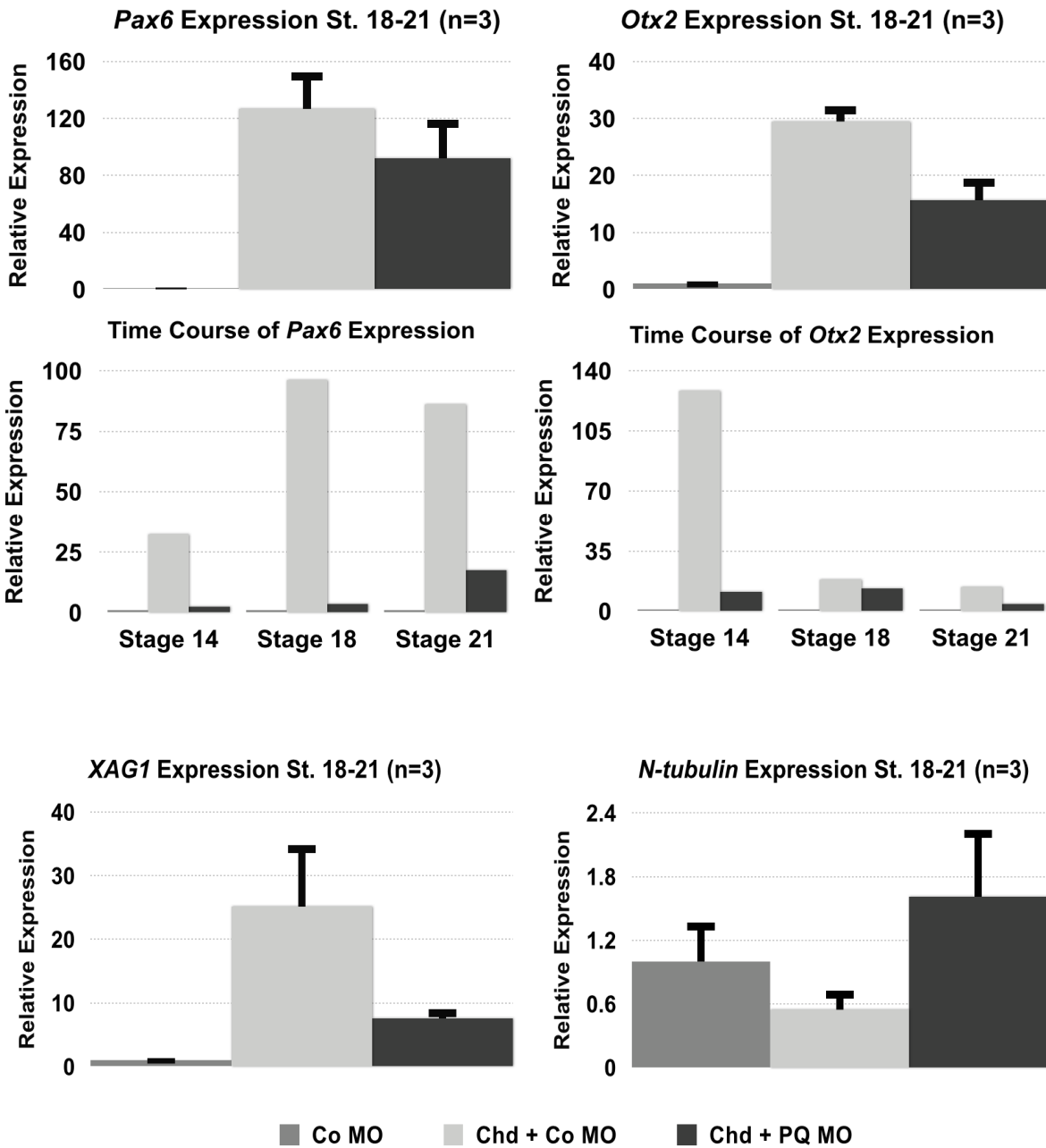


Figure 21: Expression levels at NF Stages 18-21 and time courses of neural marker expression (and the cement gland marker *XAG1*) in animal caps injected with either control MO, *chordin* mRNA + control MO, or *chordin* mRNA + PQBP1 MO. Levels were set relative to control MO-injected caps. Note that time courses for *XAG1* and *N-tubulin* are not shown. Error bars represent the standard error of the mean.

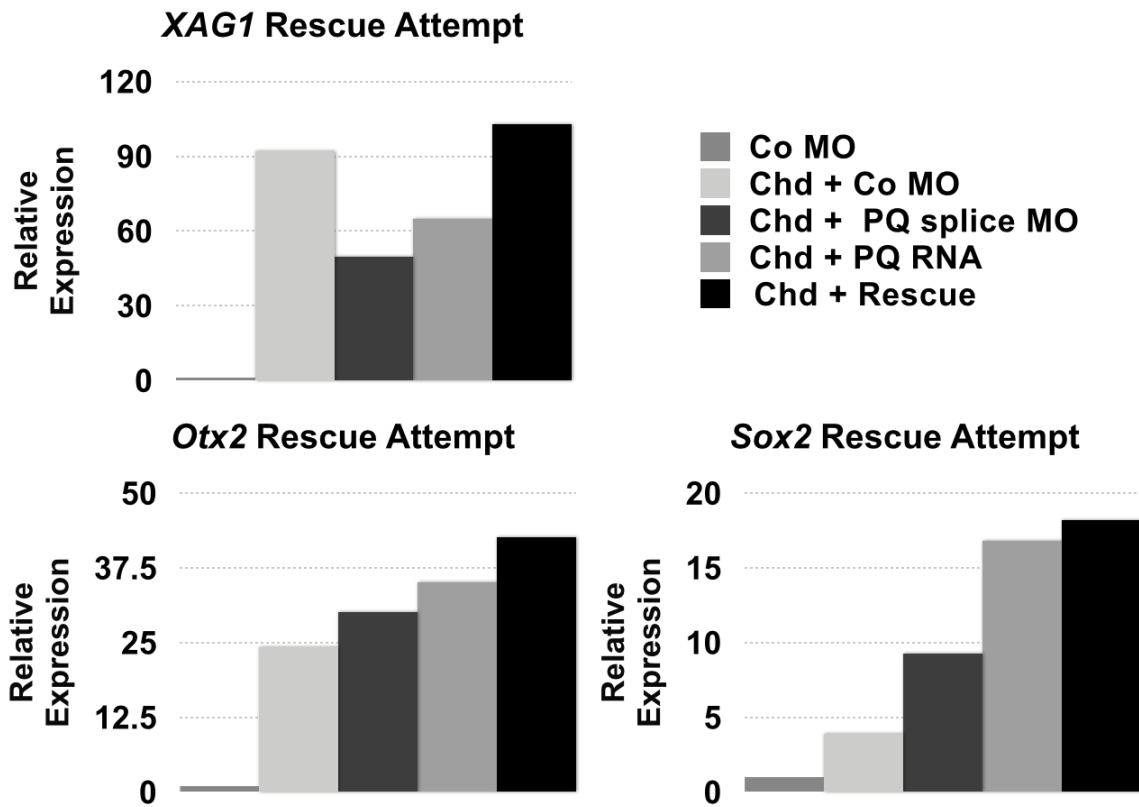


Figure 22: PQBP1 morpholino and *pqbp1* mRNA appear to induce similar changes in marker expression. PQBP1 morpholino-induced marker expression changes cannot be rescued by co-injection of *pqbp1* mRNA.

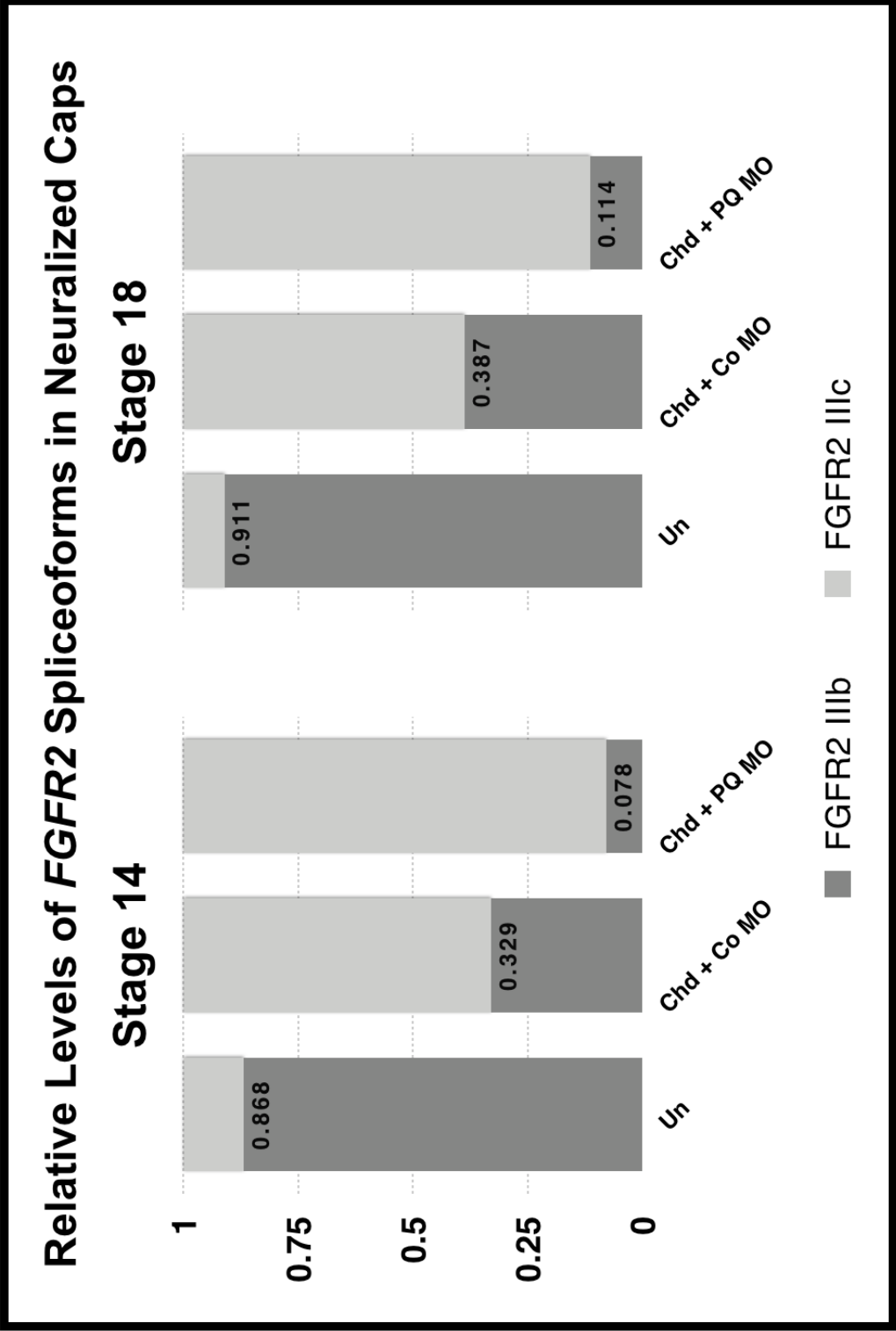


Figure 23: PQBP1 morpholino injection changes the relative levels of the *FGFR2* spliceoforms IIIb (KGFR form) and IIIc (bek form) in neuralized animal caps. This change is the opposite of that observed in whole embryos following PQBP1 morpholino injection (see Iwasaki & Thomsen 2014).

Chapter 5: PQBP1 selectively influences the neural developmental circuit

5.1 Introduction

To complement the data on PQBP1 knockdown phenotypes in tailbud stage embryos as well as marker expression in neuralized caps, whole mount *in situ* hybridization was performed on both neurula and tailbud stage embryos to further investigate relevant marker expression in the context of the intact embryo. The markers and their role during neural and cement gland development are described in Table 1.

For these experiments, neural-fated blastomeres were targeted and successful targeting was identified through magenta-gal staining. Only embryos showing staining in the head region were utilized for the *in situs*. Although it is likely that some of the effects observed are due to mesodermal influences, the injected PQBP1 morpholino would be expected to be concentrated in the head region in these embryos.

5.2 Results

5.2.1 Targeted PQBP1 knockdown in early neurula stages impacts a subset of neural markers

Morpholino injections were targeted into one dorsal blastomere at the 4-8 cell stage. The morpholino was injected along with β -galactoside as a lineage tracer. The uninjected sides of the embryos served as internal controls. Table 8 shows a summary of the effect of PQBP1 knockdown on marker expression at mid-neurula

stages (NF Stages 15-17). *NCAM*, *pax6*, *XAG1*, and *otx2* showed the most robust changes. Figure 24 shows representative expression patterns seen in each marker following knockdown.

Control embryos were also stained alongside the PQBP1 knockdown embryos. No changes in expression were seen in the injected versus uninjected sides of the embryos for any of the markers (data not shown).

5.2.2 Marker expression is altered in tailbud stage embryos

Tailbud (NF Stage 27) embryos were also used to examine marker expression using whole mount *in situ* hybridization (Figure 25). A number of markers showed increased or ectopic expression following PQBP1 knockdown, including *en2* and *pax6*. Others showed a reduction, namely *coe2*, *zic2*, and *zic1*. Although the concentration of *N-tubulin* appears to be reduced, especially in the anterior head region, the expression domain seems to be expanded. *Sox2*, *neuroD*, and *xag1* were unchanged. The higher level of *pax6* expression, as well as the reduced levels of *N-tubulin*, *zic2*, and *coe2* are consistent with the changes observed in mid-neurula stage embryos. However, the expression of *sox2* seemed to have recovered by this stage, while *zic2* was ectopically expressed, despite no change being recorded in the younger embryos.

5.3 Discussion

Modified marker expression was observed in neurula and tailbud stage embryos following neural-targeted PQBP1 knockdown. The changes seen at the two stages were

not always equivalent. The results of these *in situs* were largely consistent with RT-qPCR data, with the exception of *N-tubulin*, whose expression appeared to be reduced in neurula stage embryos but increased in the neuralized animal caps. However, as discussed in Chapter 4, this may be due to a delayed neurogenesis because of earlier interference with determination and differentiation in PQBP1 knockdown conditions. Interestingly, the expression domain of *N-tubulin* in the tailbud stage embryos appears to be expanded, although the concentration of transcript may be reduced. Therefore, it is difficult to determine whether the overall level of *N-tubulin* is in fact decreased or increased.

In neurulae, PQBP1 knockdown resulted in an expanded region of *pax6* expression. In tailbud embryos, *Pax6* was expressed in a discrete patch in the posterior head region, in which no expression was seen on the uninjected side. Interestingly, the *pax6* overexpression / ectopic expression induced by PQBP1 knockdown does not lead to the formation of additional eye structures, but rather, reduced or missing eyes. *Pax6* is subject to complex transcriptional regulation. In vertebrates, at least two *pax6* transcripts (*pax6* and *pax6(5a)*) are produced by alternative splicing and/or the use of alternative promoters (Nakayama et al. 2015; Martha et al. 1995; Epstein et al. 1994). In addition, *pax6* is involved in an autoregulatory positive feedback loop in which the introduction of additional *pax6* increases further expression levels, and it appears that any isoform can stimulate expression of all *pax6* transcripts (Pinson et al. 2006). Although it is unclear whether *Xenopus* produces multiple *pax6* transcripts through alternative splicing, a number of transcripts (and corresponding protein products) of different lengths are found on RefSeq. Presumably, these alternate transcripts may

have different functions during the process of eye development. It is possible that this differential expression may be altered in PQBP1 knockdown conditions, and thus can influence the function of PAX6.

Sox2 expression, although decreased in a substantial subset of neurula stage embryos, appeared to recover by NF Stage 27. However, since Stage 27 is well past the primary period of early neural induction during which *sox2* is essential, any neural defects due to the early change in *sox2* levels probably cannot be rescued by this later normalization of expression. To further investigate this, it would be useful to obtain *sox2* in situ on intermediate stages of embryos (between NF Stages 15 and 27), which might provide a clearer picture of when during development the *sox2* transcriptional level is recovered.

Consistent with RT-qPCR data, *XAG1* expression is reduced in neurula-stage embryos, although its expression also appears to recover by NF Stage 27. No defects in the phenotypic appearance of the cement gland were seen in the older embryos, consistent with prior observations.

Although *zic1* and *zic2* are both involved in promoting neural ectoderm competence, they responded differently to PQBP1 knockdown. In neurulae, *zic2* expression was reduced in about 40% of stained embryos; a reduction was also observed in the tailbud embryos. However, there was no apparent change in *zic1* expression at the earlier stage, while a reduction was seen in tailbud embryos. These results imply that PQBP1 may play a role in neural competence. If this is indeed a function of PQBP1, I would expect this role to be minor, based on the observations that in the majority of neurulae *zic2* transcript levels appeared unchanged, and *zic1*

expression was not impacted until later developmental stages, at least until neurulation was well underway.

The apparent reduction in *coe2* expression in the NF Stage 27 embryos may indicate that knockdown embryos have a defect in neuronal differentiation, which is promoted by *coe2*. In addition, *coe2* promotes expression of *N-tubulin*, so a reduction in *coe2* transcripts could be correlated with the observed decrease in *N-tubulin* in knockdown embryos (Green & Vetter 2011).

En2 marks the mid/hindbrain region. One of the functions of *En2* is to promote neuronal differentiation and cell cycle exit. A reduction in *en2* levels has been shown to lead to a variety of defects in both model organisms and humans, including absence of the midbrain and upper pons and autism-like phenotypes (Koenig et al. 2010; Sarnat et al. 2002; Cheh et al. 2006; Rossman et al. 2014). In PQBP1 knockdown tailbud embryos, *en2* levels appear to be increased. Since PQBP1 knockdown overall appears to help maintain neural regions in an undifferentiated state, perhaps this increased expression is an indirect defect of delayed neural differentiation.

Overall, PQBP1 appears to have a function in neural specification and differentiation, as knockdown decreases expression of early neural specifiers and later differentiation markers, as well as shifting the expression pattern of other markers to later developmental stages.

5.4 Future Directions

There are several possibilities for expanding on the *in situ* experiments presented here. Additional replicates could be done in order to obtain a more robust picture of markers for which few replicates were available. In addition, marker expression could be examined over shorter time intervals, which would help define when during development changes in expression are occurring. More neural markers could be utilized to obtain a better overview of the position of PQBP1 in the neural developmental circuit.

Further examination of possible *pax6* isoforms by the creation of isoform-specific *in situ* probes, as well as the use of homeolog-specific probes, would refine the data presented here. Data from an RNA-seq experiment on neuralized caps (as proposed in Chapter 4) would also provide more relevant markers to look at by *in situ* hybridization, and may narrow down the focus on a particular aspect of neural development.

5.5 Materials and Methods

5.5.1 Microinjection and embryo culture

Microinjection and embryo culture were performed as in 3.5.2.

5.5.2 Whole mount *in situ* hybridization

The same methods were followed as in 2.5.1, with the modification that embryos were generally stained for several hours at room temperature (and if necessary, at 4

degrees thereafter). The *pqbp1* in situ probes used were mostly obtained from the European *Xenopus* Resource Center. Some of these were not used in the *in situ* pictures shown here, but I have included them for future reference.

Probe sources:

<i>Pqbp1</i>	Iwasaki & Thomsen 2014
<i>PAX6</i>	Thomsen lab stock
<i>Brachyury</i>	Thomsen lab stock
<i>Tbx5</i>	Thomsen lab stock
<i>En2</i>	Thomsen lab stock
<i>Hoxb9</i>	Thomsen lab stock
<i>NCAM</i>	EXRC, Clone NP-33
<i>FGF4</i>	EXRC, Clone NP-70
<i>Krox20</i>	EXRC, Clone 6
<i>Otx2</i>	EXRC, Clone KL-70
<i>N-tubulin</i>	EXRC, Clone 5571885
<i>En2</i>	EXRC, Clone p33
<i>XAG1</i>	EXRC, Clone XAG-1-pGEM-T
<i>Zic1 (Opil)</i>	EXRC, Clone Opil
<i>Zic2</i>	EXRC, Clone NP-152
<i>Geminin</i>	EXRC, Clone NP-252
<i>Coe2 (Ebf2-a)</i>	EXRC, Clone NP-52
<i>Cbfa2t2 (XETOR)</i>	EXRC, Clone 790

<i>NeuroD</i>	EXRC, Clone KL-77
<i>Pax3</i>	EXRC, Clone 863
<i>Neurogenin2</i>	EXRC, Clone NP-32

5.6 Figures and Tables

Table 8: Expression Changes By Marker (NF Stage 18-21 Embryos)

Marker	Percent (Number) with Decreased Expression	Percent (Number) with Unchanged Expression	Percent (Number) with Increased Expression	Total Number of Embryos	Total Number of Experiments
<i>Pax6</i>	4 (1)	17 (4)	78 (18)	23	8
<i>N-tubulin</i>	100 (14)	0 (0)	0 (0)	14	6
<i>Zic2</i>	40 (8)	55 (11)	5 (1)	20	5
<i>Ngnr-1</i>	17 (2)	83 (10)	0 (0)	12	3
<i>Elf2 (Coe2)</i>	64 (7)	27 (3)	9 (1)	11	4
<i>XAG1</i>	88 (7)	12 (1)	0 (0)	8	3
<i>Sox2</i>	37 (6)	63 (10)	0 (0)	16	5
<i>NCAM</i>	86 (6)	14 (1)	0 (0)	7	3
<i>Otx2</i>	100 (3)	0 (0)	0 (0)	3	2
<i>Zic1</i>	0 (0)	100 (4)	0 (0)	4	1
<i>En2</i>	0 (0)	100 (4)	0 (0)	4	1

Embryos were injected with 18.75 ng control or PQBP1 splice morpholino, into one dorsal blastomere at the 4 or 8 cell stage.

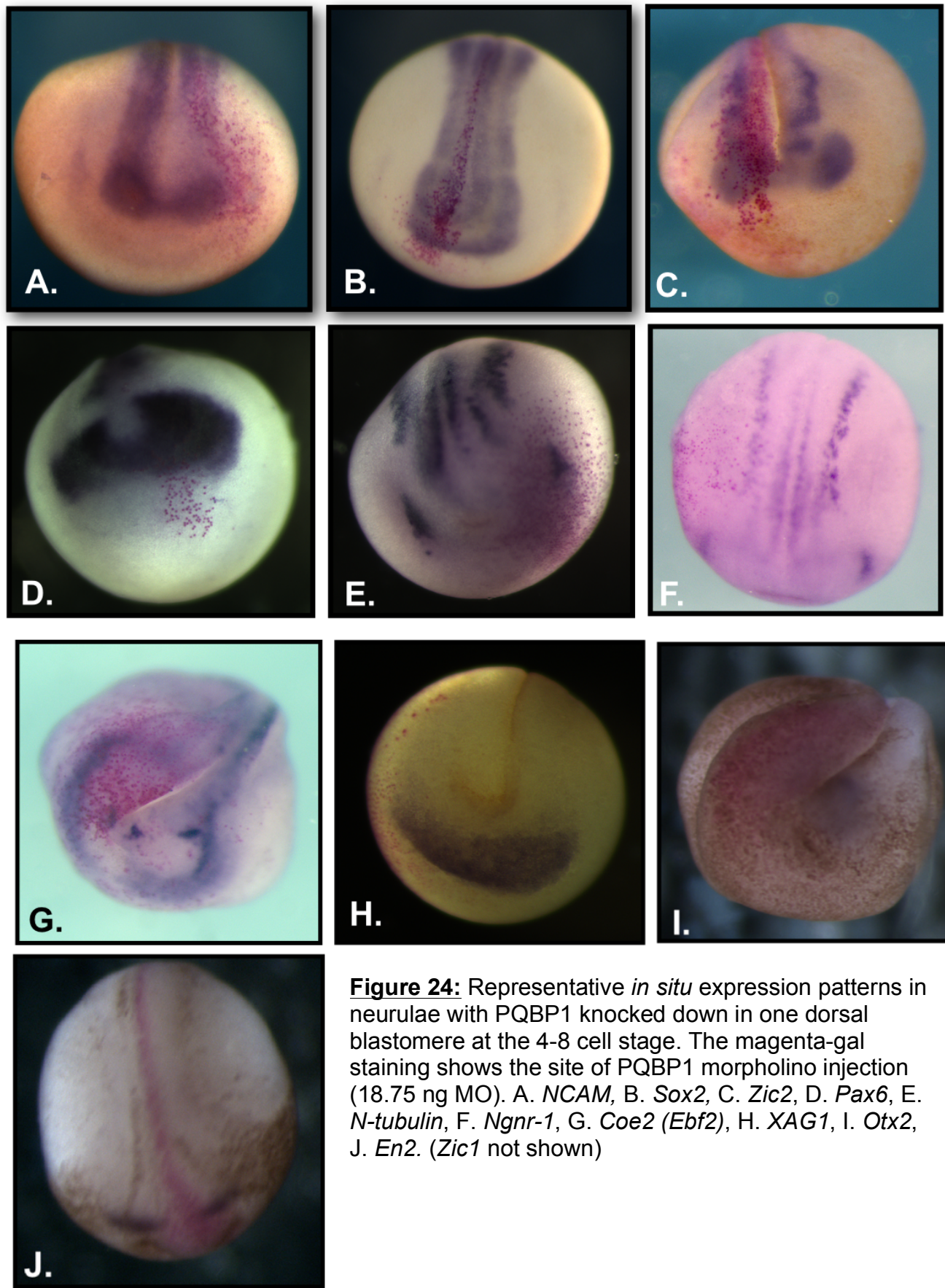


Figure 24: Representative *in situ* expression patterns in neurulae with PQBP1 knocked down in one dorsal blastomere at the 4-8 cell stage. The magenta-gal staining shows the site of PQBP1 morpholino injection (18.75 ng MO). A. *NCAM*, B. *Sox2*, C. *Zic2*, D. *Pax6*, E. *N-tubulin*, F. *Ngnr-1*, G. *Coe2 (Ebf2)*, H. *XAG1*, I. *Otx2*, J. *En2*. (*Zic1* not shown)

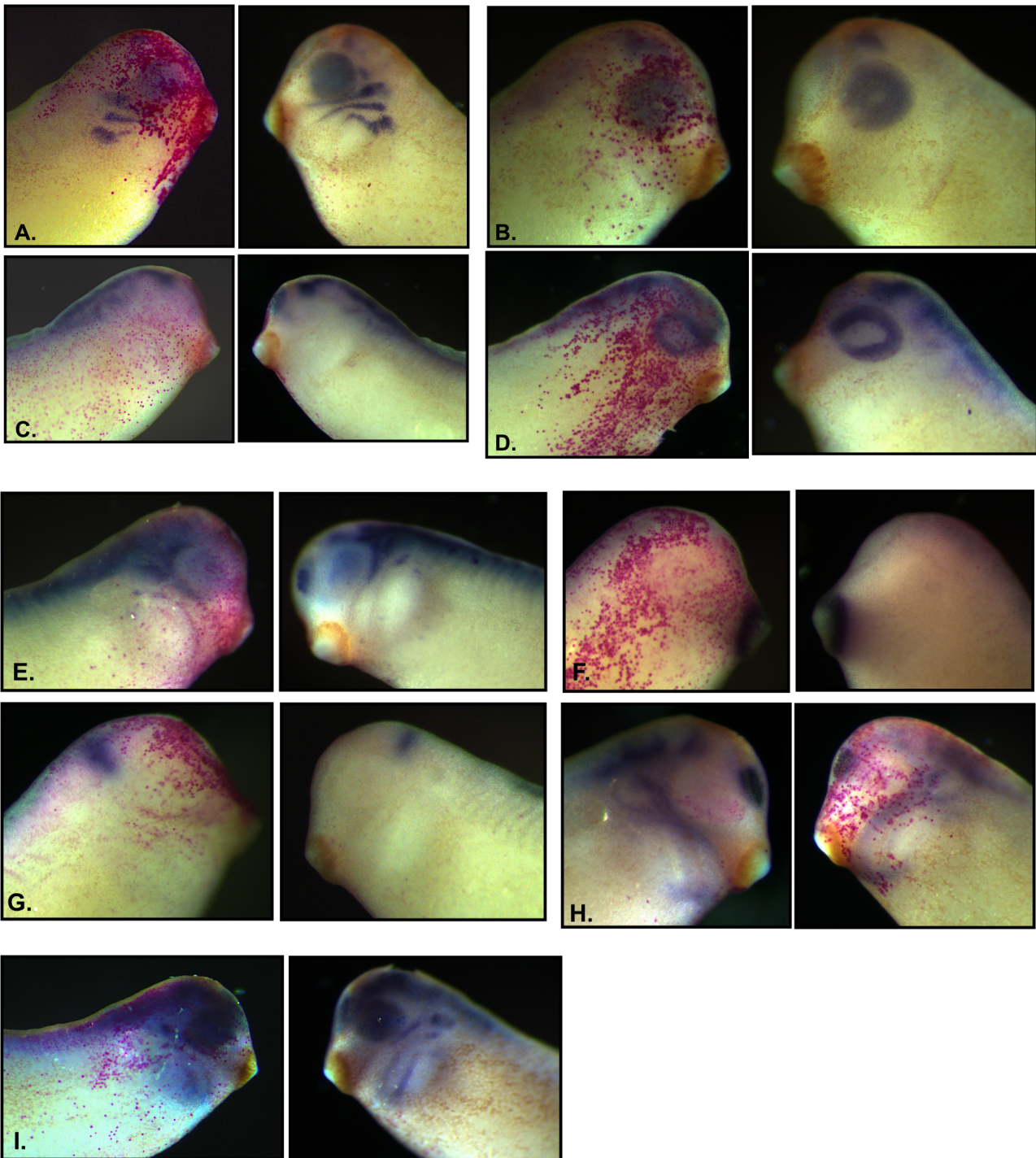


Figure 25: Representative *in situ* expression patterns in NF Stage 27 embryos with PQBP1 knocked down in one dorsal blastomere at the 4-8 cell stage. The magenta-gal staining shows the site of PQBP1 morpholino injection (18.75 ng MO). A. *NeuroD*, B. *Pax6*, C. *Zic1*, D. *Zic2*, E. *N-tubulin*, F. *XAG1*, G. *En2*, H. *Coe2 (Ebf2)*, I. *Sox2*.

Chapter 6: PQBP1 likely acts during early neural specification

Based on the data presented here, PQBP1 was placed in a simplified neural regulatory network as shown in Figure 26. It is important to note several caveats when interpreting this figure. The neural regulatory network of *Xenopus laevis* is by no means completely understood, and it is highly likely that there are many additional interactions involved. Moreover, only the major factors implicated in early neural induction and specification are shown. However, based on what has been discovered regarding the effect of PQBP1 protein knockdown on embryonic phenotype and neural marker expression, a number of logical inferences can be made. Here, I have built upon a network initially proposed by Rogers et al. (2009).

Given the impact of PQBP1 knockdown on both *geminin* and *sox2*, as well as the knowledge that *sox2* is involved in the regulation of *pqbp1*, it is probable that *pqbp1* is involved in early aspects of neural specification and induction (Li et al. 2013). As *geminin* is involved in maintaining an immature neural state, the increase in *geminin* expression following PQBP1 knockdown suggests a possible role for PQBP1 in promoting neural specification or differentiation. The decreased expression seen in *sox2*, which is known to be involved in the maintenance of ectoderm competence and neural progenitor states, also suggests that PQBP1 is involved in the process by which the embryo establishes the correct number of neural progenitors.

Given the prevalence of eye defects following knockdown, PQBP1 likely affects eye development either directly or indirectly. In fact, *sox2* overexpression promotes the formation of neural tissue at the expense of epidermis, and, conversely, *sox2* mutations can lead to anophthalmia or microphthalmia in human patients through a reduction in

retinal neural progenitor competence (Ellis et al. 2004; Bakrania et al. 2007; Taranova et al. 2006). *Sox2* is also known to regulate *pax6*, which is a definitive eye field marker. Therefore, the observed reduction in *sox2* expression following PQBP1 knockdown could be expected to have a significant impact on eye development, and the observed whole embryo phenotypes are consistent with those seen in human patients.

Interestingly, while PQBP1 knockdown in *Xenopus* animal cap explants leads to a reduction in *pax6* expression, knockdown in the whole embryo appears to change the region of expression. Either a reduction in or misexpression of *pax6* could influence proper development of the eye field.

PQBP1 knockdown reliably produces a reduction in *otx2* expression. *Otx2* is involved in the development of brain structures as well as the cement gland (through its induction of *XAG1*). The lowered level of *XAG1* expression seen in neurulae following PQBP1 knockdown is likely an indirect effect through *otx2*, since both *XAG1* expression and cement gland formation appear to recover by later tadpole stages. It is possible that *pqbp1* impacts *otx2* directly; however, *pqbp1* could also be exerting these effects through its influence on *geminin* and/or *sox2* expression. This also applies to the changes observed in *zic1*, *zic2*, *en2*, and *NCAM*.

It is likely that the changes observed in the bHLH transcription factors, including *ngnr-1*, *neuroD*, *ebf2*, and *N-tub*, are indirect effects as well, since the impact of PQBP1 knockdown is greater and more consistent on the more downstream factors, primarily *N-tubulin*. It is possible that this effect is due to smaller changes upstream, that eventually have a greater impact on the downstream targets.

While the data shown suggest that PQBP1 targets factors involved in early neural specification, the complexity of neural regulation and our incomplete knowledge of the players involved in the regulatory network prevent more specific conclusions from being drawn. Further study is critical to inform us of the precise mechanism of action of PQBP1. It would be useful to combine PQBP1 knockdown with overexpression of potential direct targets, to observe whether similar changes are still observed. Increasing the number and broadening the scope of neural factors examined could also help pinpoint the timing and targets of PQBP1 activity. Additional information about the precise cellular localization of PQBP1 during a range of developmental stages, gleaned from studies such as whole brain and brain section *in situs*, would help narrow down the possible molecular pathways, as well as developmental time frames, in which PQBP1 is playing an important role.

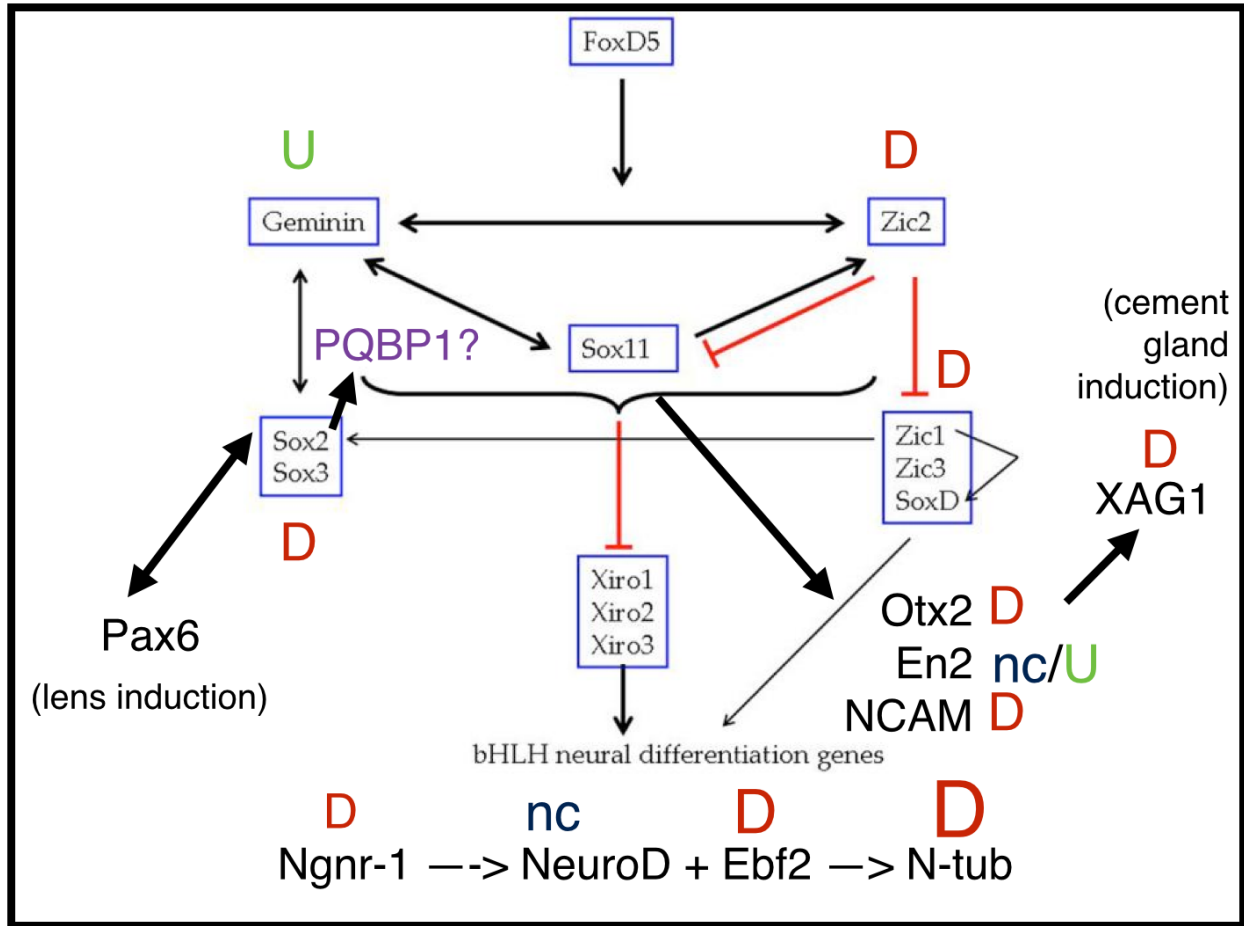


Figure 26: Proposed placement of PQBP1 in a simplified neural regulatory network. D= downregulated expression, U = upregulated expression, nc = no change (all as assayed by *in situ* hybridization). The size of the letters corresponds to the strength of the effect on expression following *pqbp1* knockdown (modified from Rogers et al. 2009).

Bibliography

- Alexandrova, E.M. & Thomsen, G.H., 2006. Smurf1 regulates neural patterning and folding in *Xenopus* embryos by antagonizing the BMP/Smad1 pathway. *Developmental Biology*, 299(2), pp.398–410.
- Appler, J.M. & Goodrich, L. V., 2011. Connecting the ear to the brain: Molecular mechanisms of auditory circuit assembly. *Progress in Neurobiology*, 93(4), pp.488–508.
- Aranda, P.S., Lajoie, D.M. & Jorcyk, C.L., 2012. Bleach gel: A simple agarose gel for analyzing RNA quality. *Electrophoresis*, 33(2), pp.366–369.
- Archidiacono, N. et al., 1987. X-linked mental retardation. II. Renpenning syndrome and other types (report of 14 families). *Journal de genetique humaine*, 35(5), pp.381–398.
- Baker, C.V.. & Bronner-Fraser, M., 1997. The origins of the neural crest. Part I: embryonic induction. *Mechanisms of Development*, 69(1-2), pp.3–11.
- Bakrania, P. et al., 2007. SOX2 anophthalmia syndrome: 12 new cases demonstrating broader phenotype and high frequency of large gene deletions. *The British journal of ophthalmology*, 91(11), pp.1471–1476.
- Barrios-Rodiles, M. et al., 2005. High-throughput mapping of a dynamic signaling network in mammalian cells. *Science (New York, N.Y.)*, 307(5715), pp.1621–1625.
- Bentaya, S. et al., 2012. The RNA-binding protein XSeb4R regulates maternal Sox3 at the posttranscriptional level during maternal-zygotic transition in *Xenopus*. *Developmental Biology*, 363(2), pp.362–372.
- Bill, B.R. et al., 2009. A primer for morpholino use in zebrafish. *Zebrafish*, 6(1), pp.69–77.
- Bradley, L., Wainstock, D. & Sive, H., 1996. Positive and negative signals modulate formation of the *Xenopus* cement gland. *Development (Cambridge, England)*, 122(9), pp.2739–2750.
- Busch, A. et al., 2003. Mutant huntingtin promotes the fibrillogenesis of wild-type huntingtin: A potential mechanism for loss of huntingtin function in Huntington's disease. *Journal of Biological Chemistry*, 278(42), pp.41452–41461.
- Cheh, M.A. et al., 2006. En2 knockout mice display neurobehavioral and neurochemical alterations relevant to autism spectrum disorder. *Brain Research*, 1116(1), pp.166–176.

- Cossée, M. et al., 2006. Exonic microdeletions in the X-linked PQBP1 gene in mentally retarded patients: a pathogenic mutation and in-frame deletions of uncertain effect. *European journal of human genetics : EJHG*, 14(4), pp.418–425.
- Dawid, I.B. & Sargent, T.D., 1988. *Xenopus laevis* in developmental and molecular biology. *Science (New York, N.Y.)*, 240(4858), pp.1443–1448.
- Eisen, J.S. & Smith, J.C., 2008. Controlling morpholino experiments: don't stop making antisense. *Development (Cambridge, England)*, 135(10), pp.1735–1743.
- Ekker, S.C., 2000. Morphants: a new systematic vertebrate functional genomics approach. *Yeast (Chichester, England)*, 17(4), pp.302–306.
- Ellis, P. et al., 2004. SOX2, a persistent marker for multipotential neural stem cells derived from embryonic stem cells, the embryo or the adult. *Developmental Neuroscience*, 26(2-4), pp.148–165.
- Epstein, J.A. et al., 1994. Two independent and interactive DNA-binding subdomains of the Pax6 paired domain are regulated by alternative splicing. *Genes and Development*, 8(17), pp.2022–2034.
- Fletcher, R.B., Baker, J.C. & Harland, R.M., 2006. FGF8 spliceforms mediate early mesoderm and posterior neural tissue formation in *Xenopus*. *Development (Cambridge, England)*, 133(9), pp.1703–1714.
- Fletcher, R.B. & Harland, R.M., 2008. The role of FGF signaling in the establishment and maintenance of mesodermal gene expression in *Xenopus*. *Developmental Dynamics*, 237(5), pp.1243–1254.
- Flynn, M., Zou, Y.S. & Milunsky, A., 2011. Whole gene duplication of the PQBP1 gene in syndrome resembling Renpenning. *American Journal of Medical Genetics, Part A*, 155(1), pp.141–144.
- Fukuchi-Shimogori, T. & Grove, E.A., 2001. Neocortex patterning by the secreted signaling molecule FGF8. *Science (New York, N.Y.)*, 294(5544), pp.1071–1074.
- Garel, S., Huffman, K.J. & Rubenstein, J.L.R., 2003. Molecular regionalization of the neocortex is disrupted in Fgf8 hypomorphic mutants. *Development (Cambridge, England)*, 130(9), pp.1903–1914.
- Germanaud, D. et al., 2011. The Renpenning syndrome spectrum: new clinical insights supported by 13 new PQBP1-mutated males. *Clinical genetics*, 79(3), pp.225–235.
- Golabi, M., Ito, M. & Hall, B.D., 1984. *A new X-linked multiple congenital anomalies/mental retardation syndrome.*

- Gould, S.E. & Grainger, R.M., 1997. Neural induction and antero-posterior patterning in the amphibian embryo: Past, present and future. *Cellular and Molecular Life Sciences*, 53(4), pp.319–338.
- Graziadei, P.P.C. & Monti-Graziadei, A.G., 1992. The influence of the olfactory placode on the development of the telencephalon in *Xenopus laevis*. *Neuroscience*, 46(3), pp.617–629.
- Green, Y.S. & Vetter, M.L., 2011. EBF factors drive expression of multiple classes of target genes governing neuronal development. *Neural development*, 6, p.19.
- Guo, X. et al., 2014. Efficient RNA/Cas9-mediated genome editing in *Xenopus tropicalis*. *Development (Cambridge, England)*, 141(3), pp.707–14.
- Gurdon, J., 1971. Use of Frog Eggs and Oocytes for the Study of Messenger RNA and its Translation. *Nature*.
- Gurdon, J.B. & Hopwood, N., 2000a. The introduction of *Xenopus laevis* into developmental biology: Of empire, pregnancy testing and ribosomal genes. *International Journal of Developmental Biology*, 44(1 SPEC. ISS. 1), pp.43–50.
- Gurdon, J.B. & Hopwood, N., 2000b. The introduction of *Xenopus laevis* into developmental biology: Of empire, pregnancy testing and ribosomal genes. *International Journal of Developmental Biology*, 44(1 SPEC. ISS. 1), pp.43–50.
- Harland, R.M., 1991. Appendix G: In Situ Hybridization: An Improved Whole-Mount Method for *Xenopus* Embryos BT - Methods in cell biology. In *Methods in cell biology*. pp. 685–695.
- He, X. et al., 1989. Expression of a large family of POU-domain regulatory genes in mammalian brain development. *Nature*, 340(6228), pp.35–41.
- Heasman, J., 2002. Morpholino oligos: making sense of antisense? *Developmental biology*, 243(2), pp.209–214.
- Heasman, J., Kofron, M. & Wylie, C., 2000. Beta-catenin signaling activity dissected in the early *Xenopus* embryo: a novel antisense approach. *Developmental biology*, 222(1), pp.124–134.
- Heeg-Truesdell, E. & LaBonne, C., 2006. Neural induction in *Xenopus* requires inhibition of Wnt- β -catenin signaling. *Developmental Biology*, 298(1), pp.71–86.
- Hogel, M., Laprairie, R.B. & Denovan-Wright, E.M., 2012. Promoters are differentially sensitive to N-terminal mutant huntingtin-mediated transcriptional repression. *PLoS ONE*, 7(7).

- Holzmann, K. et al., 2012. Alternative splicing of fibroblast growth factor receptor IgIII loops in cancer. *Journal of Nucleic Acids*, 2012.
- Huch, S. & Nissan, T., 2014. Interrelations between translation and general mRNA degradation in yeast. *Wiley Interdisciplinary Reviews: RNA*.
- Imafuku, I. et al., 1998. Polar amino acid-rich sequences bind to polyglutamine tracts. *Biochemical and biophysical research communications*, 253(1), pp.16–20.
- Ip, C. et al., 2014. Head formation: OTX2 regulates Dkk1 and Lhx1 activity in the anterior mesendoderm. *Development*, 141(20), pp.3859–67.
- Ito, H. et al., 2014. In utero gene therapy rescues microcephaly caused by Pqbp1-hypofunction in neural stem progenitor cells. *Molecular Psychiatry*, (April), pp.1–13.
- Ito, H. et al., 2009. Knock-down of PQBP1 impairs anxiety-related cognition in mouse. *Human Molecular Genetics*, 18(22), pp.4239–4254.
- Iwamoto, K., Huang, Y. & Ueda, S., 2000. Genomic organization and alternative transcript of the human PQBP-1 gene. *Gene*, 259(1-2), pp.69–73.
- Iwasaki, Y. & Thomsen, G.H., 2014. The splicing factor PQBP1 regulates mesodermal and neural development through FGF signaling. *Development (Cambridge, England)*, 141(19), pp.3740–51.
- Jaglin, X.H. et al., 2009. Mutations in the beta-tubulin gene TUBB2B result in asymmetrical polymicrogyria. *Nature genetics*, 41(6), pp.746–752.
- Josephson, R. et al., 1998. POU transcription factors control expression of CNS stem cell-specific genes. *Development (Cambridge, England)*, 125(16), pp.3087–3100.
- Kao, K.R. & Elinson, R.P., 1988. The entire mesodermal mantle behaves as Spemann's organizer in dorsoanterior enhanced *Xenopus laevis* embryos. *Developmental biology*, 127(1), pp.64–77.
- Keller, R., Clark, W.H. & Griffin, F. eds., 1992. *Gastrulation*, Boston, MA: Springer US.
- Khokha, M.K. et al., 2005. Depletion of three BMP antagonists from Spemann's organizer leads to a catastrophic loss of dorsal structures. *Developmental Cell*, 8(3), pp.401–411.
- Khokha, M.K. et al., 2002. Techniques and probes for the study of *Xenopus tropicalis* development. *Developmental Dynamics*, 225(4), pp.499–510.

- Kleefstra, T. et al., 2004. Genotype-phenotype studies in three families with mutations in the polyglutamine-binding protein 1 gene (PQBP1). *Clinical Genetics*, 66(4), pp.318–326.
- Koenig, S.F. et al., 2010. En2, Pax2/5 and Tcf-4 transcription factors cooperate in patterning the *Xenopus* brain. *Developmental biology*, 340(2), pp.318–28.
- Kok, F.O. et al., 2014. Reverse Genetic Screening Reveals Poor Correlation between Morpholino-Induced and Mutant Phenotypes in Zebrafish. *Developmental Cell*, 32(1), pp.97–108.
- Komiyama, T. et al., 2003. From lineage to wiring specificity: POU domain transcription factors control precise connections of *Drosophila* olfactory projection neurons. *Cell*, 112(2), pp.157–167.
- Komuro, A., Saeki, M. & Kato, S., 1999a. Association of two nuclear proteins, Npw38 and NpwBP, via the interaction between the WW domain and a novel proline-rich motif containing glycine and arginine. *Journal of Biological Chemistry*, 274(51), pp.36513–36519.
- Komuro, A., Saeki, M. & Kato, S., 1999b. Npw38, a novel nuclear protein possessing a WW domain capable of activating basal transcription. *Nucleic Acids Research*, 27(9), pp.1957–1965.
- Kunde, S.A. et al., 2011. The X-chromosome-linked intellectual disability protein PQBP1 is a component of neuronal RNA granules and regulates the appearance of stress granules. *Human Molecular Genetics*, 20(24), pp.4916–4931.
- Kuroda, H., Wessely, O. & De Robertis, E.M., 2004. Neural induction in *Xenopus*: Requirement for ectodermal and endomesodermal signals via Chordin, Noggin, β -Catenin, and Cerberus. *PLoS Biology*, 2(5).
- Kurosaki, T., Gojobori, J. & Ueda, S., 2012. Comparative genetics of the poly-Q tract of ataxin-1 and its binding protein PQBP-1. *Biochemical Genetics*, 50(3-4), pp.309–17.
- Laskey, R. et al., 1977. Protein synthesis in oocytes of *Xenopus laevis* is not regulated by the supply of messenger RNA. *Cell*.
- Latchman, D.S., 1999. POU family transcription factors in the nervous system. *Journal of Cellular Physiology*, 179(2), pp.126–133.
- Lei, Y. et al., 2012. Efficient targeted gene disruption in *Xenopus* embryos using engineered transcription activator-like effector nucleases (TALENs). *Proceedings of the National Academy of Sciences*, 109(43), pp.17484–17489.

- Lenski, C. et al., 2004. Novel truncating mutations in the polyglutamine tract binding protein 1 gene (PQBP1) cause Renpenning syndrome and X-linked mental retardation in another family with microcephaly. *American journal of human genetics*, 74(4), pp.777–80.
- Li, C. et al., 2013. Sox2 transcriptionally regulates PQBP1, an intellectual disability-microcephaly causative gene, in neural stem progenitor cells. *PLoS ONE*, 8(7), p.e68627.
- Liang, P. et al., 2015. CRISPR/Cas9-mediated gene editing in human tripronuclear zygotes. *Protein & cell*.
- Lubs, H. et al., 2006. Golabi-Ito-Hall syndrome results from a missense mutation in the WW domain of the PQBP1 gene. *Journal of medical genetics*, 43(6), p.e30.
- Maggio, I. & Gonçalves, M.A.F. V, 2015. Genome editing at the crossroads of delivery, specificity, and fidelity. *Trends in biotechnology*, 33(5), pp.280–291.
- Mai, S. et al., 2010. The missense mutation W290R in Fgfr2 causes developmental defects from aberrant IIIb and IIIc signaling. *Developmental dynamics : an official publication of the American Association of Anatomists*, 239(6), pp.1888–900.
- Martha, A. et al., 1995. Three novel aniridia mutations in the human PAX6 gene. *Human Mutation*, 6(1), pp.44–49.
- Martínez-Garay, I. et al., 2007. A two base pair deletion in the PQBP1 gene is associated with microphthalmia, microcephaly, and mental retardation.,
- Michalik, A. & Van Broeckhoven, C., 2003. Pathogenesis of polyglutamine disorders: aggregation revisited. *Human molecular genetics*, 12 Spec No, pp.R173–R186.
- Michiue, T. et al., 2007. Xenopus galectin-VIa shows highly specific expression in cement glands and is regulated by canonical Wnt signaling. *Gene Expression Patterns*, 7(8), pp.852–857.
- Mizuguchi, M. et al., 2014. Mutations in the PQBP1 gene prevent its interaction with the spliceosomal protein U5-15kD. *Nature communications*, 5, p.3822.
- Moody, S.A., 1987a. Fates of the blastomeres of the 16-cell stage Xenopus embryo. *Developmental biology*, 119(2), pp.560–578.
- Moody, S.A., 1987b. Fates of the blastomeres of the 32-cell-stage Xenopus embryo. *Developmental biology*, 122(2), pp.300–319.
- Moody, S.A. & Kline, M.J., 1990. Segregation of fate during cleavage of frog (*Xenopus laevis*) blastomeres. *Anatomy and Embryology*, 182(4), pp.347–362.

- Musante, L. et al., 2010. Common pathological mutations in PQBP1 induce nonsense-mediated mRNA decay and enhance exclusion of the mutant exon. *Human Mutation*, 31(1), pp.90–98.
- Nakajima, K. et al., 2013. Targeted Gene Disruption in the *Xenopus tropicalis* Genome using Designed TALE Nucleases. *Zoological science*, 30(6), pp.455–60.
- Nakayama, T. et al., 2013. Simple and efficient CRISPR/Cas9-mediated targeted mutagenesis in *Xenopus tropicalis*. *Genesis*, 51(12), pp.835–843.
- Nakayama, T. et al., 2015. *Xenopus pax6* mutants affect eye development and other organ systems, and have phenotypic similarities to Human aniridia patients. *Developmental Biology*.
- Nasevicius, A. & Ekker, S.C., 2000. Effective targeted gene “knockdown” in zebrafish. *Nature genetics*, 26(2), pp.216–220.
- Nasu, M., Mizuno, F. & Ueda, S., 2012. Comparative aspects of polyglutamine binding domain in PQBP-1 among Vertebrata. *Gene*, 511(2), pp.243–7.
- Nicolaescu, E. et al., 2008. Nature of the nuclear inclusions formed by PQBP1, a protein linked to neurodegenerative polyglutamine diseases. *European Journal of Cell Biology*, 87(10), pp.817–829.
- Nieuwkoop, P., 1977. Origin and establishment of embryonic polar axes in amphibian development. *Current topics in developmental biology*.
- Nieuwkoop, P., 1973. The organization center of the amphibian embryo: its origin, spatial organization, and morphogenetic action. *Advances in morphogenesis*.
- Nieuwkoop, P. & Faber, J., 1956. *Normal table of Xenopus laevis (Daudin). A systematical and chronological survey of the development from the fertilized egg till the end of metamorphosis*. P. Nieuwkoop & J. Faber, eds., Amsterdam: North-Holland Publishing Company. Guilders.
- Nieuwkoop, P., Faber, J. & Gurdon, J., 1995. Normal table of *Xenopus laevis* (Daudin). *Trends in Genetics*, 11(10), p.418.
- Nutt, S.L. et al., 2001. Comparison of Morpholino based translational inhibition during the development of *Xenopus laevis* and *Xenopus tropicalis*. *Genesis*, 30(3), pp.110–113.
- Okazawa, H. et al., 2002. Interaction between mutant ataxin-1 and PQBP-1 affects transcription and cell death. *Neuron*, 34(5), pp.701–713.

- Okuda, T. et al., 2003. PQBP-1 transgenic mice show a late-onset motor neuron disease-like phenotype. *Human Molecular Genetics*, 12(7), pp.711–725.
- Ornitz, D.M. et al., 1996. Receptor specificity of the fibroblast growth factor family. *The Journal of biological chemistry*, 271(25), pp.15292–15297.
- Orr-Urtreger, A. et al., 1993. Developmental localization of the splicing alternatives of fibroblast growth factor receptor-2 (FGFR2). *Developmental biology*, 158(2), pp.475–486.
- Pera, E.M. et al., 2014. Active signals, gradient formation and regional specificity in neural induction. *Experimental Cell Research*, 321(1), pp.25–31.
- Pinson, J. et al., 2006. Positive autoregulation of the transcription factor Pax6 in response to increased levels of either of its major isoforms, Pax6 or Pax6(5a), in cultured cells. *BMC developmental biology*, 6, p.25.
- Des Portes, V., 2013. X-linked mental deficiency. *Handbook of clinical neurology*, 111, pp.297–306.
- Qi, Y. et al., 2005. PQBP-1 is expressed predominantly in the central nervous system during development. *European Journal of Neuroscience*, 22(6), pp.1277–1286.
- Ramakers, C. et al., 2003. Assumption-free analysis of quantitative real-time polymerase chain reaction (PCR) data. *Neuroscience Letters*, 339(1), pp.62–66.
- Rash, B., Tomasi, S. & Lim, H., 2013. Cortical gyrification induced by fibroblast growth factor 2 in the mouse brain. *The Journal of ...*, 33(26), pp.10802–10814.
- Rejeb, I. et al., 2011. A novel frame shift mutation in the PQBP1 gene identified in a Tunisian family with X-linked mental retardation. *European journal of medical genetics*, 54(3), pp.241–6.
- Renpenning, H. et al., 1962. Familial sex-linked mental retardation. *Canadian Medical Association Journal*, 3(87), pp.954–6.
- Reuss, B. & Von Bohlen Und Halbach, O., 2003. Fibroblast growth factors and their receptors in the central nervous system. *Cell and Tissue Research*, 313(2), pp.139–157.
- De Robertis, E.M., 2006. Spemann's organizer and self-regulation in amphibian embryos. *Nature reviews. Molecular cell biology*, 7(4), pp.296–302.
- De Robertis, E.M. & Kuroda, H., 2004. Dorsal-ventral patterning and neural induction in *Xenopus* embryos. *Annual review of cell and developmental biology*, 20, pp.285–308.

- Robertson, A.L. & Bottomley, S.P., 2010. Towards the treatment of polyglutamine diseases: the modulatory role of protein context. *Current medicinal chemistry*, 17(27), pp.3058–3068.
- Rodnina, M. V., Vintermeyer, W. & Green, R. eds., 2011. *Ribosomes: Structure, Function, and Dynamics* 1st ed.,
- Rogers, C.D., Moody, S.A. & Casey, E.S., 2009. Neural induction and factors that stabilize a neural fate. *Birth Defects Research Part C - Embryo Today: Reviews*, 87, pp.249–262.
- Rossmann, I.T. et al., 2014. Engrailed2 modulates cerebellar granule neuron precursor proliferation, differentiation and insulin-like growth factor 1 signaling during postnatal development. *Molecular autism*, 5(1), p.9.
- Sarnat, H.B. et al., 2002. Agenesis of the mesencephalon and metencephalon with cerebellar hypoplasia: Putative mutation in the EN2 gene - Report of 2 cases in early infancy. *Pediatric and Developmental Pathology*, 5(1), pp.54–68.
- Schaefer, M.H., Wanker, E.E. & Andrade-Navarro, M.A., 2012. Evolution and function of CAG/polyglutamine repeats in protein-protein interaction networks. *Nucleic Acids Research*, 40(10), pp.4273–4287.
- Schlosser, G., 2006. Induction and specification of cranial placodes. *Developmental Biology*, 294(2), pp.303–351.
- Schlosser, G. & Ahrens, K., 2004. Molecular anatomy of placode development in *Xenopus laevis*. *Developmental Biology*, 271(2), pp.439–466.
- Schoenwolf, G.C. & Smith, J.L., 2000. Mechanisms of neurulation. *Methods in molecular biology (Clifton, N.J.)*, 136, pp.125–34.
- Schreiber, E. et al., 1993. cDNA cloning of human N-Oct3, a nervous-system specific POU domain transcription factor binding to the octamer DNA motif. *Nucleic acids research*, 21(2), pp.253–258.
- Shapiro, H. & Zwarenstein, H., 1935. A test for the early diagnosis of pregnancy on the South African clawed toad (*Xenopus laevis*). *South African MJ*.
- Shi, G. et al., 2010. Brn2 is a transcription factor regulating keratinocyte differentiation with a possible role in the pathogenesis of lichen planus. *PLoS ONE*, 5(10).
- Shimohata, T. et al., 2002. Expanded polyglutamine stretches form an “aggresome.” *Neuroscience Letters*, 323(3), pp.215–218.

- Shimohata, T., Onodera, O. & Tsuji, S., 2000. Interaction of expanded polyglutamine stretches with nuclear transcription factors leads to aberrant transcriptional regulation in polyglutamine diseases. In *Neuropathology*. pp. 326–333.
- Sive, H., Grainger, R. & Harland, R., 2000. Early development of *Xenopus laevis*: a laboratory manual.
- Stainier, D.Y.R., Kontarakis, Z. & Rossi, A., 2015. Making Sense of Anti-Sense Data. *Developmental Cell*, 32(1), pp.7–8.
- Stevenson, R.E. et al., 2005. Renpenning syndrome comes into focus. *American Journal of Medical Genetics*, 134 A(4), pp.415–421.
- Stevenson, R.E. et al., 1998. *Renpenning syndrome maps to Xp11.*
- Stout, R.P. & Graziadei, P.P.C., 1980. Influence of the olfactory placode on the development of the brain in *Xenopus laevis* (Daudin). *Neuroscience*, 5(12), pp.2175–2186.
- Sudol, M., McDonald, C.B. & Farooq, A., 2012. Molecular insights into the WW domain of the Golabi-Ito-Hall syndrome protein PQBP1. *FEBS Letters*, 586(17), pp.2795–2799.
- Takahashi, K. et al., 2009. Nematode homologue of PQBP1, a mental retardation causative gene, is involved in lipid metabolism. *PLoS ONE*, 4(1).
- Tamura, T. et al., 2013. A restricted level of PQBP1 is needed for the best longevity of *Drosophila*. *Neurobiology of Aging*, 34(1), pp.356.e11–20.
- Tamura, T. et al., 2010. *Drosophila* PQBP1 regulates learning acquisition at projection neurons in aversive olfactory conditioning. *The Journal of neuroscience : the official journal of the Society for Neuroscience*, 30(42), pp.14091–101.
- Tapia, V.E. et al., 2010. Y65C missense mutation in the WW domain of the Golabi-Ito-Hall syndrome protein PQBP1 affects its binding activity and deregulates pre-mRNA splicing. *Journal of Biological Chemistry*, 285(25), pp.19391–19401.
- Taranova, O. V. et al., 2006. SOX2 is a dose-dependent regulator of retinal neural progenitor competence. *Genes and Development*, 20(9), pp.1187–1202.
- Thisse, B. & Thisse, C., 2005. Functions and regulations of fibroblast growth factor signaling during embryonic development. *Developmental Biology*, 287(2), pp.390–402.

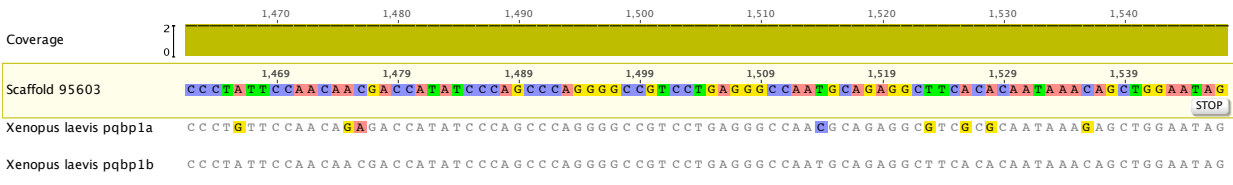
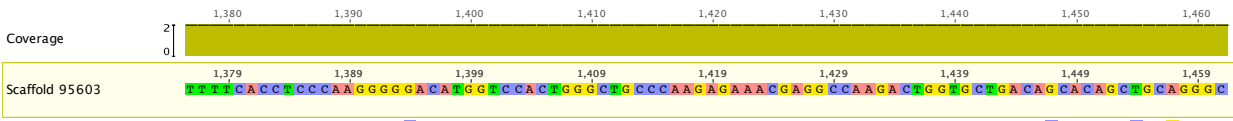
- Thurber, A.E. et al., 2011. Inverse expression states of the BRN2 and MITF transcription factors in melanoma spheres and tumour xenografts regulate the NOTCH pathway. *Oncogene*, 30(27), pp.3036–3048.
- Tong, X. et al., 2011. Ataxin-1 and Brother of ataxin-1 are components of the Notch signalling pathway. *EMBO reports*, 12(5), pp.428–435.
- Waldman, Y.Y. et al., 2011. Selection for translation efficiency on synonymous polymorphisms in recent human evolution. *Genome Biology and Evolution*, 3(1), pp.749–761.
- Wallingford, J.B. & Harland, R.M., 2001. Xenopus Dishevelled signaling regulates both neural and mesodermal convergent extension: parallel forces elongating the body axis. *Development (Cambridge, England)*, 128(13), pp.2581–2592.
- Wang, F. et al., 2015. Targeted gene disruption in *Xenopus laevis* using CRISPR/Cas9. *Cell & bioscience*, 5, p.15.
- Wang, Q. et al., 2013. PQBP1, a factor linked to intellectual disability, affects alternative splicing associated with neurite outgrowth. *Genes and Development*, 27(6), pp.615–626.
- Wapinski, O.L. et al., 2013. Hierarchical mechanisms for direct reprogramming of fibroblasts to neurons. *Cell*, 155(3).
- Waragai, M. et al., 1999. PQBP-1, a novel polyglutamine tract-binding protein, inhibits transcription activation by Brn-2 and affects cell survival. *Human Molecular Genetics*, 8(6), pp.977–987.
- Waragai, M. et al., 2000. PQBP-1/Npw38, a nuclear protein binding to the polyglutamine tract, interacts with U5-15kD/dim1p via the carboxyl-terminal domain. *Biochemical and biophysical research communications*, 273(2), pp.592–595.
- Wardle, F.C. & Sive, H.L., 2003. What's your position? The *Xenopus* cement gland as a paradigm of regional specification. *BioEssays*, 25(7), pp.717–726.
- Whetzel, P.L. et al., 2011. BioPortal: Enhanced functionality via new Web services from the National Center for Biomedical Ontology to access and use ontologies in software applications. *Nucleic Acids Research*, 39(SUPPL. 2).

Appendix A: *Pqbp1* Homeolog Alignment to Genomic Scaffold Showing Intron/Exon Boundaries and Morpholino Target Sites

The genomic scaffold containing *pqbp1* was identified by searching the *Xenopus laevis* genome using the *Xenopus laevis pqbp1* homeologs found on NCBI. This was done using blastn at the BLAST interface found on Xenbase (<http://www.xenbase.org/genomes/blast.do>). The genomic scaffold was set as the reference, and the homeologs were aligned to it with Geneious software (6.1.7) using their proprietary algorithm.







Appendix B: TGF- β Interactants Morpholino Screen Preliminary Data

A preliminary screen was conducted looking at the function of a number of TGF- β pathway interactants during *Xenopus laevis* early embryonic development.

Candidates for this screen were narrowed down from a study published by the Wrana lab (Barrios-Rodiles et al. 2005), as well as online datasets such as Biogrid and Flybase. A list of 239 potential targets was compiled and arranged according to the number and strength of their interactions with TGF- β components. For the final selection, preference was given to targets with multiple interactions. Targets were excluded if they 1) had been previously knocked down by morpholino or other method in *Xenopus*, or 2) had already been extensively studied. Translation-blocking morpholinos were designed for each target.

The following pages include background information about the targets already knocked down, morpholino sequences, as well as phenotypes observed upon knockdown. The narrowed down table of possible targets is included at the end of this Appendix.

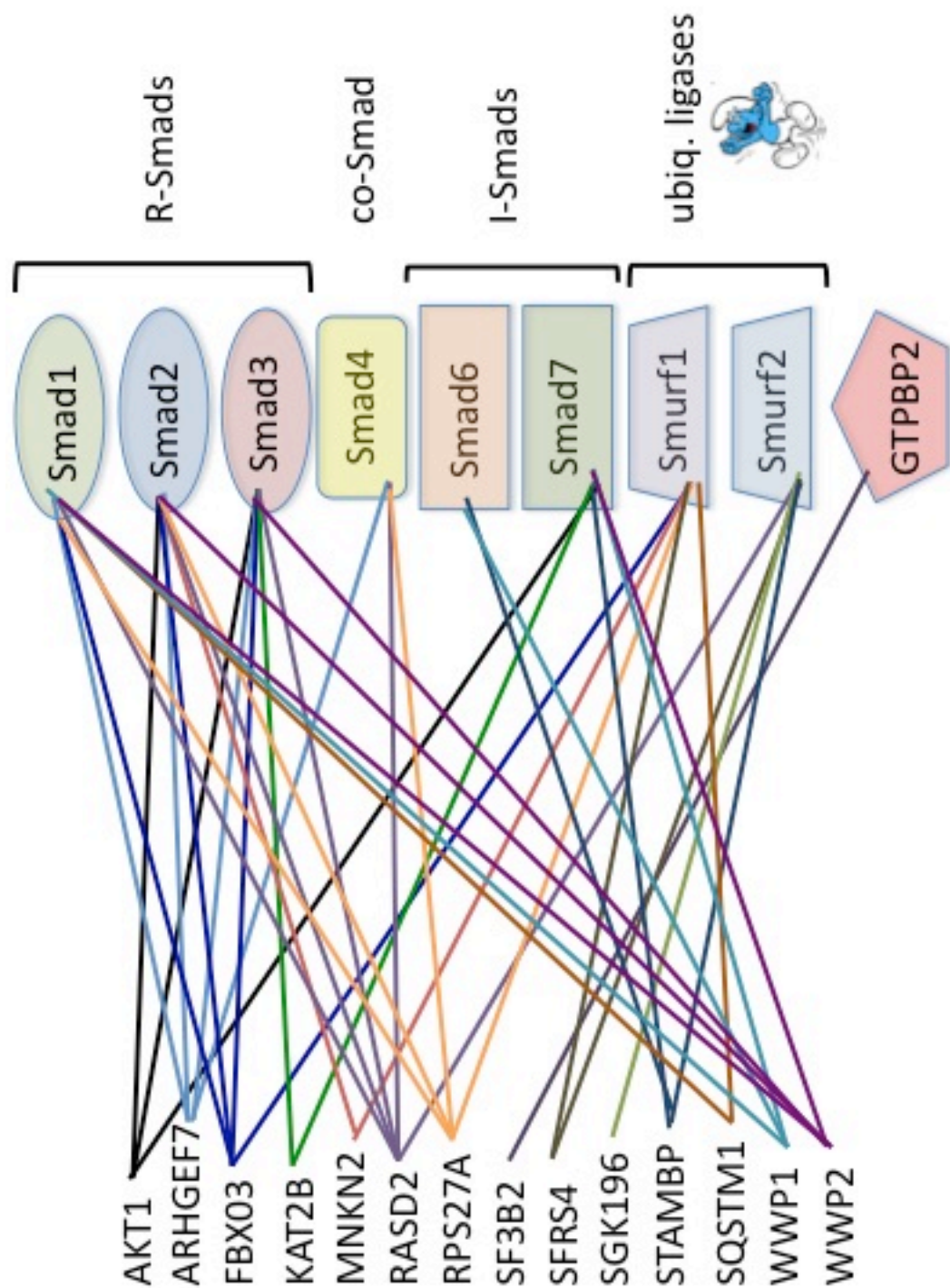


Figure B-1: TGF-β pathway interactants knocked down during the preliminary morpholino screen. Interactions with specific TGF-β pathway components are shown.

Protein	Known functions and interacting proteins
AKT1	Functions in cell survival, insulin signaling, angiogenesis and tumor formation. In the developing nervous system it is a critical mediator of growth factor-induced neuronal survival. (SMAD 2, SMAD 3, SMAD 7)
ARHGGEF7	Acts as a RAC1 guanine nucleotide exchange factor (GEF) and can induce membrane ruffling. May function as a positive regulator of apoptosis. May function in cell migration. (SMAD 1, SMAD 2, SMAD 3, SMAD 4)
FBX03	Substrate recognition component of the SCF (SKP1-CUL1-F-box protein)-type E3 ubiquitin ligase complex. Mediates the ubiquitination of HIPK2 and probably that of EP300, leading to rapid degradation by the proteasome. (SMAD 1, SMAD 2, SMAD 3, SMURF 1)
KAT2B	Functions as a histone acetyltransferase (HAT) to promote transcriptional activation. Has significant histoneacetyltransferase activity with core histones (H3 and H4), and also with nucleosome core particles. (SMAD 3, SMAD 7)
MNKN2	May play a role in the response to environmental stress and cytokines. Appears to regulate transcription by phosphorylating EIF4E, thus increasing the affinity of this protein for the 7-methylguanosine-containing mRNA cap. (SMAD 2, SMURF 1)
RASD2	GTPase signaling protein that binds to and hydrolyzes GTP. Regulates signaling pathways involving G-proteins-coupled receptor and heterotrimeric proteins such as GNB1, GNB2 and GNB3. May be involved in selected striatal competencies, mainly locomotor activity and motor coordination. (SMAD 1, SMAD 2, SMAD 3, SMAD 4, SMURF 2)

Protein	Known functions and interacting proteins
RPS27A	<p>This gene encodes a fusion protein consisting of ubiquitin at the N terminus and ribosomal protein S27a at the C terminus. When expressed in yeast, the protein is post-translationally processed, generating free ubiquitin monomer and ribosomal protein S27a. Ribosomal protein S27a is a component of the 40S subunit of the ribosome and belongs to the S27AE family of ribosomal proteins. (SMAD 1, SMAD 2, SMAD 4, SMURF 1)</p>
SF3B2	<p>This gene encodes subunit 2 of the splicing factor 3b protein complex. Splicing factor 3b, together with splicing factor 3a and a 12S RNA unit, forms the U2 small nuclear ribonucleoproteins complex. (GTPBP2)</p>
SFRS4	<p>This gene encodes a member of the arginine/serine-rich splicing factor family. The encoded protein likely functions in mRNA processing. (SMURF 1, SMURF 2)</p>
SGK196	<p>Not much known. The protein kinase domain is predicted to be catalytically inactive. Belongs to the protein kinase superfamily. Ser/Thr protein kinase family. STKL subfamily. (SMURF 2)</p>
STAMBP	<p>Potentiates BMP (bone morphogenetic protein) signaling by antagonizing the inhibitory action of SMAD6 and SMAD7. (SMAD 6, SMAD 7, SMURF 2)</p>

Protein	Known functions and interacting proteins
SQSTM1	<p>Adapter protein which binds ubiquitin and may regulate the activation of NFKB1 by TNF-alpha, nerve growth factor (NGF) and interleukin-1. May play a role in titin/TTN downstream signaling in muscle cells. May regulate signaling cascades through ubiquitination. Adapter that mediates the interaction between TRAF6 and CYLD (by similarity). May be involved in cell differentiation, apoptosis, immune response and regulation of K(+) channels. (SMAD 1, SMURF 1)</p>
WWP1	<p>E3 ubiquitin-protein ligase which accepts ubiquitin from an E2 ubiquitin-conjugating enzyme in the form of thioester and then directly transfers the ubiquitin to targeted substrates. Ubiquitinates ERBB4 isoforms JM-A CYT-1 and JM-B CYT-1, KLF2, KLF5 and TP63 and promotes their proteasomal degradation. Ubiquitinates RNF11 without targeting it for degradation. Ubiquitinates and promotes degradation of TGFBR1; the ubiquitination is enhanced by SMAD7. Ubiquitinates SMAD6 and SMAD7. (SMAD 1, SMAD 6, SMAD 7)</p>
WWP2	<p>E3 ubiquitin-protein ligase (see WWP1). Polyubiquitinates POU5F1 by 'Lys-63'-linked conjugation and promotes it to proteasomal degradation; in embryonic stem cells (ESCs) the ubiquitination is proposed to regulate POU5F1 protein level. Ubiquitinates EGR2 and promotes it to proteasomal degradation; in T-cells the ubiquitination inhibits activation-induced cell death. Ubiquitinates SLC11A2; the ubiquitination is enhanced by presence of NDFIP1 and NDFIP2. Ubiquitinates RPB1 and promotes it to proteasomal degradation. (SMAD 1, SMAD 2, SMAD 3, SMAD 7)</p>

<u>MO Name</u>	<u>Sequence</u>
XIStampBP-MO1	CTGGCATCACTGTGTTCTGGCATG
XIFBXO3-MO1	CGCTCGGACTAGCGCCATCTTGCAA
XIWWP2-MO1	TTTGAGTAGAACCTGATGATGCCAT
XISFRS4-MO1	TCATCTTGTCTAGTCCGTCCGACGA
XIArhGef7-MO1	AATTCATGGCTCGCCAGCCACACGC
WWP1-MO1	GCCATGTCAGGTTACAGGTCAGGCC
XISf3b2-MO1	TTCCGTCCGCAGTTTCCGCCATGTT
XIAkt1-MO1	CACCATCACTTCATTCATGTTGGTA
XISgk196-MO1	CAGACACTAGGTTTTCTCTCCATAT
XIRnf146-MO1	GCTAACCTCCCCACAACCAGCCATC
XIEIF2AK4-MO1	TGCCATGCTAAGCCGGACTCATCCC
XINat5-MO1	CGTTGTCATCTTCTTATGAAGTCTC
XINeddL4-MO1	GGTGCAATTTCCCCTAATCCTTTGC
XIRhebL1-MO1	AAAACGAAATACGGGCTTCCACTTT
XICANK2A2-MO1	TTTCGGGTTAGCAGGCCCCCTAAGCC

MO	Gastrulation	Neurulation	Shortened Axis	Bent Body
AKT1		X		X
ARHGEF7		X	X	X
FBX03		X	X	X
KAT2B		X	X	X
MNKN2 (no phenol)				
RASD2	X			
RPS27A				X
SF3B2	X			
SFRS4		X	X	X
SGK196			X	X
STAMBP			X	
SQSTM1	X	X	X	
WWP1		X	X	
WWP2	X (high dose)		X (low dose)	X (low dose)

Summary of Observed Defects

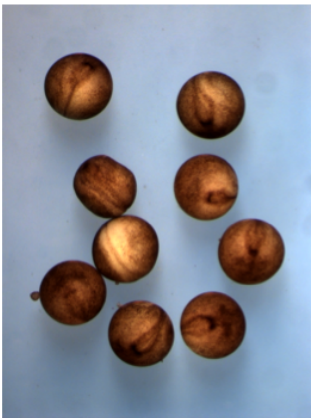
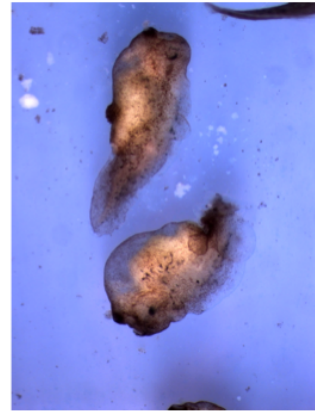
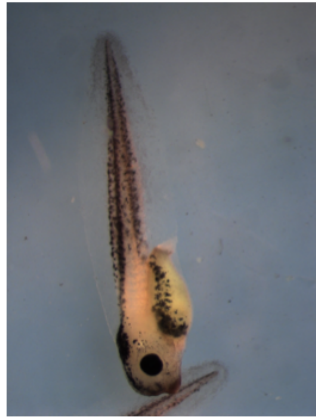
Morpholino	Amount	Results	Pass to second screen?
FBXO3	50 ng total	Head defects/missing structures, shortened axis	Yes
SF3B2	50 ng total, 25 ng total	All died with higher dose, gastrulation defect apparent with lower dose	Yes
STAMPB	50 ng total	Missing most head and tail structures, but have cement gland (ventralized?)	Yes
SFRS4	50 ng total	Dissociation from neural plate, shortened AP axis, missing eyes	Yes
WWP2	50 ng total, 25 ng total	All died with higher dose, shortened AP axis in some embryos at lower dose	Yes
WWP1	50 ng total	Neurulation block - neural plate not well defined	Yes
ARHGEF7	50 ng total	Open blastopore (some), variety of phenotypes	Yes (may need more specific targeting)
AKT1	50 ng total	Embryos look "narrow" and have dissociation, some have open blastopore and neurulation defects	Yes (may need more specific targeting)
KAT2B	50 ng total	Dissociation, shortened AP axis, missing anterior head structures	Yes
MKNK2	50 ng total	No observable phenotype	No
SQKL96	50 ng total	Possible gastrulation defect	Yes
RSP27A	50 ng total	Shortened AP axis, reduced anterior structures (cement gland present)	Yes
RASD2	50 ng total	Dissociation on one side of embryos, died by approx. stage 24	Yes

Target

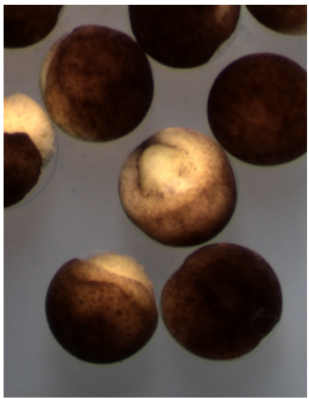
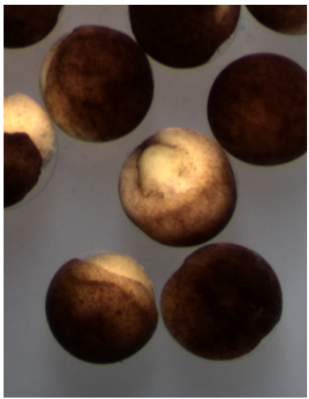

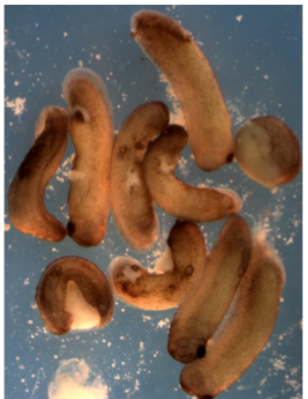


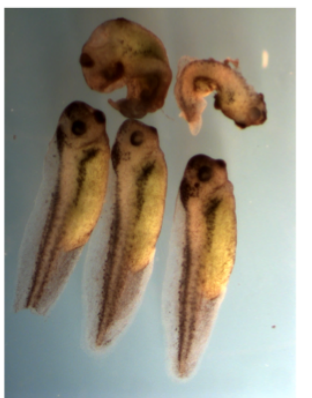



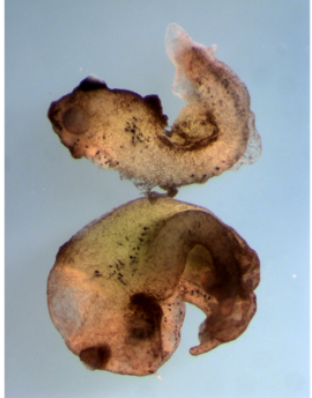

Control MO
(50 ng)

STAMPBP
(50 ng)

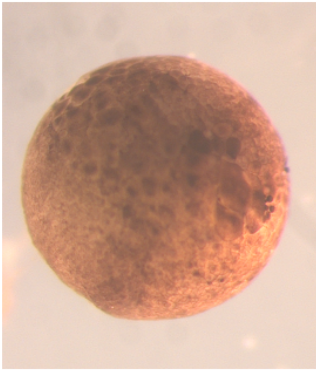
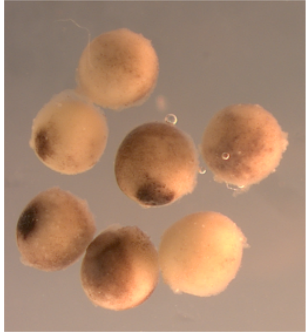

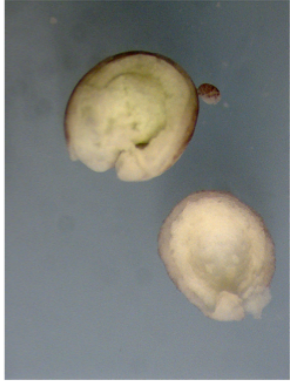
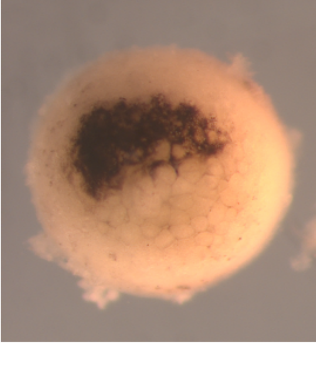
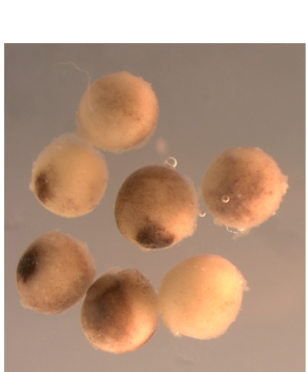
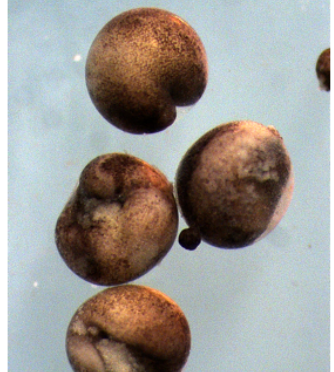

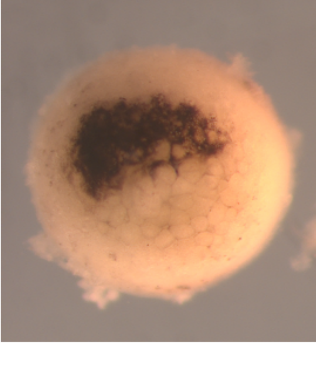
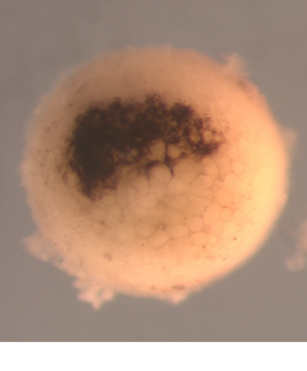
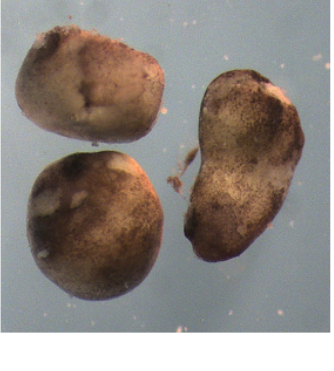

SFRS4
(50 ng)



<p>Target</p>	<p>WWP2 (25 ng)</p>	<p>FBXO3 (50 ng)</p>	<p>RSP27A (50 ng)</p>
			
			
			

Target	<p>RASD2 (50 ng)</p>	<p>ARHGEF7 (50 ng)</p>	<p>AKT1 (50 ng)</p>
			
			
			

<p>Target</p>	<p>WWP1 (50 ng)</p>	<p>MKNIK2 (50 ng)</p>	<p>KAT2B (50 ng)</p>
			
			
			

<p>Target</p>	<p>SF3B (50 ng)</p>	<p>SQSTM1 (50 ng)</p>	<p>SGK196 (25 ng)</p>
			
			
			

ClonellD	Role	Label	Mm Unigene	Hs Unigene	hRL-SMAD2	hRL-SMAD2+TGFβ signal	hRL-SMAD3	hRL-SMAD3+TGFβ signal	TGFβR1-RL (T204D)	hRL-SMAD1	hRL-SMAD1+BMP signal	ACVR1-hRL WT	ACVR1-hRL (K235R)	ACVR1-hRL (Q207D)
1300010006	WW	WWP2	Mm.294777	Hs.315485	2.321254801	1.752698153	1.18	1.304740699	1.845528284	1.817	1.348102364	1.194	0.976101918	1.276